Petersburg Quantum Weeks 2025

The International Summer Conference on Theoretical Physics 2025

Book of Abstracts

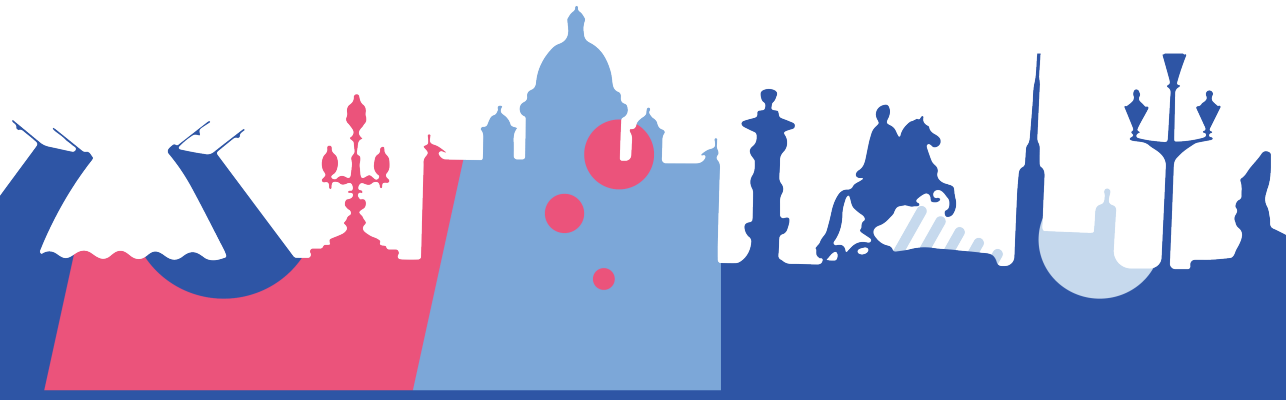

Plenary talks

Skyrmion crystals as a complex field theory

D.N. Aristov[1,2]

[1] NRC "Kurchatov Institute" – PNPI, 188300, Gatchina, Russia

[2] Faculty of Physics, St. Petersburg State University, 199034, St. Petersburg, Russia

aristov_dn@pnpi.nrcki.ru

Magnetic skyrmions are topological objects at the scale of tens of nanometers, that are actively discussed in the last decade. The interest in the fundamental properties of these objects is accompanied by the possibility of their possible use in the future memory devices. Experimentally, skyrmions were observed by neutron scattering and by Lorentz transmission electron microscopy as skyrmion lattices in a tightly packed triangular configuration, see Fig. 1. The main focus of experimental investigations and numerical modeling shifted nowadays to the preparation and manipulation of individual skyrmions, with the hope to use these topologically protected bits in electronic devices. The dynamics or heat transport properties of regular arrays of skyrmions, usually called skyrmion crystals (SkX), attract less attention.

In my talk I plan to briefly review theoretical efforts to describe magnetic skyrmions in 2D ferromagnets, starting from the seminal paper by Belavin and Polyakov [1]. The usual way of modeling includes the determination of the skyrmionic ground state, which has topologically non-trivial vector field configuration. The dynamics is studied at the second stage, either in linear spin-wave theory or within collective coordinate method (Thiele equation).

In our group we suggest to use the unified formalism to describe both the static configuration and the dynamics of SkX. We use the method of stereographic projection, which maps the vector field of local magnetization to complex-valued field. The static configuration of SkX is described by a simple trial function, with optimal parameters found numerically. [2] The dynamics is determined by considering the second variation of the action and eventual semi-classical quantization. [4] The calculation of the spectra shows that several magnon branches have non-trivial topology and non-zero Chern numbers. [3] The topological character of low-energy magnon branches may change upon variation of external magnetic field. [5] We argue that the latter topological transition in magnon spectra should be visible in thermal Hall effect at low temperatures.

This work was supported by the Russian Science Foundation, grant No. 25-12-00212.

References

1. A. A. Belavin and A. M. Polyakov, JETP Lett. 22, 245 (1975).
2. V. E. Timofeev, A. O. Sorokin, and D. N. Aristov, JETP Lett. 109, 207 (2019).
3. V. E. Timofeev and D. N. Aristov, Phys. Rev. B 105, 024422 (2022).
4. R. Rajaraman, *Solitons and Instantons* (North Holland, Amsterdam, 1982).
5. V. E. Timofeev and D. N. Aristov, JETP Lett. **117**, 9 (2023); ibid. **118**, 448 (2023); ibid. **118**, 911 (2023).

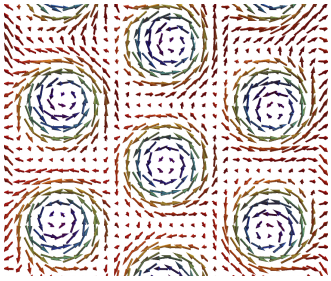

Figure 1: Magnetization pattern in 2D skyrmion crystal.

Metamaterials: from linear basics to nonlinear complications

M. Lapine[1,2,3]

[1] ITMO University, Russia

[2] University of Technology Sydney, Australia

[3] Qingdao Innovation and Development Centre of Harbin Engineering University, China

mikhail.lapine@gmail.com

The research area of metamaterials — as long as we adhere to the explicit use of terminology, as indeed some of the relevant ideas are more than a century old — is currently at a mature age of a quarter of a century, and a wide range of specific research directions has emerged in this context. [1] It is certainly impossible to address all the relevant aspects within a single review talk, and I will present a brief overview of the approaches to design artificial magnetic response with metamaterials, and highlight various phenomena which can be observed in magnetic metamaterials.

Specific attention will be offered to specific properties of finite-size samples [2], and enhanced role of metamaterial boundaries where the observed properties deviate significantly from the effective medium predictions [3].

Strong mutual interaction also paves a route towards implementation of nonlinear response [4] in magnetic metamaterials, enabling novel degrees of freedom in metamaterial design and some peculiarities of nonlocal nonlinear response [5] in layered structures [6]. In particular, I will discuss various links between mechanical and magnetic response, emerging in a range of intriguing phenomena including electro-magneto-mechanical self-oscillations [7].

A somewhat related direction points to opto-acoustic metamaterial designs, which offer artificial electrostriction [8]. On this track, a simple and non-resonant composite medium, such as an array of spheres embedded in a matrix of a different material, attains an artificial term in the electrostriction coefficient so the resulting photoelasticity can exceed that of the individual components.

Another example of non-resonant metamaterials is a simple but efficient design of artificial diamagnetics [9]. Diamagnetic metamaterials are scalable to work in a huge range of frequencies, and provide exceptionally strong diamagnetism compared to conventional materials . The strong role of mutual interaction in a very dense uniaxial lattice of meta-atoms, is once again a key feature here, leading to a magnitude of effective permeabilities below 0.1, further armed with efficient reconfigurability, and playing a step on the way to light-weight magnetic levitation.

Research work related to peculiar properties of discrete structures is supported by the Russian Science Foundation (grant no. 22-11-00153).

References

1. M. Gorkunov, M. Lapine and S. A. Tretyakov, Methods of crystal optics for studying electromagnetic phenomena in metamaterials: Review, *Crystallography Reports*, **51** (6), 1048–1062 (2006).

2. M. Lapine, L. Jelinek and R. Marqués, Surface mesoscopic effects in finite metamaterials, *Opt. Express*, **20** (16), pp. 18297–18302 (2012).

3. M. Lapine, R. C. McPhedran, and C. G. Poulton, Slow convergence to effective medium in finite discrete metamaterials, *Phys. Rev. B*, **93**, 235156 (2016).

4. M. Lapine, New degrees of freedom in nonlinear metamaterials, *Phys. Status Solidi B* **254** (4), 1600462 (2017).

5. M. A. Gorlach, T. A. Voytova, M. Lapine, Yu. S. Kivshar, and P. A. Belov, Nonlocal homogenization for nonlinear metamaterials, *Phys. Rev. B*, **93**, 165125 (2016).

6. M. Lapine, M. A. Gorlach, Current trends and nonlinear effects in multilayered metamaterials, *Ceramics International* **49**, 24422–24427 (2023).

7. Mingkai Liu, D. A. Powell, I. V. Shadrivov, M. Lapine, and Yu. S. Kivshar, Self-oscillations in nonlinear torsional metamaterials, *New J. of Physics*, **15**, 073036 (2013).

8. M. J. A. Smith, B. T. Kuhlmey, C. M. de Sterke, C. Wolff, M. Lapine, and C. G. Poulton, Electrostriction enhancement in metamaterials, *Phys. Rev. B*, **91**, 214102 (2015).

9. M. Lapine, A. K. Krylova, P. A. Belov, C. G. Poulton, R. C. McPhedran and Yu. S. Kivshar, Broadband diamagnetism in anisotropic metamaterials, *Phys. Rev. B*, **87**, 024408 (2013).

Oral talks

Generation of vortex electrons in tunneling ionization of polyatomic molecules: Exact results in the zero-range potential model

Kirill V. Bazarov[1,2] and Oleg I. Tolstikhin[1]

[1] Moscow Institute of Physics and Technology, Dolgoprudny 141700, Russia

[2] NRC "Kurchatov Institute", Moscow 123182, Russia

bazarov.kv@phystech.edu

This note is based on [1]. Tunneling ionization of polyatomic molecules is considered. This process can be described within the framework of the single active electron approximation. The orientation of the molecule is frozen, and the external electric field acts in the dipole approximation. Thus, we have the following Schrödinger equation:

$$\left[-\frac{1}{2}\Delta + V(\mathbf{r}) + Fz - E\right]\phi(\mathbf{r}) = 0, \tag{1}$$

satisfying the outgoing-wave boundary condition

$$\phi(\mathbf{r})|_{z\to-\infty} = \int A(\mathbf{k}_\perp) e^{i\mathbf{k}_\perp \mathbf{r}_\perp} g(z, k_\perp) \frac{d\mathbf{k}_\perp}{(2\pi)^2}, \tag{2}$$

where

$$g(z, k_\perp) = \frac{1}{|2Fz|^{1/4}} \exp\left[\frac{iF^{1/2}|2z|^{3/2}}{3} - \frac{i(k_\perp^2 - 2E)|z|^{1/2}}{(2F)^{1/2}}\right]. \tag{3}$$

The solution of (1) represents tunneling ionization and contain two important observables. First, the eigenvalue, represented in the form

$$E = \mathcal{E} - \tfrac{i}{2}\Gamma, \tag{4}$$

where Γ describes the ionization rate. And $A(\mathbf{k}_\perp)$, the transverse momentum distribution amplitude. The structure of the electron flux from the ionized molecule is coded in $A(\mathbf{k}_\perp)$. The flux contains vortex photoelectrons. To analyze the generation of such vortex electrons, it is convenient to introduce:

$$A(\mathbf{k}_\perp) = \sum_{m=-\infty}^{\infty} A_m(k_\perp) e^{im\varphi_k}, \quad P_m = \frac{1}{2\pi}\int_0^\infty |A_m(k_\perp)|^2 k_\perp dk_\perp, \quad P = \sum_{m=-\infty}^{\infty} P_m. \tag{5}$$

We can analyze these observables within the zero-range potential model:

$$V(\mathbf{r}) = \sum_{i=1}^{N} V_{\mathrm{ZRP}}(\mathbf{r} - \mathbf{R}_i; \varkappa_i), \quad V_{\mathrm{ZRP}}(\mathbf{r}; \varkappa) = \frac{2\pi}{\varkappa}\delta(\mathbf{r})\frac{\partial}{\partial r}r. \tag{6}$$

Within this model, it is possible to carry out exact calculations.

One of the main conclusions of our calculations is the following: vortex electrons can be generated even at a relatively weak field. For this purpose, partial ionization fluxes characterizing the rate of generation of plane-wave ($m = 0$) or vortex ($|m| > 0$) electrons were analyzed.

Also, we see that as the electric field strength increases, the ionization process changes from being dominated by plane wave electrons to including vortex electrons, whose contribution becomes noticeable. The transverse momentum distribution evolves from a Gaussian shape to a more complex structure associated with vortex channels. Furthermore, the study suggests a promising direction for enantiosensitive photoelectron spectroscopy by exploiting the behavior of vortex electrons, especially in large chiral molecules, with ongoing studies to quantify this sensitivity.

This work was supported by the Russian Science Foundation (Grant No. 24-12-00055).

References

1. Bazarov, K. & Tolstikhin, O. Generation of vortex electrons in tunneling ionization of polyatomic molecules: Exact results in the zero-range potential model. *Phys. Rev. A.* **110**, 033107 (2024,9), https://link.aps.org/doi/10.1103/PhysRevA.110.033107

Arrays of Josephson artificial atoms with topologically nontrivial band structure

G. Fedorov[1], E. Konopleva[2,1], O. Astafiev[2,1]

[1] Moscow Institute of Physics and Technology

[2] Skolkovo Institute of Science and Technology

gleb.fedorov@phystech.edu

Recently, significant interest was attracted towards developing and scaling quantum simulators of various kinds based on various physical platforms, which pave an alternative way to reach quantum utility in the NISQ era. Numerous works were devoted to the Bose-Hubbard model where quantum walks were extensively studied on processors with dozens of transmons. Systems with non-trivial topological properties are also now entering the focus of research, with 1D and 2D arrays simulating the Aubry-Andre-Harper models and direct discretized quantum Hall structures.

An interesting new direction in this context is to extend the work done on topological simulators built using optical lattices by incorporating Josephson quantum circuits into the problem. In this talk, we share our preliminary results and propose a scheme that uses a new type of superconduting artificial atom that we name the "polarization transmon" to build a quantum version of the well-known Zig-zag model with ultra-low losses and inherent quantumness ensured by working at the single-photon levels.

This work was supported by Russian Science Foundation, project №25-22-00280

Non-equilibrium bosonization technique and it's applications in mesoscopic physics

Edvin G. Idrisov

Department of Physics, United Arab Emirates University, P.O. Box 15551 Al-Ain, United Arab Emirates

edvin.idrisov@uaeu.ac.ae

The research focuses on a theoretical study of fundamental questions such as dephasing, charge quantization, equilibration, and entanglement in hybrid mesoscopic systems based on the quantum Hall effect, where one-dimensional edge states play a central role [1, 2, 3, 4]. To account for strong electron-electron interactions in such systems, the non-equilibrium bosonization technique is employed. Particular attention is given to quantum point contacts and floating Ohmic contacts, which serve as examples of non-equilibrium sources [5]. This study is partly motivated by recent experimental advances in mesoscopic physics.

This work was supported by the United Arab Emirates University under the Startup Grant No. G00004974 and Sure Plus Grant.

References

1. E. G. Idrisov, I. P. Levkivskyi, and E. V. Sukhorukov, Phys. Rev. Lett. **121**, 026802 (2018)

2. E. G. Idrisov, I. P. Levkivskyi, and E. V. Sukhorukov, Phys. Rev. B **101**, 245426 (2020)

3. E. G. Idrisov, I. P. Levkivskyi, E. V. Sukhorukov, and T. L. Schmidt, Phys. Rev. B **106**, 085405 (2022)

4. E. G. Idrisov and J. Ekstrom, Phys. Rev. B **110**, L041402 (2024).

5. E. G. Idrisov, I. P. Levkivskyi, E. V. Sukhorukov, Phys. Rev. Research **7**, 013042 (2025)

Predicting properties of quantum systems by regression on a quantum computer

A. Kardashin[1], Ye. Balkybek[1], V. V. Palyulin[1], K. Antipin[1,2]

[1] Skolkovo Institute of Science and Technology, Moscow, Russia

[2] Lomonosov Moscow State University, Moscow, Russia

andrey.kardashin@skoltech.tu

Quantum machine learning (QML) is among the most promising applications of quantum computers [1]. In our work [2], we consider solving regression QML problems for quantum data, i.e., data represented by quantum states.

Suppose we are given a training set of the form $\mathcal{T} = \left\{(\rho_{\alpha_j}, \alpha_j)\right\}_{j=1}^{T}$, where ρ_{α_j} are labeled n-qubit quantum states and $\alpha_j \in \mathbb{R}$ are their corresponding labels. Our goal is to use the given training set $\mathcal{T}$ for learning how to predict the label α for an unseen datum ρ_α. Since the data points ρ_α are quantum states, it is natural to obtain the prediction a for the labels α as the expected value of an observable H measured in ρ_α, i.e., $\mathsf{a} \equiv \operatorname{Tr} H\rho_\alpha = \alpha + b(\alpha)$, where $b(\alpha)$ is the prediction bias.

We parametrize the Hermitian operator H as $H(\boldsymbol{x}, \boldsymbol{\theta}) = \sum_i x_i \Pi_i(\boldsymbol{\theta})$, where $\boldsymbol{x} = \{x_i\}_i$ are the eigenvalues, and the eigenprojectors $\Pi_i(\boldsymbol{\theta}) = U^\dagger(\boldsymbol{\theta})\,|i\rangle\langle i|\,U(\boldsymbol{\theta})$ are the projectors onto the ith state of the computational basis transformed by a unitary $U(\boldsymbol{\theta})$ parametrized by $\boldsymbol{\theta} \subset \mathbb{R}$. Schematically, the label prediction can be represented as

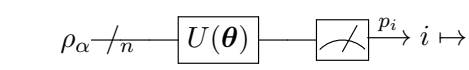

That is, given an n-qubit labeled state ρ_α, we transform it by a variational quantum circuit $U(\boldsymbol{\theta})$, measure the resultant state $\rho_\alpha(\boldsymbol{\theta}) \equiv U(\boldsymbol{\theta})\rho_\alpha U^\dagger(\boldsymbol{\theta})$ in the computational basis, with probability $p_i(\rho_\alpha, \boldsymbol{\theta}) = \langle i|\rho_\alpha(\boldsymbol{\theta})|i\rangle$ get the outcome i associated with x_i, which gives the prediction in the form $\mathsf{a}(\rho_\alpha, \boldsymbol{x}, \boldsymbol{\theta}) = \sum_i x_i p_i(\rho_\alpha, \boldsymbol{\theta})$.

To find optimal parameters $\boldsymbol{x}^*$ and $\boldsymbol{\theta}^*$, we solve the following minimization problem:

$$(\boldsymbol{x}^*, \boldsymbol{\theta}^*) = \arg\min_{\boldsymbol{x},\boldsymbol{\theta}} \left[w_{\text{ls}} \sum_{j=1}^{T} \Big(\alpha_j - \mathsf{a}\big(\rho_{\alpha_j}, \boldsymbol{x}, \boldsymbol{\theta}\big)\Big)^2 + w_{\text{var}} \sum_{j=1}^{T} \Delta^2_{\rho_{\alpha_j}} H(\boldsymbol{x}, \boldsymbol{\theta}) \right], \quad (1)$$

with $w_{\text{ls}}, w_{\text{var}} > 0$ being weights. In (1), the first term is the sum of the squared differences between the given labels α and our predictions $\mathsf{a} = \langle H\rangle_{\rho_\alpha} \equiv \operatorname{Tr} H\rho_\alpha$, while the second term is the sum of the variances $\Delta^2_{\rho_\alpha} H \equiv \langle H^2\rangle_{\rho_\alpha} - \langle H\rangle^2_{\rho_\alpha}$. For the variance of H in ρ_α, from the quantum Cramer-Rao bound [3] we derive $\Delta^2_{\rho_\alpha} H / \big|\partial_\alpha \langle H\rangle_{\rho_\alpha}\big|^2 \geqslant 1/I_q(\rho_\alpha)$, where $\partial_\alpha \equiv \frac{\partial}{\partial\alpha}$ and $I_q(\rho_\alpha)$ is the quantum Fisher information; we use this relation to assess the quality of the solution obtained via solving (1).

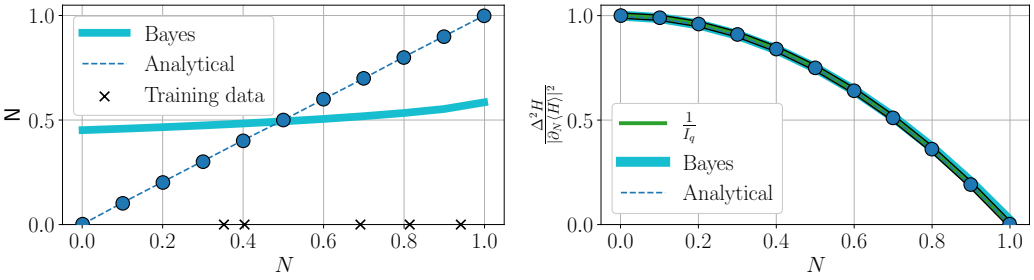

Figure 1: Left: Predicted N vs. the true N negativity of the Bell-type states. Right: Variance of the optimized observable H^* together with lower bound $1/I_q$. The blue circles show the results obtained via solving (1), the solid blue line stands for the results obtained after the minimization of the Bayesian MSE ($w_{\text{ls}} = w_{\text{var}}$ in (1)), and the dashed line indicates the results from solving (2).

We note that if $w_{\text{ls}} = w_{\text{var}}$ and if the distribution of α is uniform, then (1) reduces to the minimization of the Bayesian mean squared error (MSE) [3]. Additionally, in our work [2], we show that the observable $H^* \equiv H(\boldsymbol{x}^*, \boldsymbol{\theta}^*)$ can be found by solving

$$\frac{1}{2}\left(\tilde{\rho}_\alpha H^* + H^* \tilde{\rho}_\alpha\right) - \frac{k}{T}\sum_{j=1}^{T} \alpha_j \rho_{\alpha_j} + \frac{(k-1)}{T}\sum_{j=1}^{T} \mathrm{Tr}\big(H_0 \rho_{\alpha_j}\big)\rho_{\alpha_j} = 0, \tag{2}$$

where $\tilde{\rho}_\alpha = \frac{1}{T}\sum_{j=1}^{T} \rho_{\alpha_j}$ and $k = w_{\text{ls}}/w_{\text{var}}$; that is, H^* delivers a minimum to (1).

Consider the task of predicting the entanglement of the Bell-type states $\left|\Phi_p^+\right\rangle = \sqrt{p}\,|00\rangle + \sqrt{1-p}\,|11\rangle$. We applied our method (1) to the training set $\mathcal{T} = \left\{|\Phi_{p_j}^+\rangle, N_j\right\}_{j=1}^{5}$, where the coefficients p_j are picked randomly and N_j is the negativity of $|\Phi_{p_j}^+\rangle$; the negativity of a state ρ is defined as $N(\rho) = \left\|\rho^{T_2}\right\|_1 - 1$, where $\|\cdot\|_1$ is the trace norm, and $\rho^{T_2} \equiv (\mathbb{1} \otimes T)[\rho]$ is the partial transpose of ρ. As can be seen in Figure 1, with our method we can find an observable H^* giving accurate predictions $\mathsf{N} = \langle \Phi_p^+ | H^* | \Phi_p^+ \rangle$ of the negativity $N(\Phi_p^+)$, as well as having low variance $\Delta^2_{\Phi_p^+} H^*$. Additionally, we can see that the minimization of the Bayesian MSE produces a large prediction bias $b(N)$.

References

1. J. Biamonte *et al.*, Nature **549**, 195–202 (2017).

2. A. Kardashin *et al.*, Phys. Rev. Research **7**, 013201 (2025).

3. J. Sidhu *et al.*, AVS Quantum Sci. **2**, 014701 (2020)

Helical metamaterials with strong spatial dispersion.

P.O. Kazinski[1] and P.S. Korolev[1]

[1] Tomsk State University

kpo@phys.tsu.ru, kizorph.d@gmail.com

The propagation of electromagnetic waves in helical media with strong spatial dispersion is investigated. The general form of the permittivity tensor with spatial dispersion obeying the helical symmetry [1, 2] is derived. Its particular form describing the medium of conducting spiral wires - helical metamaterial - has been studied in detail [3, 4]. The presence of a strong spatial dispersion revealing as the pole in the permittivity tensor has given rise to the appearance of the additional degree of freedom—the field of plasmons propagating along the conducting wires in the wired medium. The solution of the corresponding Maxwell's equations is obtained in the paraxial and shortwave approximations. The dispersion law of electromagnetic field modes, their polarization and integral curves of the Poynting vector are analyzed. The photon dispersion law in such a medium possesses polarization-dependent forbidden bands. The width of these bands and their positions are tunable over a wide range of energies. The scattering of electromagnetic waves by a plate made of a helical metamaterial is considered. A design scheme for a cholesteric-like helical metamaterial whose electromagnetic properties reproduce the known properties of cholesteric liquid crystals [5, 6] and possess an additional total forbidden band in the dispersion law is proposed.

The research was carried out with the support of a grant from the Government of the Russian Federation (Agreement No. 075-15-2025-009 of 28 February 2025).

References

1. P. O. Kazinski, P. S. Korolev, J. Phys. A: Math. Th., **55**, 395301 (2022).

2. P. O. Kazinski, P. S. Korolev, J. Phys. A: Math. Th., **58**, 095701 (2025).

3. M. G. Silveirinha, IEEE Trans. Antenn. and Prop.,**56**, 390-401 (2008).

4. J. Kaschke, M. Wegener, Nanophotonics, **5**, 510-523 (2016).

5. P. G. De Gennes, J. Prost, The physics of liquid crystals, Oxford university press (1993).

6. V. A. Belyakov, A. S. Sonin, Optics of Cholesteric Liquid Crystals [in Russian]. Nauka: Moscow, Russia (1982).

Electron-positron pair creation at heavy ion-atom collisions involving deexcitation processes

Y. S. Kozhedub[1], V. A. Zaytsev, V. M. Shabaev[1,2], D. Yu[3]

[1]Department of Physics, St. Petersburg State University, 199034 St. Petersburg, Russia

[2]National Research Centre "Kurchatov Institute" B. P. Konstantinov Petersburg Nuclear Physics Institute, 188300 Gatchina, Leningrad district, Russia

[3]Institute of Modern Physics, Chinese Academy of Sciences, 730000 Lanzhou, China

y.kozhedub@spbu.ru

The work aims to explore the strongly relativistic domain and investigate the non-perturbative phenomena of quantum electrodynamics (QED) in the presence of extreme electromagnetic fields. Low-energy collisions of heavy ions provide a unique opportunity to probe our understanding of quantum electron dynamics in the scarcely explored regime of critical fields [1, 2, 3]. When the total charge of the colliding nuclei exceeds the critical value, $Z_1 + Z_2 > Z_{\rm cr} \approx 173$, and the internuclear distance is smaller than the critical distance, the ground-state $1s\sigma$ of the quasimolecule submerges into the Dirac sea below $-2m_ec^2$, making spontaneous electron-positron pair production (spontaneous vacuum decay) possible. Observing spontaneous pair production in such collisions may provide valuable insights into QED under supercritical fields [4, 5, 6].

Future facilities dedicated to atomic physics research with highly charged ions, such as FAIR in Darmstadt, Germany, NICA in Dubna, Russia, and the rapidly developing HIAF in Huizhou, China, offer unique conditions for studying heavy ion-atom collisions. A broad range of experimental research is planned, focusing on comprehensive investigations of various processes, including those in the supercritical regime. These experimental efforts require complementary theoretical studies to provide guidance and support.

The fundamental prediction of spontaneous electron-positron pair production remains unconfirmed experimentally. In addition to technical challenges, the study of this process is complicated by the presence of a dynamical pair-production channel, driven by the time dependence of the two-center potential. This dynamical mechanism operates in both subcritical and supercritical regimes and, in the latter case, generally dominates over the spontaneous mechanism at collision energies near the Coulomb barrier—energies most suitable for investigating the phenomenon of interest [7]. However, our recent works [8, 9, 10] have demonstrated the theoretical possibility of observing spontaneous vacuum decay by analyzing the dependence of the total positron creation probability on collision trajectories. Nonetheless, the proposed procedure is extremely

difficult to implement in practice, making the search for alternative approaches highly desirable.

In this work, we consider a new channel of spontaneous electron-positron pair production during heavy ion-atom collisions involving deexcitation processes. In these processes, an electron may transition from an excited state of the quasimolecule to the ground state, with the released energy being used to produce an electron-positron pair. Although the rate of this channel is suppressed by a factor of $1/Z_{\rm cr}^2$ compared to the domain pair-creation process, it operates in both subcritical and supercritical regimes and can contribute significantly to the total positron creation probability. Notably, this channel does not require a supercritical field, allowing it to be explored in lower-energy collision regimes (and at larger shortest internuclear distances) where the dynamical pair-production mechanism is suppressed relative to the spontaneous one. It is also worth mentioning that the energy spectra of positrons in the standard and proposed channels of electron-positron pair production are expected to differ significantly due to the energy of the excited electron. All these factors make this process highly promising for the potential observation of spontaneous electron-positron pair production. Moreover, this process is of particular interest due to the involvement of electron-electron interactions, which are expected to be highly sensitive to QED effects in such extremely relativistic particles.

This work was supported by the Russian Science Foundation (Grant No. 22-62-00004).

References

1. J. Eichler and W.E. Meyerhof, Relativistic Atomic Collisions, (Academic Press, New York, 1995).

2. J. Eichler and Th. Stöhlker, Phys. Rep. **439**, 1 (2007).

3. V.M. Shabaev, Phys. Rep. **356**, 119 (2002).

4. S.S. Gershtein and Y.B. Zeldovich, Zh. Eksp. Teor. Fiz. **57**, 654 (1969) .

5. W. Pieper and W. Greiner, Z. Phys. **218**, 327 (1969).

6. W. Greiner, B. Müller, and J. Rafelski, Quantum Electrodynamics of Strong Fields (Springer-Verlag, Berlin, 1985).

7. I.A. Maltsev *et al.*, Phys. Rev. A **91**, 032708 (2015).

8. I.A. Maltsev *et al.*, Phys. Rev. Lett. **123**, 113401 (2019).

9. R.V. Popov *et al.*, Phys. Rev. D **102**, 076005 (2020).

10. N.K. Dulaev *et al.*, Phys. Rev. D **109**, 036008 (2024).

Quantum electrodynamics calculations of energy levels in highly charged ions

A. V. Malyshev[1,2]

[1] Department of Physics, St. Petersburg State University, Universitetskaya 7/9, 199034 St. Petersburg, Russia

[2] Petersburg Nuclear Physics Institute named by B. P. Konstantinov of National Research Center "Kurchatov Institute", Orlova roscha 1, 188300 Gatchina, Leningrad region, Russia

a.v.malyshev@spbu.ru

Highly charged ions are ideal mini-laboratories for probing high-precision methods of bound-state quantum electrodynamics (BS-QED) in the presence of strong electromagnetic fields [1, 2, 3, 4, 5]. This is because a rather small number of electrons in such systems allows accurate treatment of electron-electron correlations without masking QED effects, which are significantly enhanced compared to light atoms. To date, the most stringent tests of the BS-QED methods in the strong-coupling regime are provided by the ground-state Lamb-shift measurement in H-like uranium [6, 7] and the precise determination of the $2p_{1/2} \to 2s$ transition in Li-like uranium [8, 9, 10]. The transition energies in helium-, beryllium-, and boronlike ions are also the object of active experimental studies.

In the report, a brief review of modern approaches used to calculate the energy levels in highly charged ions will be given. Comparison of the obtained theoretical predictions with the results of high-precision experiments provides a unique opportunity to test the developed QED methods [11, 12]. Such tests are necessary, in particular, as a basis for applying the previously proposed schemes for measuring fundamental constants in experiments with highly charged ions.

Acknowledgments

The work was supported by the the Foundation for the Advancement of Theoretical Physics and Mathematics BASIS (Project No. 24-1-2-74-1).

References

1. J. Sapirstein and K. T. Cheng, Can. J. Phys. **86**, 25 (2008).

2. P. Beiersdorfer, J. Phys. B: At. Mol. Opt. Phys. **43**, 074032 (2010).

3. V. M. Shabaev *et al.*, Hyp. Interact. **239**, 60 (2018).

4. M. G. Kozlov *et al.*, Rev. Mod. Phys. **90**, 045005 (2018).

5. P. Indelicato, J. Phys. B: At. Mol. Opt. Phys. **52**, 232001 (2019).

6. Th. Stöhlker *et al.*, Phys. Rev. Lett. **85**, 3109 (2000).

7. A. Gumberidze *et al.*, Phys. Rev. Lett. **94**, 223001 (2005).

8. J. Schweppe *et al.*, Phys. Rev. Lett. **66**, 1434 (1991).

9. C. Brandau *et al.*, Phys. Rev. Lett. **91**, 073202 (2003).

10. P. Beiersdorfer *et al.*, Phys. Rev. Lett. **95**, 233003 (2005).

11. A. V. Malyshev, Y. S. Kozhedub, and V. M. Shabaev, Phys. Rev. A **107**, 042806 (2023).

12. A. V. Malyshev, Y. S. Kozhedub, V. M. Shabaev, and I. I. Tupitsyn, Phys. Rev. A **110**, 062824 (2024).

Flat bands in anisotropic p-mode honeycomb lattice

M. Mazanov[1], D. Román-Cortés[2], R. A. Vicencio[2], M. A. Gorlach[1]

[1] School of Physics and Engineering, ITMO University, Saint Petersburg 197101, Russia

[2] Departamento de Física and Millenium Institute for Research in Optics-MIRO, Facultad de Ciencias Físicas y Matemáticas, Universidad de Chile, 8370448 Santiago, Chile

maxim.mazanov@metalab.ifmo.ru

Flat bands have been a recurring topic of condensed matter physics research for the last several decades, as understanding of this physics and systematic construction of artificial flat bands could help increase particle interactions, boosting such nonlinear phenomena as superconductivity and superfluidity [1]. Originally proposed in magnetic materials, flat bands have since been discovered in multiple other physical settings such as photonics [2], acoustics, topoelectric circuits and more, with photonic platforms being of special interest for the proof-of-principle experiments thanks to their reconfigurable nature and precise fabrication techniques. Among the flat band physics research, all-bands-flat lattices push the concept to the limit by creating a finite Aharonov-Bohm cage for any input excitation, suppressing any diffraction.

In one dimension, several condensed matter proposals are known, with most prominent examples being the Creutz ladder and rhombic lattice in magnetic field [3], along with their photonic counterparts [4]. On the other hand, two-dimensional realizations of all-bands-flat physics remain challenging, with a single condensed matter proposal involving the Dice lattice in magnetic field [5], followed by experiments in superconducting wire networks [6].

Here, we propose an alternative approach for achieving two-dimensional all-bands-flat physics by utilizing the concept of invisibility angle (coupling cancellation) arising for dipolar modes at certain geometrical lattice anisotropy. Although this physics could be in principle achieved for electronic lattices in condensed matter, we propose a proof-of-principle experiment in the optical waveguide lattice fabricated via the femtosecond laser writing technique. Due to more prominent long-range couplings and effects of mode non-orthogonality in optics, our theory and experiment demonstrate nearly-all-bands physics, with band dispersion limited by such effects.

Nevertheless, we experimentally observe more than three cycles of Aharonov-Bohm caging for the bulk point excitation, suggesting diffraction suppression similar to one-dimensional optical analogues. Moreover, we observe almost diffraction-free propagation for the initial excitation at the corner waveguide due to its significant overlap with the tightly localized topological corner state [7]. Localization characteristics such as inverse participation ratio extracted from our experiment show excellent correspondence with

theory accounting for both long-range interactions and non-orthogonality corrections, which start playing a major role close to the flat-band limit and for larger wavelengths. The caging effect is more prominent for smaller wavelengths close to 700 nm due to the diminished effect of long-range couplings of more tightly localized individual waveguide modes. This case is relevant for electronic lattices where the tight-binding approximation (approximation of highly localized electrons) is valid.

In summary, our study provides an alternative approach to creating two-dimensional all-bands-flat phases in condensed matter and beyond, while our optical experiment simultaneously highlights its limitations for materials with less localized electrons. The invisibility angle phenomenon could also be generalized to higher-order modes and multiple no-coupling angles, as has been appreciated in chemical literature [8]. In photonics context, our model could find applications in wavelength-tunable diffractionless signal transmission for optical on-chip technologies [9]. Additionally, if properly modulated, our structure could achieve diffractionless transfer of the input state across the lattice in analogy to one-dimensional proposal [10].

References

1. D. Leykam et al, Advances in Physics: X **3**, 1473052 (2018).

2. C. Danieli et al, Nanophotonics **13**, 3925-3944 (2024).

3. M. Creutz, Phys. Rev. Lett. **83**, 2636 (1999).

4. C. Jörg et al, Light Sci. Appl. **9**, 150 (2020).

5. J. Vidal et al., Phys. Rev. Lett. **81**, 5888 (1998).

6. C. C. Abilio et al., Phys. Rev. Lett. **83**, 5102 (1999).

7. W. A. Benalcazar et al, Phys. Rev. B **99**, 245151 (2019).

8. P. M. Kazmaier et al., J. Am. Chem. Soc. **116**, 9684 (1994); N. Hestand et al., Chem. Rev. **118**, 7069 (2018).

9. B. Jang et al, Opt. Lett. **44**, 4016-4019 (2019); J. Yang et al, Opt. Lett. **36**, 772-774 (2011).

10. G. Cáceres-Aravena et al, Phys. Rev. Lett. **128**, 256602 (2022).

Spontaneous transitions under the influence of noise in a Brillouin laser in hard excitation mode with exceptional point

A. R. Mukhamedyanov[1,2], A. A. Zyablovsky[1,2], E. S. Andrianov[1,2]

[1] Dukhov Research Institute of Automatics (VNIIA)

[2] Moscow Institute of Physics and Technology

mukhamedianov.a@phystech.edu

Optomechanical systems have a great potential for the creation of coherent radiation sources, sensors, and high sensitive gyroscope [1]. We consider a Brillouin laser consisting of two optical modes a_1, a_2 that interact with each other via phonon mode b [2]. In such system, there are two states: the zero state (no coherent generation) and the non-zero state (coherent generation). The stability conditions of the states and the position of the exceptional point of the Brillouin laser are determined by the pumping amplitude of the external wave Ω [3]. Here Ω_{ex}, Ω_{EP} and Ω_{th} correspond to pump amplitude when exist the non-zero state, position of exceptional point and threshold value respectively. In the range $0 < \Omega < \Omega_{th}$ the zero state of the system is stable, furthermore there is $\Omega_{ex} < \Omega_{EP} < \Omega_{th}$ when the non-zero state is stable [3]. Therefore, when $\Omega_{ex} < \Omega < \Omega_{th}$ both states (zero and non-zero) exist and stable.

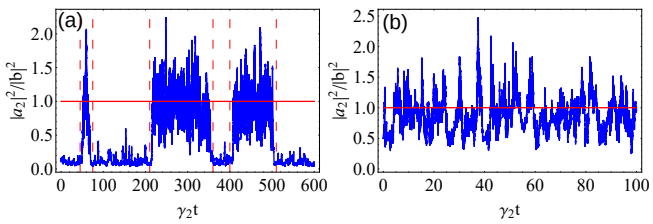

Figure 1: Time dependence of the ratio of the intensity of the second optical mode to the intensity of the phonon mode. $\Omega_{ex} < \Omega < \Omega_{EP}$ (a); $\Omega_{EP} < \Omega < \Omega_{th}$ (b). The dashed lines separate the time intervals when the system evolves near the symmetric state ($|a_2|^2/|b|^2 = 1$) and when it evolves near the non-symmetric state ($|a_2|^2/|b|^2 << 1$).

Theoretical and numerical studies have shown that in case when exceptional point exists and the time evolution occurs near the zero state, the system is in an asymmetric state ($|a_2|^2 \neq |b|^2$). When evolution occurs near a non-zero state, the system is in a symmetric state ($|a_2|^2 = |b|^2$). Numerical calculation demonstrates that noise causes random transitions between symmetric and asymmetric states (Figure 1). These transitions are accompanied by abrupt changes in the intensities of optical modes and phonon mode, which opens up new opportunities for studying spontaneous

symmetry breaking (SSB) or parity-time (PT) symmetry breaking. The obtained results demonstrate the SSB effect in optomechanical systems. Numerical calculations show that thermal noise plays a crucial role in transitions between symmetric and asymmetric states in optomechanical systems.

Optomechanical system is non-Hermitian system, therefore we use a theoretical approach for open quantum systems. To simulate an open quantum system, we use the Heisenberg-Langevin approach and derive the equation of motion. For evaluation of the time dependence of the intensities, we use numerical Huen's method [4] where the noise is represented as a thermal noise (Brownian motion).

Noise-induced transitions can be used in the creation of new sensors based on optomechanical systems using the method of intracavity laser spectroscopy [5]. For example, transitions between asymmetric and symmetric states can be used to increase the sensitivity of sensors by increasing the intensity ratio of the optical mode in the generation mode and in the non-generation mode.

References

1. B. B. Li *et al.*, Nanophotonics **10**(11), p. 2799-2832 (2021).

2. I. S. Grudinin *et al.*, Phys. Rev. Lett. **104**, 083901 (2010).

3. A. Mukhamedyanov *et al.*, Opt. Lett. **49**(4), p. 782-785 (2024).

4. H. P. Breuer and F. Petruccione, *The theory of open quantum systems*, Oxford University Press, USA, 2002.

5. P. Melentiev *et al.*, App. Phys. Lett. **111**(21), (2017).

Intracavity squeezing for a Kerr quantum nondemolition measurement scheme

D.I. Salykina[1,2] and F.Ya. Khalili[1]

[1] Russian Quantum Center, Skolkovo IC, Bolshoy Bulvar 30, bld. 1, Moscow, 121205, Russia

[2] Faculty of Physics, M.V. Lomonosov Moscow State University, Leninskie Gory 1, Moscow 119991, Russia

koil257@mail.ru

According to quantum physics, conducting a measurement over a micro-object necessarily entails a disturbance that affects the object in an unpredictable way and worsens the sensitivity of the measurement. In the 1970s, Braginsky and his co-authors proposed the concept of quantum nondemolition measurements [1]. The idea behind this is the following: if only one of the two noncommuting quantities is of interest to us, then we should create a scheme that will hold the disturbance resulting from the measurement in the observable that we are not interested in without communicating it to the quantity that we measure. In this case, repeated measurements can be performed with any desired accuracy.

This approach can be implemented in a photon-number measurement scheme within a Kerr nonlinear medium, where entanglement of the probe and signal fields via cross-phase modulation induces a phase shift in the probe wave that carries information about the photon count in the signal channel [2]. This shift can be detected using interferometric techniques, providing us with information about the number of photons in signal mode without destruction of the signal.

A promising platform for such measurements is whispering gallery mode microresonator, which exhibits low optical losses and small effective volume of the e.m. field localization, enabling efficient exploitation of nonlinear effects [3]. However, there are two primary factors that limit the sensitivity of this scheme: optical losses (including detectors inefficiencies) and phase fluctuations in the probe field caused by self-phase modulation (SPM) [4].

To reduce the effect of external losses on the sensitivity of the scheme, we will use the method proposed by Caves in [5]. We will add an additional degenerate optical parametric amplifier (DOPA) to our scheme before detecting quadrature, which will amplify (anti-squeeze) our signal. Another improvement in sensitivity can be achieved by applying squeezed states of probe light at the input of the scheme. However, these methods do not fully eliminate the influence of SPM, which sets the lower limit of the measurement [6].

An alternative approach involves generating squeezed states of light directly within the nonlinear resonator. In this work, we demonstrate that the utilization of intracavity squeezing in a quantum nondemolition measurement scheme completely cancels the

self-phase modulation effect. We analyze the impact of input, internal and output losses, accounting for mode bandwidths, and provide estimates of the achievable sensitivity. Our results indicate that increasing the probe beam power enables one to approach single-photon-level sensitivity under realistic system parameters. Estimates show that generation and verification of bright non-Gaussian quantum states with mean photon numbers up to 10^3 is feasible [7].

The work was supported by the Russian Science Foundation (project 25-12-00263)

References

1. V. B. Braginsky, Y. I. Vorontsov, F. Ya. Khalili, Sov. Phys. JETP **46**, 705 (1977).
2. G. J. Milburn and D. F. Walls, Phys. Rev. A **28**, 2065 (1983).
3. D. V. Strekalov *et al.*, Journal of Optics **18**, 123002 (2016).
4. S. N. Balybin *et al.*, Phys. Rev. A **106**, 013720 (2022).
5. C. M. Caves, Phys. Rev. D **23**, 1693 (1981).
6. S. N. Balybin, D. I. Salykina and F. Ya. Khalili, Phys. Rev. A **108**, 053708 (2023).
7. D. I. Salykina, S. N. Balybin and F. Ya. Khalili, Phys. Rev. A **111**, 013715 (2025).

Worldline instanton approach to Schwinger-like particle production

P. Satunin[1]

[1] Institute for Nuclear Research of RAS

petr.satunin@gmail.com

We apply the semiclassical method of Worldline Instanons [1] to the non-perturbative calculation for the Schwinger-like processes assisted by an external neutral particle: the photon decay to an electron-positron pair in a constant external electric or magnetic field [2], neutrino decay to W-boson and electron in a constant magnetic field [3]. Further, we consider the cross-section for the Breit-Wheeler process (two photon scattering to electron-positron pair) in a constant external electric or magnetic field below the perturbative threshold with Worldline instantons [4]. The latter process is generalized to so-called Double assisted Schwinger: the Schwinger pair production assisted by both a high energy photon and an intermediate plane wave which is considered by a many-photon state. It is shown that the probability is significantly enhanced compared with the standard Schwinger process.

References

1. I. Affleck, O. Alvarez, N. Manton. Nucl. Phys. B, **197**, 509 (1982).

2. P. Satunin. Phys. Rev. D, **87** 105015, (2013)

3. P. Satunin. JETP Lett., **101** 657, (2015).

4. P. Satunin. EPJ Web Conf. **191** 02019 (2018)

Precise modeling of structural parameters for crystals with compound-tunable embedding potential method

V.M. Shakhova[1], A.A. Lutchenko[1,2], Y.V. Lomachuk[1], D.A. Maltsev[1], A.V. Titov[1,2]

[1] Petersburg Nuclear Physics Institute named by B.P.Konstantinov of NRC «Kurchatov Institute»

[2]St Petersburg University

shakhova_vm@pnpi.nrcki.ru

Theoretical studies of crystals containing lanthanides are typically limited by current capabilities of modern quantum chemical methods for describing periodic structures: density functional theory, scalar-relativistic versions of “soft” (projected augment wave) pseudopotentials and atomic basis sets of moderate size. Precise theoretical study of such structures could become a powerful tool that allows one to solve many new fundamental and practical problems.

In this research, the electronic structures of ytterbium halide crystals and lanthanide orthophosphates are studied. For investigating such structures the combined method is applied. It contains "compound-tunable pseudopotentials" (CTPP) and "compound-tunable embedding potentials" (CTEP) [1-4].

The investigation of a crystal by the CTEP method is carried out in three stages. First, a perfect crystal with periodic boundary conditions is calculated by the CRYSTAL code. Second, short-range large-core CTPP is built for the chosen crystal by using the CRYSTAL code as well. Third, cluster calculations of the crystal fragment are performed, and the long-range Coulomb potential of the environment is constructed as a part of CTEP. A crystal fragment of a "required minimal size” (minimal cluster include a heavy atom and its immediate environment) is cut out, within which the electron density must be reproduced with high accuracy. The atoms of the near environment of the crystal fragment are described by point charges and CTPPs ("pseudoatoms" below) to take into account the influence on a chosen fragment of the "whole crystal" excluding the atoms of the fragment. It is important to note that the relaxation of the crystal fragment environment is considered as negligible by appropriate choosing the fragment, and the whole system is generally electroneutral taking into account the charged pseudoatoms of the near environment.

The crystal fragment built by the CTEP method using CTPP reproduces the electron density from periodic calculations in the vicinity of the central atom with the error less than 0.25%. In the framework of periodic calculations, the use of precise small-core PP and saturated basis sets is practically impossible. Consequently, the accuracy of such calculations is at best at the level of 0.1 eV for the energetic characteristics, which is insufficient for precise study of materials with f- and heavy

d-elements. In turn, such a problem does not arise in cluster CTEP calculations, since both good basis sets and PPs are used, and the calculation errors associated with them are drastically reduced. Thus, knowing the correct electron density from cluster calculations, it is possible to build a "new" CTPP which could be used in crystal calculations to obtaine more accurate data to build advanced version of CTEP.

References

1. Lomachuk Y. V., Maltsev D. A., Mosyagin N. S., Skripnikov L. V., Bogdanov R. V. and Titov A. V., Phys. Chem. Chem. Phys., 22:17922-17931, (2020).

2. Maltsev D. A., Lomachuk Y. V., Shakhova V. M., Mosyagin N. S., Skripnikov L. V. and Titov A. V., Phys. Rev. B., 103:205105, (2021).

3. Shakhova V. M., Maltsev D. A., Lomachuk Y. V., Mosyagin N. S., Skripnikov L. V. and Titov A. V, Phys. Chem. Chem. Phys., 24:19333-19345, (2022).

4. Maltsev D. A., Lomachuk Y. V., Shakhova V. M., Mosyagin N. S., Kozina, D. and Titov A. V, Sci. Rep., 15:10645, (2025).

Absorption of a twisted photon by an electron in strong magnetic field

A.A. Shchepkin*, D.V. Grosman, I.I. Shkarupa, D.V. Karlovets

School of Physics and Engineering, ITMO University, 197101, St. Petersburg, Russia

a.shchepkin@metalab.ifmo.ru

The work investigates absorption of a twisted photon, which possesses quantized total angular momentum (TAM), by a relativistic electron in a strong magnetic field up to the Schwinger limit, $H_c = 4.4 \cdot 10^{13}$ G. The absorption cross sections and their dependence on the parameters of the incident photon and the initial Landau electron are examined.

It is found that total absorption cross sections decrease as angular momentum of the incident photon increases and increase as angular momentum of the initial electron grows, as seen in upper row of Fig. 1. The process is also compared across different magnetic field strengths, and the contribution of various electron spin transitions to total absorption cross section is analyzed. It is also found that the processes without an electron spin flip dominate and, on top of that, an asymmetry in the "spin-down" $\rightarrow$ "spin-up" and the "spin-up" $\rightarrow$ "spin-down" transitions is observed (lower row of Fig. 1). Specifically, the cross sections for the "spin-down" $\rightarrow$ "spin-up" transition are larger, which can be interpreted as an analogy of the Sokolov-Ternov effect present for photon emission [1, 2]. Our findings can help improve the understanding of the QED processes in critical fields, typical for astrophysical environments such as neutron stars.

The work was carried out with the support of the Russian Science Foundation (Grant No. 23-62-10026) and the Foundation for the Advancement of Theoretical Physics and Mathematics "BASIS".

References

1. A. Sokolov and I. Ternov, Relativistic electron, "Nauka", Moscow (1974);

2. I. Pavlov and D. Karlovets, Phys. Rev. D, **109**, 036017 (2024).

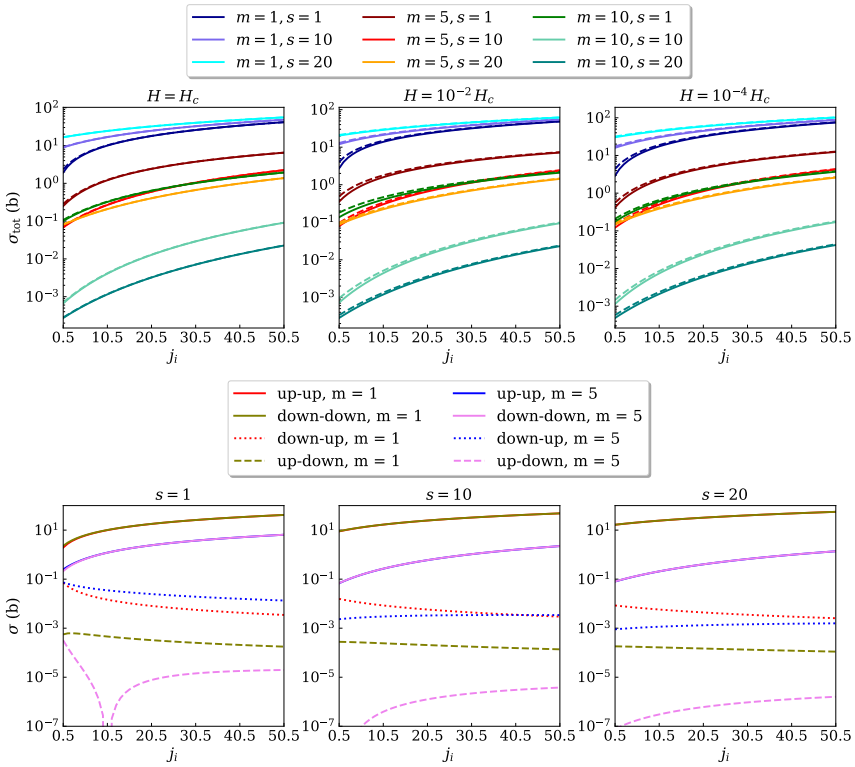

Figure 1: Upper row: total cross sections of the twisted photon absorption as function of the total angular momentum of initial electron, j_i, for different total angular momenta of the photon, m and different radial quantum numbers of the initial electron, s. Lower row: absorption cross sections for different spin states (up and down, relative to the magnetic field) of initial and final electron

A study of the nuclear charge radius of ^{26m}Al for testing CKM matrix unitarity

L.V. Skripnikov[1,2] and S.D. Prosnyak[1]

[1]Petersburg Nuclear Physics Institute named by B.P. Konstantinov of National Research Center "Kurchatov Institute" (NRC "Kurchatov Institute" – PNPI), 1 Orlova roscha, Gatchina, 188300 Leningrad region, Russia

[2]Saint Petersburg State University, 7/9 Universitetskaya nab., St. Petersburg, 199034, Russia

[1]skripnikov_lv@pnpi.nrcki.ru

Accurate determination of nuclear charge radii serves as a sensitive test of various aspects of nuclear structure and provides an important benchmark for the development of nuclear models [1]. Precise charge radius measurements can also constrain the parameters of the nuclear matter equation of state. The knowledge of nuclear charge radii for certain isotopes is crucial for testing fundamental particle physics models. The Cabibbo-Kobayashi-Maskawa (CKM) matrix plays a central role in describing quark-flavour mixing via the weak interaction within the Standard Model (SM). According to the SM, the CKM matrix must be unitary, but this property requires experimental verification. Any deviation from unitarity could signal new physics beyond the SM. Significant efforts are underway to test this unitarity [2]. The deviation from unitarity in the top row of the CKM matrix can be quantified by the parameter $\Delta_{\mathrm{CKM}} = 1 - (|V_{ud}|^2 + |V_{us}|^2 + |V_{ub}|^2)$, which should be zero if the matrix is unitary. The largest V_{ud} element can be extracted from a global analysis of superallowed $0^+ \to 0^+$ nuclear β decays of certain isotopes [2]. Among these, the superallowed β decay of the isomer ^{26m}Al is of particular importance, as it exhibits the smallest nuclear-structure-dependent corrections [2]. Several corrections must be calculated to relate the experimentally measured ft value (which characterizes the superallowed β decay) to the V_{ud}. One of these corrections is the isospin-symmetry-breaking term, which depends on the nuclear mean-square (ms) charge radius. This radius can be extracted from isotope shift (IS) measurements, which in turn require accurate knowledge of atomic parameters known as the field and mass shifts—a challenge for modern many-body atomic theory.

A method for calculating the field shift contribution to isotope shifts in many-electron atoms, including quantum electrodynamics (QED) effects, has been introduced [3]. We also implement a model QED approach to incorporate QED corrections to the nuclear recoil effect proposed in Ref. [4]. The developed computational scheme utilizes advanced methods such as coupled cluster with single, double, triple and perturbative quadruple excitations, CCSDT(Q), to accurately account for electron correlation effects beyond the 6 order of perturbation theory. For the first time for

a many-electron atom, achieved theoretical uncertainty required consideration of the QED effects.

By combining our calculated atomic factors with the recently measured isotope shift of the $3s^2 3p\ ^2P_{3/2} \to 3s^2 4s\ ^2S_{1/2}$ transition in Al, we obtain a difference in ms charge radii between ^{27}Al and ^{26m}Al of 0.443(44)(19) fm^2, where the first and second uncertainties are experimental and theoretical, respectively. The theoretical uncertainty has been reduced by a factor of four compared to previous works. Using this result and the known charge radius of ^{27}Al, we derive $R_c(^{26m}\mathrm{Al}) = 3.132(10)$ fm. With the improved accuracy of the calculated IS factors, the uncertainty in $R_c(^{26m}\mathrm{Al})$ is now dominated by experimental error. We also revise charge radii of ^{28}Al, ^{29}Al, ^{30}Al, ^{31}Al, and ^{32}Al using existing IS data. Additionally, we compute atomic factors for the $3s^2 3p\ ^2P_{3/2} \to 3s^2 4s\ ^2S_{1/2}$, $3s^2 3p\ ^2P_{1/2} \to 3s^2 5s\ ^2S_{1/2}$, and $3s^2 3p\ ^2P_{3/2} \to 3s^2 5s\ ^2S_{1/2}$ transitions in Al, which can be used in future experiments. The improved rms charge radius of ^{26m}Al directly affects the evaluation of the V_{ud} element of the CKM matrix and, consequently, has important implications for testing the unitarity of the CKM matrix.

Electronic structure calculations were supported by the Russian Science Foundation (Grant No. 24-12-00092 (https://rscf.ru/en/project/24-12-00092/). Analysis of results were supported by the Foundation for the Advancement of Theoretical Physics and Mathematics BASIS (Project No. 24-1-1-36-1).

References

1. X. F. Yang, S. J. Wang, S. G. Wilkins, and R. F. Garcia Ruiz, Prog. Part. Nucl. Phys. **125**, 104005 (2022).

2. J. C. Hardy and I. S. Towner, Phys. Rev. C **102**, 045501 (2020).

3. L. V. Skripnikov, S. D. Prosnyak, A. V. Malyshev et al., Phys. Rev. A **110**, 012807 (2024).

4. M. Anisimova, D. A. Glazov, A. V. Volotka, V. M. Shabaev, and G. Plunien, Phys. Rev. A **106**, 062823 (2022).

Light quasi-molecular compounds comprising the antiproton

D. Solovyev[1,2], A. Anikin[2,3], A. Danilon[1], A. Kotov[1], D. Glazov[4,2]

[1] The Faculty of Physics, St. Petersburg State University

[2] PNPI named by B.P.Konstantinov of NRC "Kurchatov Institute"

[3] The D.I. Mendeleev All-Russian Institute for Metrology (VNIIM)

[4] Faculty of Physics, ITMO University)

d.solovyev@gmail.com

Our ongoing research focuses on lightweight dinuclear quasi-molecular compounds. In the framework of the fully relativistic approach the Dirac equation with two-center potential is solved [1, 2]:

$$\hat{H}_{\rm D} = \boldsymbol{\alpha}\cdot\mathbf{p} + V(Z_1, Z_2, \boldsymbol{r}) + \beta,$$
$$V(Z_1, Z_2, \boldsymbol{r}) = V_{\rm nucl}(Z_1, |\boldsymbol{r} - \boldsymbol{R}_1|) + V_{\rm nucl}(Z_2, |\boldsymbol{r} - \boldsymbol{R}_2|)$$

The coordinate system used is schematically depicted in Fig. 1.

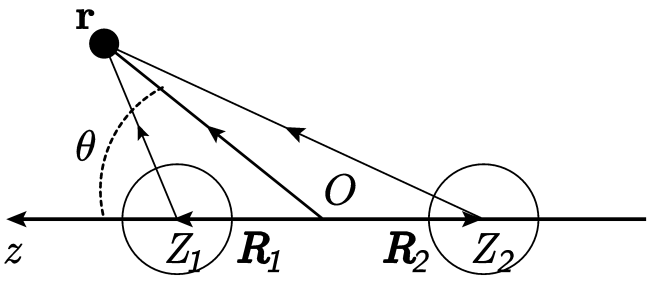

Figure 1: The coordinate system for diatomic one-electron system oriented along the z-axis. The bound electron is marked with a filled circle, the nuclei are marked with circles with the nucleus charges Z_1 and Z_2. The corresponding position vectors from the coordinate origin O are indicated as $\boldsymbol{r}$, $\boldsymbol{R}_1$ and $\boldsymbol{R}_2$. Since axial symmetry, the azimuth angle θ is introduced.

The numerical calculation is performed by the B-splines method with the dual kinetic balance condition generalized to the case of axial symmetry - the A-DKB method. As results, the electronic spectra of one-electron compounds are obtained, relativistic effects as well as the effect of finite size of nuclei are discussed [3, 3, 4, 5, 6]. In the framework of the considered problems, the influence of an external magnetic

field is also studied. A separate interesting direction is the detailed description of the interaction of one-electron atoms (ions) with the antiproton. The critical distance (Fermi-Teller radius) at which electronic autoionization occurs is discussed. The phenomenon is considered both in zero and various laboratory magnetic fields. A comparative analysis with data from modern scientific literature is presented for all the results obtained.

References

1. A.A. Kotov, D.A. Glazov, A.V. Malyshev, A.V. Vladimirova, V.M. Shabaev, G. Plunien, X-Ray Spectrometry **49**, 110 (2020)

2. A.A. Kotov, D.A. Glazov, V.M. Shabaev, G. Plunien, Atoms **9**, 44 (2021)

3. A. Anikin, A. Danilov, D. Glazov, A. Kotov, D. Solovyev, J. Chem. Phys. **159**, 214304 (2023).

4. A.A. Danilov, A.A. Anikin, D.A. Glazov, E.Y. Korzinin, A.A. Kotov, D.A. Solovyev, Opt. Spectr. **131**(11), 1477 (2023).

5. D. Solovyev, A. Anikin, A. Danilov, D. Glazov, A. Kotov, Phys. Scr. **99**, 045401 (2024).

6. A. Anikin, A. Danilov, D. Glazov, A. Kotov, D. Solovyev, Mol. Phys. e2435466 (2024).

Sequential and correlated double tunnel ionization in ultrashort electromagnetic pulses

D. Tyurin[1], S. Popruzhenko[1,2], V. Strelkov[3]

[1]National Research Nuclear University MEPhI

[2]Prokhorov General Physics Institute RAS

[3]Lebedev Physics Institute RAS

[1]Denisturin1999@yandex.ru

Ionization of atomic systems by intense laser fields is the key phenomenon of contemporary nonlinear optics. The most common theoretical approach to description of multiple tunnel ionization is based on the single-active electron (SAE) approximation in which the ionization of several electrons proceeds sequentially and independently. Howewer, the electron-electron interaction can significantly affect the ionization dynamics leading to effects not treatable within the SAE approximation. One of the ionization mechanisms caused by electron-electron correlations is the rescattering of an electron on its parent ion. This ionization channel is studied in detail theoretically and examined experimentally [1]. In this contribution, we investigate alternative pathways of correlated multiple ionization.

We examine the ionization dynamics of a two-electron atomic system in the field of an unipolar electromagnetic pulse in which the rescattering channel is entirely eliminated. This makes possible to investigate other nonsequential mechanisms. By solving numerically the time-dependent Schödinger equation for a two-electron system modeling the negative bromine ion in one and two dimensions, we demonstrate that the effect of electron-electron correlations on the probability of double ionization strongly depends on the pulse duration. For electromagnetic pulses with duration of several tens of femtoseconds, the SAE approximation describes the ionization dynamics with accuracy of the order of a per cent. In contrast, for extremely short (~ 1 fs) pulses the electron-electron interaction suppresses the rate of ionization by approximately one order of magnitude, compared to the SAE approximation.

Besides, we envisage the collective tunneling ionization channel theoretically discussed in [2, 3, 4, 5]. This channel of double tunnel ionization has not been observed in experiment so far. Numerical solution of the time-dependent Schrödinger equation demonstrates weak but clear signatures of the collective tunneling in the photoelectron density distribution. Our results show that the electron-electron repulsion noticeably suppresses the collective ionization channel, compared to analytic theoretical predictions based on the complete discard of this interaction. Yet however, this exotic channel appears theoretically detectable.

References

1. W. Becker *et al.*, Reviews of Modern Physics. **84**, 3, 1011 (2012).
2. B. A. Zon, JETP **89**, 219-222 (1999).
3. U. Eichmann, M. Dörr, H. Maeda *et al.*, Phys. Rev. Lett. **84**, 3550 (2000).
4. S. V. Popruzhenko, T. A. Lomonosova, JETP Lett. **113**, 5, 317-321 (2021).
5. S. V. Popruzhenko, D. I. Tyurin, Bull. Lebedev Phys. Inst. **50**, 8, S922-S927 (2023).

Two-photon states in planar atomic lattices

I.A. Volkov[1], D.F. Kornovan[1], A.S. Sheremet[1], R.S. Savelev[1], M.I. Petrov[1]

[1] School of Physics and Engineering, ITMO University, St. Petersburg 197101, Russia

ilya.volkov@metalab.ifmo.ru

In this work we consider two-photon states in infinite quadratic lattice of similar two-level atoms with out-of-plane polarization of dipolar transition. To obtain dispersion, we apply quasi-infinite lattice method, in which center of mass of two photons can propagate in infinite lattice with a wavevector $\mathbf{K}$ with no restrictions, but the relative distance between these photons is restricted to some number of lattice periods N_Δ.

We demonstrate different kinds of subradiant two-photon states, consisting of single photon states similar to bound states in continuum (BIC) and band edge (BE) states. At the same time we explore localized and quasi-localized two-photon states with continuous distributions in $\mathbf{k}$-space. Similar variety of states was previously obtained for 1D system of atoms interacting via guided mode [1].

Some results about these states are presented in Figure 1. On (a) we show dispersion dispersion dependence on $\mathbf{K}$ in $K_x = K_y$ direction. Scattered states consisted of two single photon states form 3 continuous zones, which were calculated by outer summation of analytical dispersions [2]. Localized states for which average distance between excitations, or localization length (LL) doesn't depend on N_Δ, are laying inside the bandgaps, see (b)-(d). Moreover, the hybrid localized state (e) s_h with a radiative lifetime 3 orders larger than $1/\Gamma_0$, where Γ_0 is a single atom decay rate.

References

1. Poshakinskiy, A.V. et al. Quantum Hall phases emerging from atom–photon interactions. npj Quantum Inf 7, 34 (2021).

2. Volkov, I. et al. Strongly subradiant states in planar atomic arrays. Nanophotonics, 13(3), 289-298 (2024).

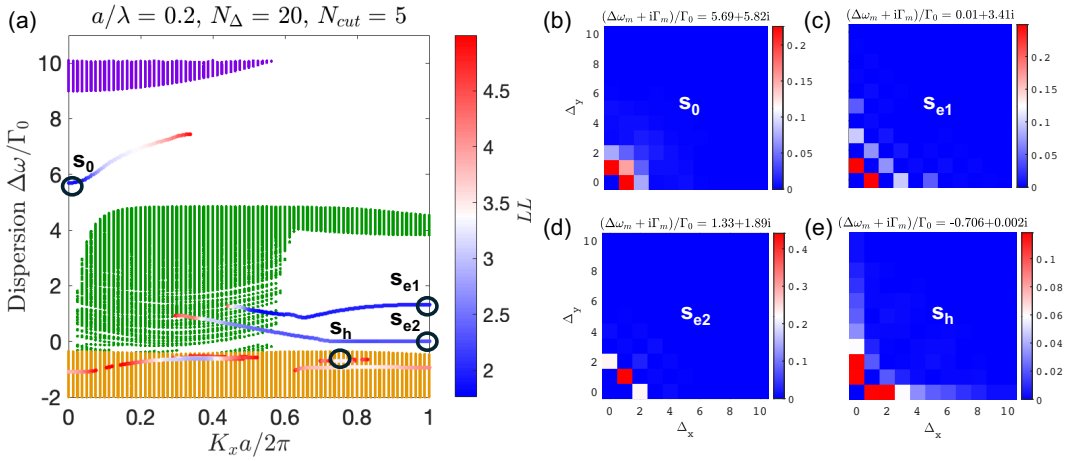

Figure 1: Variety of two-photon states in square atomic lattice with period $a = 0.2\lambda$. Maximal distance between excitations is restricted to $N_\Delta = 20$. (a) Dispersion dependence of collective frequency shift $\Delta\omega/\Gamma_0$ on center of mass wavevector $\mathbf{K}$ in $K_x = K_y$ direction. Three continuous zones, painted purple, green and yellow correspond to scattered states. Dispersions of localized or quasi-localized hybrid states are depicted by lines, with a color dependent on localization length (LL) in units of a. $|\psi|^2$ profiles of localized or hybrid states are shown on (b)-(e). Radiative decay rates and collective frequency shifts are specified above the profiles.

Quantum algorithm for PDE using system dynamics

I. Zacharov, B. Arseniev, D. Guskov

Skolkovo Institute of Science and Technology
I.Zacharov@skoltech.ru

Quantum computers represent an innovative technology with the potential to surpass classical computers in specific algorithmic classes, notably in solving partial differential equations (PDE). For particular types of PDEs, applying order-reducing transformations followed by spatial differential discretization enables the derivation of a system Hamiltonian. The evolution of this Hamiltonian within Hilbert space yields quantum states that reflect the solutions to the original PDE.

Our research centers around expressing the Hamiltonian using Pauli basis, since these quantum gates are specifically suitable for straightforward execution on quantum computers. We have developed an algorithm for this decomposition that possesses characteristics allowing to handle varying parameters in PDEs, thereby broadening the range of PDEs that can benefit from this method. Additionally, our method leads to the intuitive classification of commuting collections of quantum gates, which facilitates further optimizations like simultaneous diagonalization.

Although the methodology is developed for one-dimensional PDEs, it can be directly extended to higher dimensions, where the quantum algorithm demonstrates an advantage by circumventing the "curse of dimensionality." Classical algorithms scale as $O(N^D)$, whereas the quantum algorithm scales as $O(N \cdot D)$. This disparity in scaling is a key factor fueling our expectation of achieving a quantum advantage in real-world applications.

Time evolution of the multi-dimensional system Hamiltonian employs Pauli string-based Trotterization, which updates each coordinate axis alternately at every Trotter step, thereby achieving reduced gate depth by splitting operators based on dimensions. Numerical trials performed on a specific example of the Wave equation exhibit a significant quantum advantage with the utilization of more than four qubits per axis. This advantage arises from both the expo nential compression of memory and polynomial scaling of gates, in contrast to traditional grid-based methods on classical computing platforms.

Hexatomic $RaOCH_3$ molecule as a platform for studying interactions with the Dark matter halo

P.D. Zakharova[1,2]

[1]St. Petersburg State University, St. Petersburg, Russia

[2]Petersburg Nuclear Physics Institute named by B.P.Konstantinov of NRC «Kurchatov Institute»

zakharova.annet@gmail.com

In this work, we study the interaction of the electron shell of a hexatomic "symmetric top" molecule with the Dark Matter halo under the assumption that it is formed by a condensate of a pseudoscalar axion field. In the linear order, the contribution of the corresponding interaction vanishes for non-chiral molecules in equilibrium configurations, so chiral molecules were previously considered for its search. In this paper, we point out the possibility of this interaction for non-chiral "symmetric top" molecules through transitions between excited rovibrational states, and consider it using the example of the RaOCH3 molecule. For this molecule, the effect is strongly suppressed, but the mechanism considered can lead to the observed effects in other molecules of this type.

The work was supported by the Russian Science Foundation (grant No. 24-72-10060).

The International Summer Conference on Theoretical Physics 2025
Faculty of Physics of ITMO University
Abrikosov Center for Theoretical Physics

Exploring the Properties of Light Diatomic Molecules in Strong Magnetic Fields

T. Zalialiutdinov [1, 2] and D. Solovyev [1, 2]

[1]Department of Physics, St. Petersburg State University, Petrodvorets, Oulianovskaya 1, 198504, St. Petersburg, Russia

[2]Petersburg Nuclear Physics Institute named by B.P. Konstantinov of National Research Centre 'Kurchatov Institut', St. Petersburg, Gatchina 188300, Russia

t.zalialiutdinov@spbu.ru

Abstract

In this study, we develop and implement a specialized coupled-cluster (CC) approach tailored for accurately describing atoms and molecules in finite magnetic fields. Using the open-source Ghent Quantum Chemistry Package (`GQCP`) in conjunction with the Python-based Simulations of Chemistry Framework (`PySCF`), we compute potential energy curves, as well as permanent and transition dipole moments and vibrational spectra, for the diatomic molecules HeH^+, LiH, and H_2 under various magnetic field strengths, adopting a fully non-perturbative treatment. The main computational difficulties stem from the inclusion of the magnetic field in the Hamiltonian, in particular the presence of the angular momentum operator, which leads to a complication of the wave function and introduces a gauge-origin dependence. Addressing these challenges requires advanced modifications to existing routines, which we achieve by implementing gauge-including atomic orbitals (GIAOs) with the use of `GQCP`, and the capabilities offered by `PySCF`. This approach enhances the accuracy and reliability of the CC theory, opening pathways for more comprehensive investigations in molecular quantum chemistry at finite magnetic fields.

Introduction

The study of atoms and molecules subjected to strong magnetic fields has garnered substantial interest in recent years [1, 2, 3]. Although magnetic fields of 1000 Tesla and above B_0, where one atomic unit, B_0, corresponds to 2.35×10^5 Tesla, cannot be generated or directly investigated on Earth, such extreme conditions are naturally present in the atmospheres of magnetized white dwarf stars. Observations of helium [4], hydrogen molecules [5], and more recently heavier elements [6] in these astrophysical environments underscore the critical importance of exploring the behavior of atoms and molecules under intense magnetic fields. This line of research is essential for

advancing our understanding of fundamental physical and chemical processes and also plays a pivotal role in astrophysics. In particular, it assists in the interpretation of the observational spectra of magnetic white dwarfs and neutron stars, thereby facilitating the determination of their magnetic field strengths.

The strongest sustained magnetic fields generated in terrestrial laboratories are on the order of 10 Tesla implying that it can typically be treated as a perturbation. However, this assumption breaks down as the field strength approaches B_0, where the underlying physics becomes more complex. In such a case, the magnetic forces become comparable in magnitude to the Coulomb forces, necessitating a non-perturbative treatment [7]. Furthermore, this phenomenon gives rise to a new type of chemical bond known as a paramagnetic perpendicular bond [8]. The investigation of atoms and molecules under such conditions is fraught with considerable difficulties, arising primarily from the limitations inherent in the existing experimental methods and the complex nature of the quantum systems under study. The necessity for reliable theoretical models and precise quantum-chemical calculations is particularly pronounced in this context, owing to the complex behavior of electron correlation within these extreme environments.

During the past decade, the Full Configuration Interaction (FCI) and Coupled Cluster (CC) methods have emerged as the prevalent approaches for such studies, as evidenced by several groundbreaking works in the field [7]. However, the computational demands of FCI are extraordinarily high, rendering it feasible only for very small systems with a limited number of electrons. This substantial computational cost is attributed to the requirement to consider all possible electron configurations, resulting in an exponential increase in complexity with the size of the system.

Given these constraints, there is a pressing need to develop and refine quantum-chemical methods capable of handling larger and more complex systems with a similar level of accuracy. Advancements in this area would not only facilitate the study of larger molecules and systems with more electrons but could also lead to the discovery of new phenomena or provide deeper insights into the behavior of matter under strong magnetic fields. Recently, significant progress has been made in realizing non-perturbative magnetic field effects within coupled-cluster (CC) methods. In particular, several specialized software packages have been advanced, including `ChronusQ` (Chronus Quantum), `HelFEM` (Helsinki Finite Element Suite for Atoms and Diatomic Molecules), `BAGEL` (Brilliantly Advanced General Electronic-structure Library), `QCumbre` (Quantum Chemical Utility Enabling Magnetic-Field Dependent Investigations Benefitting from Rigorous Electron-Correlation Treatment), and the `LONDON` code.

Among these software packages, `QCumbre` and `LONDON` are notable for their ability to incorporate electron correlation effects through the application of the coupled-cluster approach. Additionally, `BAGEL` offers capabilities for relativistic calculations within the framework of the full configuration interaction (FCI) method. However, this latter capability comes at the cost of significant restrictions on the size of the systems that can be considered, owing to the substantial computational demands required.

In this study, we present our computational implementation for calculating binding energies and electronic structure properties of HeH^+, LiH, and H_2 molecules exposed to strong magnetic fields. The approach utilizes complex coupled-cluster methods and is built on the open-source libraries available through The Ghent Quantum Chemistry Package (GQCP) and the Python-based Simulations of Chemistry Framework.

Acknowledgements

The work of T.Z. was supported by the Foundation for the Advancement of Theoretical Physics and Mathematics "BASIS" (grant No. 23-1-3-31-1).

References

1. Turbiner, A. V., del Valle, J. C., and Ruiz, A. M. Escobar. "Two-body neutral Coulomb system in a magnetic field at rest: From hydrogen atom to positronium." Physical Review A **103**, 032820 (2021).

2. Pemberton, M. J., Irons, T. J. P., Helgaker, T., et al. "Revealing the exotic structure of molecules in strong magnetic fields." The Journal of Chemical Physics **156**, 20 (2022).

3. Lai, D. "Matter in strong magnetic fields." Reviews of Modern Physics **73**, 629-662 (2001).

4. Jordan, S., Schmelcher, P., and Becken, W. "Stationary components of He I in strong magnetic fields - a tool to identify magnetic DB white dwarfs." Astronomy and Astrophysics **376**, 614-620 (2001).

5. Bignami, G. F., Caraveo, P. A., De Luca, A., et al. "The magnetic field of an isolated neutron star from X-ray cyclotron absorption lines." Nature **423**, 725-727 (2003).

6. Hollands, M. A., Stopkowicz, S., Kitsaras, M-P., et al. "A DZ white dwarf with a 30 MG magnetic field." Monthly Notices of the Royal Astronomical Society **520**, 3560-3575 (2023).

7. Stopkowicz, S., Gauss, J., Lange, K. K., et al. "Coupled-cluster theory for atoms and molecules in strong magnetic fields." The Journal of Chemical Physics **143**, 7 (2015).

8. Lange, K. K., Tellgren, E. I., Hoffmann, M. R., and Helgaker, T. "A Paramagnetic Bonding Mechanism for Diatomics in Strong Magnetic Fields." Science **337**, 327-331 (2012).

Poster talks

G factor of few-electron ions: a search for new physics

R. Abdullin[1,2], D. Glazov[1,2], A. Moshkin[1], A. Volotka[1]

[1] Department of Physics and Engineering, ITMO University, St. Petersburg 197101, Russia

[2] Petersburg Nuclear Physics Institute of NRC "Kurchatov Institute", Gatchina, Leningrad District 188300, Russia

rinat.abdullin@metalab.ifmo.ru

In the framework of addressing the strong CP problem in quantum chromodynamics (QCD), an additional global U(1) Peccei-Quinn (PQ) symmetry is introduced [1, 2]. The spontaneous breaking of this symmetry results in the emergence of a pseudoscalar pseudo-Nambu–Goldstone boson, known as the axion [3, 4]. Thus, axions arise naturally and contribute to the elimination of CP violation in strong interactions. Extensions of the Standard Model predict the emergence of new particles [5]. For example, additional U(1) symmetries can lead to the appearance of a dark photon—a massive vector particle that emerges as a result of extending the gauge group and is capable of mediating hidden interactions in the dark sector. The dark matter problem remains one of the key issues in modern physics, and the study of axions and dark photons opens new perspectives for a deep understanding of the fundamental mechanisms of symmetry breaking and for reconciling cosmological observations with experimental data [6].

In spite of the significant successes of the Standard Model, its incompleteness stimulates the search for extensions in which the measurement of the bound electron g factor plays a key role in verifying theoretical predictions. In recent years, research on highly charged ions (HCIs) has advanced considerably in both experimental and theoretical fields [7, 8]. One of the key factors ensuring high-precision calculations is the strong electrostatic field of the nucleus, which significantly enhances relativistic and quantum electrodynamical effects. Moreover, the electronic structure of HCIs remains relatively simple compared to that of neutral atoms, allowing for high-precision computations. Modern experimental techniques enable the measurement of the HCI g factor with outstanding relative accuracy [9, 10, 11, 12]. The comparison of these data with theoretical predictions opens up opportunities for detecting deviations that may indicate new physics [13, 14]. Even the slightest discrepancies between theory and experiment could signal the existence of previously unknown interactions beyond the Standard Model, making such studies extremely promising.

In this work, we investigate the interaction of bound electrons, mediated by new physics models (such as axions, dark photons, and others), on the g factor of few-electron ions. The study is devoted to assessing the contribution of these effects that emerge from the exchange of virtual axions or dark photons between electrons. This approach opens up the possibility of establishing stringent constraints on the

parameters of the considered models. In this work, we also examine systems and configurations in which corrections associated with new physics are enhanced.

References

1. R.D. Peccei and H.R. Quinn, Phys. Rev. Lett. **38**, 1440 (1977).
2. R.D. Peccei and H.R. Quinn, Phys. Rev. D **16**, 1791 (1977).
3. S. Weinberg, Phys. Rev. Lett. **40**, 223 (1978).
4. F. Wilczek, Phys. Rev. Lett. **40**, 279 (1978).
5. P. Fadeev et al., Phys. Rev. A **99**, 022113 (2019).
6. D. Marsh, Phys. Rep. **643**, 1–79 (2016).
7. K. Blaum et al., Quantum Sci. Technol. **6**, 014002 (2021).
8. D. Glazov et al., Atoms **11**, 119 (2023).
9. S. Sturm et al., Nature **506**, 467–470 (2014).
10. P. Micke et al., Nature **578**, 60–65 (2020).
11. T. Sailer et al., Nature **606**, 479–483 (2022).
12. J. Morgner et al., Nature **622**, 53–57 (2023).
13. V. Debierre et al., Phys. Lett. B **807**, 135527 (2020).
14. V. Debierre et al., Phys. Rev. A **106**, 062801 (2022).

The International Summer Conference on Theoretical Physics 2025
Faculty of Physics of ITMO University
Abrikosov Center for Theoretical Physics

Interelectronic interaction effects in the quadratic Zeeman splitting

V. A. Agababaev[1]

[1]ITMO University, Kronverksky pr. 49, 197101 St. Petersburg, Russia

[1]v.agababaev@yandex.ru

Abstract

We present calculation of the two-photon exchange correction to the quadratic Zeeman effect for the ground $2p_{1/2}$ and first excited $2p_{3/2}$ states in highly charged boronlike ions in the Breit approximation.

Key words: highly charged ions, bound-state quantum electrodynamics, relativistic atomic theory, Zeeman effect

Over the last quarter century, significant progress has been made in the field of high-precision measurements of the Zeeman splitting of highly charged ions. The most recent ion in which the g factor has been measured is and boron-like tin [1]. The corresponding leap in measurement precition, together with theoretical research, made it possible to determine the most accurate up to date electron mass determination [2]. It is expected that in the near future high-precision measurements of the g-factor in hydrogen-, lithium- and boronlike ions will provide a high-precision tool for independent determination of the fine structure constant α (see e.g.[3]).

The ALPHATRAP project is aimed at the g-factor measurements in the ground state for wide range of highly charged ions including boronlike ones.In the framework of this project the g factor of the ground and first excited states in boronlike argon $^{40}Ar^{13+}$ was measured [4, 5]. Quantum logic methods have made it possible to significantly improve the accuracy of g factor measurement [6]. The ARTEMIS experiment to measure the Zeeman splitting in middle-Z boronlike ions is also carried out [7]. In particular, the first of the investigated ions was also boronlike argon $^{40}Ar^{13+}$.

The studies of the quadratic Zeeman has a history of more than 80 years. Close attention of the scientific society have been attracted by the magnetars and other objects with high and extra-high (up to 10^{11} T) magnetic induction where the quadratic effect becomes principal [8]. A numerous studies of the quadratic effect have also been undertaken in molecules, atoms, solid state, Bose-Einstein condensates and exotic systems such as positronium (see e.g. [9]). The quadratic Zeeman effect is also a subject of intense study in connection with studying atomic clocks (see e.g. [10].

The theoretical treatment of the quadratic Zeeman effect in boronlike argon has recently been performed in our work [11, 12, 13]. The one-photon-exchange correction to the quadratic effect was considered in Ref. [13]. The leading order of the quadratic

Zeeman effect, the one-loop QED correction, and the one-photon-exchange correction for boronlike argon have been calculated in Ref. [11].

The main uncertainty in the calculation of the quadratic Zeeman effect is determined by the one-photon exchange correction. We present calculation of the two-photon exchange correction to the quadratic Zeeman effect in the Breit approximation.

References

1. J. Morgner *et al.* g factor of boronlike tin. Phys. Rev. Lett. **134**, 123201 (2025).
2. S. Sturm *et al.* High-precision measurement of the atomic mass of the electron. Nature **506**, 467 (2014).
3. V. A. Yerokhin *et al.* g factor of light ions for an improved determination of the fine-structure constant. Phys. Rev. Lett. **116**, 100801 (2016).
4. I. Arapoglou *et al.* g factor of boronlike argon $^{40}Ar^{13+}$. Phys. Rev. Lett. **122**, 253001 (2019).
5. T. Sailer *et al.* Measurement of the bound-electron g-factor difference in coupled ions. Nature **606**, 479 (2022).
6. P. Micke *et al.* Coherent laser spectroscopy of highly charged ions using quantum logic. Nature **578**, 60 (2020).
7. M. Vogel *et al.* Electron magnetic moment in highly charged ions: The artemis experiment. Annalen der Physik p. 1800211 (2018).
8. N. A. Huerta *et al.* An experimental platform for investigation of the zeeman effect in strong magnetic fields. Review of Scientific Instruments **95**, 043507 (2024).
9. V. V. Ivanov *et al.* Quadratic zeeman effect in hydrogen at 2–3 mg magnetic fields. Phys. Rev. E **106**, 045206 (2022).
10. A. Aeppli *et al.* Clock with 8×10^{-19} systematic uncertainty. Phys. Rev. Lett. **133**, 023401 (2024).
11. A. Agababaev, V. *et al.* Quadratic zeeman effect in boronlike argon. Nucl. Intsr. Met. B **408**, 70 (2017).
12. S. Varentsova, A. *et al.* Third-order zeeman effect in highly charged ions. Nucl. Intsr. Met. B **408**, 80 (2017).
13. A. S. Varentsova *et al.* Interelectronic-interaction contribution to the nonlinear zeeman effect in boronlike ions. Phys. Rev. A **97**, 043402 (2018).

Structure and properties of magnonic modes of dielectric ferromagnetic nanoparticles.

K. Albitskaya[1,3], F. Shuklin[1], M. Petrov[2,3], A. Chernov[1,3]

[1] MIPT, Dolgoprudny 141700, Russia

[2] ITMO University, Saint-Petersburg, 197101, Russia

[3] Russian Quantum Center, 121205 Moscow, Russia

h.alitskaya@mail.ru, m.petrov@metalab.ifmo.ru

Optomagnetism [1] is important for ultrafast, local, and reconfigurable spin control. This opens novel opportunities for fast and energy-efficient information processing. Miniaturization is one of the key problems in optomagnetism due to a diffraction limit. To overcome this limit nanoscale structures may be used to localize light at the spots of subwavelength dimensions.

For this properties we need to understand clearly the structure and interaction of magnon modes in nanoscale micromagnetic systems, where spatial quantization effects can significantly influence the dynamic properties of the structures. In relatively simple extended systems, such as antiferromagnetic and ferromagnetic films is fairly well understood theoretically and investigated experimentally [2]. However, similar effects in finite three-dimensional structures (sphere [3], [4], cylinder) are still insufficiently studied.

The study examines the issues of hybridization of exchange and dipole modes (Figure 1) in ferromagnetic structures of limited size. Numerical modeling was performed (Comsol Multiphysics package), and a semi-analytical model was constructed (couple mode theory). The effect of mode anti-crossing, which occurs when the frequencies of exchange modes coincide and are connected through the dipole overlap integral, was investigated (Figure 2).

References

1. Kimel, Alexey, et al. "The 2022 magneto-optics roadmap." Journal of Physics D: Applied Physics 55.46 463003 (2022).

2. Sud, A. et al. "Tunable magnon-magnon coupling in synthetic antiferromagnets." Physical Review B 102.10 100403 (2020).

3. Walker, Laurence R. Magnetostatic modes in ferromagnetic resonance Physical Review 105.2 390 (1957).

4. Fletcher. et al. Identification of the magnetostatic modes of ferrimagnetic resonant spheres Physical Review 114.3 739 (1959).

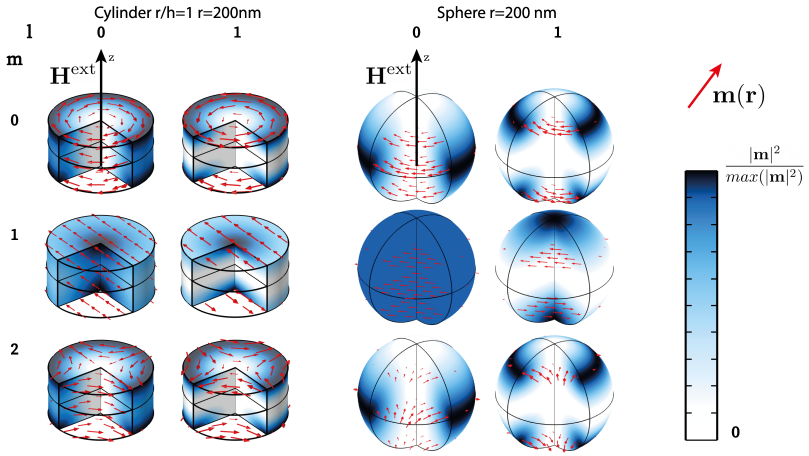

Figure 1: Types of the magnon dipole-exchange modes in cylinder (left) and in sphere (right). m - magnetic quantum number. l - number of zeros along z axis. $\mathbf{H}^{\text{ext}}$- external magnetic field, $\mathbf{m}(\mathbf{r})$ - dynamic magnetization.

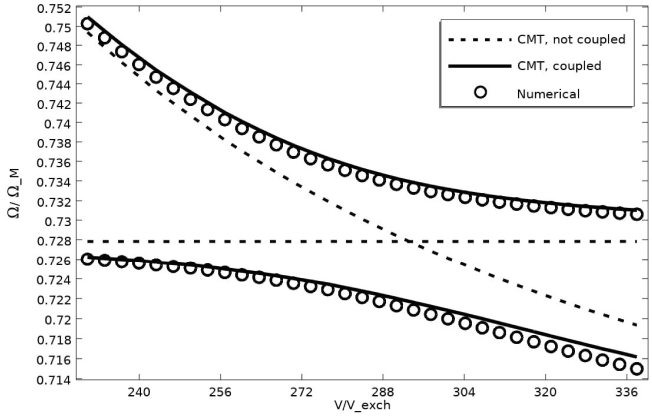

Figure 2: The dependence of the normalized frequency on the normalized volume of the cylinder, which is changed while maintaining $\frac{r_{\text{cyl.}}}{h_{\text{cyl.}}} = 1$. Demonstrates the interaction of two magnon modes obtained numerically (Numerical) and not the interaction when the dipole integrals of overlap between this modes is turned off (CMT, not coupled).

Line profile asymmetry in precision spectroscopy

A. Anikin[1,2], T. Zalialiutdinov[1,3], D. Solovyev[1,3], L Labzowsky[1,3]

[1] Department of Physics, St. Petersburg State University

[2] D.I. Mendeleev Institute for Metrology

[3] Petersburg Nuclear Physics Institute named by B.P. Konstantinov of National Research Centre 'Kurchatov Institut'

alexey.anikin.spbu@gmail.com

Precision spectroscopy plays an essential role in modern physics, providing the ability to test theoretical models and enhancing understanding of fundamental processes. Its applications span diverse domains, including dark-matter investigations [1], analysis of time variations in physical constants [2], determination of fundamental parameters, and establishment of metrological frequency standards. For example, the hyperfine transition in cesium, measured with an exceptional precision level of 10^{-18}, has facilitated the development of ultraprecise atomic timekeeping devices [3]. Progress in experimental methods has achieved precision levels of 10^{-15} for hydrogen [4] and 10^{-12} for helium spectroscopy [5], with molecular spectroscopy approaching measurement uncertainties near 10^{-12} [6].

Reaching such precision requires consideration of progressively finer phenomena and thorough examination of spectral line characteristics, now directly observable [7]. This has emerged as a significant domain in quantum electrodynamics (QED), employing the S-matrix framework to model photon-electron interactions in bound systems [8, 9, 10, 11]. A central outcome of line profile theory involves nonresonant (NR) phenomena, which induce spectral line asymmetries and distortions, influencing the determination of transition frequencies. NR effects vary with experimental conditions and encompass mechanisms such as the quantum interference effect (QIE). QIE arises when photon scattering processes involve multiple quantum pathways from adjacent energy states, producing angular-dependent asymmetries in spectral line profiles. In specific configurations, a "magic angle" neutralizes these asymmetries [12], while other scenarios require quantification of asymmetry for precise measurements [13]. Another NR phenomenon arises from frequency-dependent variations in natural line width, which manifest even in 'isolated' transitions [14]. The present investigation focuses on analyzing spectral line profiles and characterizing non-resonant phenomena.

References

1. C. Kennedy *et al.*, *Phys. Rev. Lett.*, **125**, 201302 (2020).

2. J. Webb *et al.*, *Phys. Rev. Lett.*, **87**, 091301 (2001).

3. T. Nicholson *et al. Nat. Commun.* **51**, 270 (2015).

4. A. Matveev *et al. Phys. Rev. Lett.* **110**, 230801 (2013).

5. R. Van Rooij *et al. Science* **333**, 196 (2011).

6. I. Kortunov *et al. Nat. Phys.* **17**, 569 (2021).

7. A. Beyer *et al. Science* **358** 79 (2017).

8. A. Andreev *et al. Phys. Rep.* **455**, 135 (2008).

9. T. Zalialiutdinov *et al. Phys. Rep.* **737**, 1 (2018).

10. D. Solovyev *et al. Phys. Rep.* **1114**, 1 (2025).

11. D. Solovyev *et al. J. Phys. B* **58**, 055001 (2025).

12. P. Amaro *et al. Phys. Rev. A* **92**, 062506 (2015).

13. D. Solovyev *et al. Phys. Rev. A* **109**, 022806 (2024).

14. A. Anikin *et al. Phys. Scr.* **98**, 045407 (2023).

15. J. Schwinger, Phys. Rev. **73**, 416 (1948).

16. L. D. Faddeev, Sov. Phys. JETP **12**, 1014 (1960).

17. B. P. Abbott *et al.*, Phys. Rev. Lett. **116**, 061102 (2016).

Efficient classical simulation of trotterized quantum circuits with structured unitaries

B. Arseniev

Skolkovo Institute of Science and Technology

boris.arseniev@skoltech.ru

Introduction: Simulating quantum systems on classical computers remains one of the central challenges in quantum computing. While Clifford circuits are known to be classically simulable, their lack of universality limits their ability to represent general quantum dynamics. To bridge this gap, recent research has focused on identifying broader classes of quantum circuits that remain classically tractable under certain algebraic or structural constraints, such as commutativity or group invariance [1]. A particularly important task is simulating time evolution under a general Hamiltonian, a core component of quantum algorithms and physical modeling. This evolution is typically approximated using Trotterization, where the time evolution operator $U = e^{iHt}$ is expressed as a product of simpler operators, $U(t/r)^r$, for sufficiently large r [2, 3].

Motivation and Problem Formulation: Despite its widespread use, simulating Trotterized circuits remains computationally expensive in general. Our goal is to identify structured families of such circuits that can be simulated classically with polynomial resources. We consider a parametrized unitary of the form: $U(t) = \sum_{j=1}^{M_U} \alpha_j(t) P_j$, where P_j are Pauli operators, $\alpha_j(t)$ are complex coefficients, and $N = 2^n$ is the Hilbert space dimension for an n-qubit system. The central computational task is evaluating the expectation value: $A = \langle 0| \left(U(t/r)^\dagger\right)^r \hat{O} \left(U(t/r)\right)^r |0\rangle$, for a given observable $\hat{O}$.

Main Results: We identify a structural condition that enables efficient classical simulation: if the set of Pauli operators $\{P_j\}$ and the observable $\hat{O}$ form a closed set under conjugation by $U(t)$, then the expectation value A can be computed classically in time $O(BM_U^2 \log r)$, where B is the cost of evaluating the time-dependent coefficients $\alpha_j(t)$. These coefficients can be efficiently computed using $O(N \log N)$ binary operations [4]. When the decomposition involves only polynomially many Pauli terms, i.e., $M_U = O(n^k)$, the entire simulation remains tractable, even for large n, since the complexity scales linearly with the system size. This offers a dramatic improvement over the generic diagonalization-based approach, which requires $O(N^3)$ operations.

Conclusion and Significance: Our findings extend the reach of classical simulation beyond Clifford circuits by incorporating structured, non-Clifford Trotterized dynamics. By leveraging algebraic closure properties, we provide a concrete and scalable technique for simulating a broad class of quantum circuits with potential applications in quantum algorithm design and physical system modeling. This work

complements and generalizes recent group theoretic approaches, contributing to a growing toolkit for hybrid quantum-classical simulation strategies.

References

1. I. Marvian, "Theory of quantum circuits with abelian symmetries", Physical Review Research, vol. 6, no. 4, p. 043292, 2024.

2. D.W. Berry, G. Ahokas, R. Cleve, and B.C. Sanders, "Efficient quantum algorithms for simulating sparse hamiltonians," Communications in Mathematical Physics, vol. 270, no. 2, pp. 359–371, 2007.

3. A.M. Childs, Y. Su, M.C. Tran, N. Wiebe, and S. Zhu, "Theory of trotter error with commutator scaling," Physical Review X, vol. 11, no. 1, p. 011020, 2021.

4. B. Arseniev, D. Guskov, R. Sengupta, J. Biamonte, and I. Zacharov, "Tridiagonal matrix decomposition for hamiltonian simulation on a quantum computer," Physical Review A, vol. 109, no. 5, p. 052629, 2024

Predicting bipartite entanglement by quantum regression

Y. Balkybek[1], K. Antipin[1,2], A. Kardashin[1], V. Palyulin[1]

[1]Skolkovo Institute of Science and Technology

[2]Lomonosov Moscow State University, Moscow, Russia

yerassil.balkybek@skoltech.ru

Introduction. Quantum machine learning (QML) is one of the most rapidly developing areas of research in quantum computing and is particularly relevant to the current noisy intermediate-scale quantum (NISQ) era [1, 2]. QML methods enable the modeling of complex relationships between classical data points and quantum states through various tasks, such as classification [3, 4] and regression [5, 6], among others. In this work, we focus on a regression problem aimed at quantifying entanglement in qubit–qubit and qudit–qudit systems. To this end, we propose a novel approach for constructing a problem-specific quantum neural network capable of accurately quantifying bipartite entanglement using entanglement negativity and entanglement tangle as metrics.

Problem Statement. Consider the following set:

$$\mathcal{T} = \{(\rho_i, \alpha_i)\}_{i=1}^{T}, \tag{1}$$

where $\rho_i \equiv \rho(\alpha_i)$ are data points represented by n-qubit quantum states labeled by $\alpha_i \in \mathbb{R}$. Our task is the following: Given a set $\mathcal{T}$ which is called a training set, learn how to predict the label α for a given unseen ρ_α. Essentially, we want to solve a regression problem with a peculiarity that the labeled data points are quantum states ρ_α. So, it would be natural to predict the labels α of ρ_α as an expected value of an observable H, i.e., as $\mathrm{Tr}\, H\rho_\alpha$. To find such an H, we consider solving the following minimization problem:

$$H^* \in \arg\min_H [w_{\mathrm{ls}} f_{\mathrm{ls}} + w_{\mathrm{var}} f_{\mathrm{var}}] \tag{2}$$

where

$$f_{\mathrm{ls}} = \sum_{i=1}^{T} \left(\mathrm{Tr}\, H\rho_i - \alpha_i\right)^2, \qquad f_{\mathrm{var}} = \sum_{i=1}^{T} (\mathrm{Tr}\, H^2\rho_i - \mathrm{Tr}^2\, H\rho_i)$$

That is, we want to simultaneously minimize (i) the least squares between our predictions $\mathrm{Tr}H\rho_i$ and the true labels α_i from the training set with a weight w_{ls}, and (ii) the variance of H in the states ρ_i with a weight w_{var}.

Methods and Results. Unlike variational quantum algorithms (VQAs), which rely on iterative parameter updates in parametrized quantum circuits (or ansatze), we take a different approach: we pre-define our circuit, best suitable for entanglement quantification once and perform all parameter updates classically afterwards. The core idea is as follows. We represent the observable H as

$$H_{\boldsymbol{\theta}} = \sum_{j=1}^{M} \theta_j G_j \tag{3}$$

where $\boldsymbol{\theta} = (\theta_i)_{i=1}^{M} \subset R$ are variational parameters, and G_i are Hermitian operators that are pre-defined and can be problem specific. In this work, we shall call the set $\mathcal{G} = \{G_j\}_{j=1}^{M}$ *an ansatz*.

In this project, we consider quantum entanglement negativity for qubit systems and quantum linear entropy entanglement and quantum tangle for qutrit systems. We define quantum entanglement negativity as

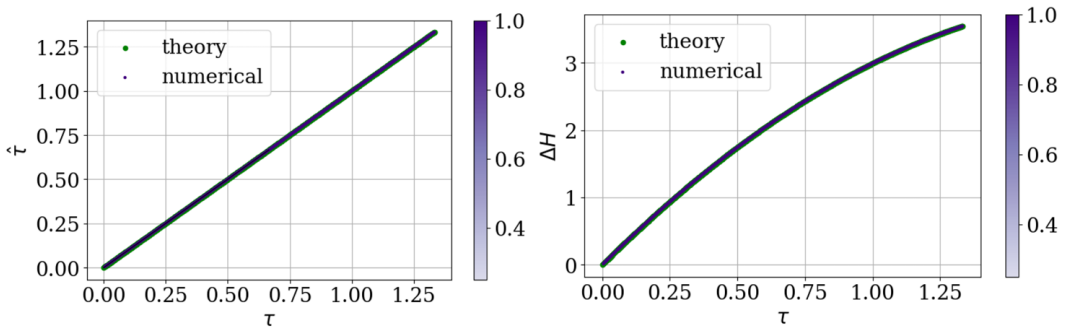

Figure 1: Left: Predicted entanglement tangle τ vs. true entanglement tangle for two copies of bipartite pure qutrit states. Right: Variance of the entanglement tangle τ vs. true entanglement tangle for two copies of bipartite pure qutrit states

$$N(\rho) = ||\rho^{T_2}||_1 - 1 \tag{4}$$

where $||\cdot||_1$ is the trace norm, and $\rho^{T_2} \equiv (1 \otimes T)[\rho]$ is the partial transpose of ρ with respect to the second qudit. In addition, we define quantum entanglement tangle and linear entropy entanglement for pure states as

$$\tau(|\psi\rangle) = 2(1 - \mathrm{Tr}(\rho_A^2)) = E|\psi\rangle \tag{5}$$

and for mixed states we optimize this value over all possible combination of pure states, which is an NP-complete problem. Theoretically, it was shown that it is

impossible to predict the entanglement of a bipartite quantum state ρ by processing solely single copies using a variational quantum circuit, but it is possible to train variational quantum circuit providing two copies of $\rho^{\otimes 2}$ to quantum neural networks to quantify quantum entanglement for pure quantum states. However, for mixed states, the accuracy of prediction grows as a number of copies of quantum states provided. In addition to the idea of processing several copies, we construct our circuit mainly based on various linear combination of swap ($\mathbb{S}$) operators to predict quantum entanglement, e.g. for two copies scenario, we take as an ansatz for H_θ in (6)

$$\mathcal{G} = \{\mathbb{1}, \mathbb{S}_{13}, \mathbb{S}_{24}, \mathbb{S}_{13}\mathbb{S}_{24}\} \tag{6}$$

This ansatz is capable of accurately estimating quantum entanglement for qubit-qubit and qutrit-qutrit cases as in Fig. (3). We also show theoretically that this ansatz can explicitly predict the entanglement using Haar-averaging over all random quantum states ρ with two copies. In Fig. (2) we consider the training set $\mathcal{T} = \left\{\rho_{N_i}^{\otimes 2}, N_i^2\right\}_{i=1}^{1000}$, where ρ_{N_i} are random qubit mixed states with the negativities N_i. So, we want to learn to predict the squared negativities. Using our intuition about predicting the negativity of mixed states, as an ansatz for $H_{\boldsymbol{\theta}}$ in Eq. (3) we take an ansatz as in Eq. (6). This way, we have only $|\boldsymbol{\theta}| = 4$ variational parameters. The results are shown in Fig. 2. With our ansatz, we obtained the results better than we had with the variational circuit of $l = 2$ layers and measuring all $m = 4$ qubits [7]. Additionally, it is significantly faster than general purpose ansatz such as hardware-efficient ansatz!

Now consider the training set $\mathcal{T} = \left\{\rho_i^{\otimes 4}, E_i\right\}_{i=1}^{100}$, where ρ_i are random mixed qutrit-qutrit states with the linear entropies E_i. As an ansatz for $H_{\boldsymbol{\theta}}$ in (3), we processed $\rho^{\otimes 4}$, i.e. four copies of ρ and our ansatz is formed by the linear combination of 33 swap operators and the result can be seen in Fig. (3).

References

1. J. Biamonte, P. Wittek, N. Pancotti, P. Rebentrost, N. Wiebe, and S. Lloyd. Quantum machine learning. *Nature*, 549(7671):195–202, 2017.

2. M. Schuld and F. Petruccione. *Machine Learning with Quantum Computers*. Springer, 2021.

3. Daniel K Park, Carsten Blank, and Francesco Petruccione. The theory of the quantum kernel-based binary classifier. *Physics Letters A*, 384(21):126422, 2020.

4. Leonardo Banchi, Jason Pereira, and Stefano Pirandola. Generalization in quantum machine learning: A quantum information standpoint. PRX *Quantum*, 2(4):040321, 2021.

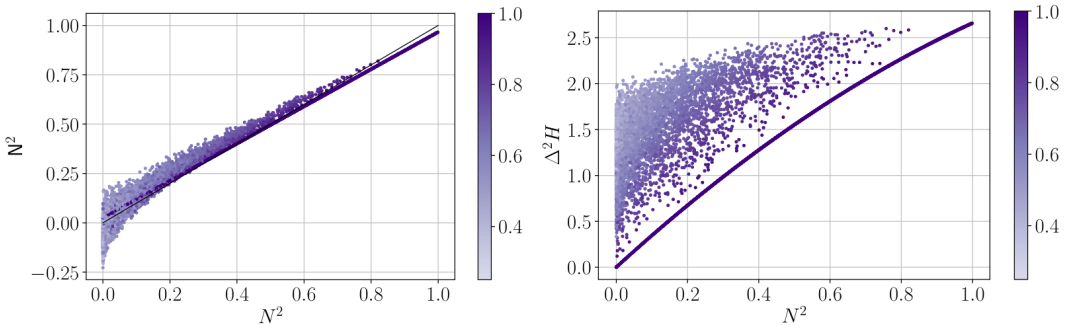

Figure 2: Left: Predicted squared negativity N^2 of 10^4 random mixed states vs. the true squared negativity N^2 for $c = 2$ copies. Right: Variance of the trained observable H. The color of the points indicates the purity of the corresponding states. The model was trained on a set $\mathcal{T} = \{(\rho_j^{\otimes 2}, N_j)\}_{j=1}^{1000}$ with random ρ_j and N_j evenly distributed on $[0, 1]$.

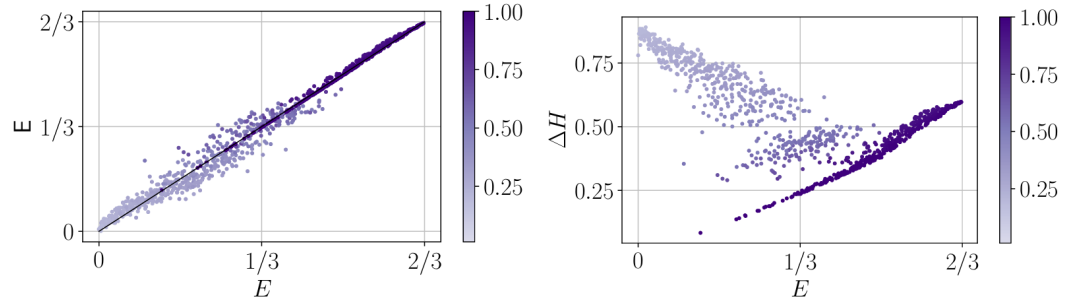

Figure 3: Left: Predicted linear entropy entanglement E of 10^4 of random mixed states vs. the linear entropy entanglement E for $c = 4$ copies. Right: Variance of the trained observable H. The color of the points indicates the purity of the corresponding states.

5. Maria Schuld, Ilya Sinayskiy, and Francesco Petruccione. Prediction by linear regression on a quantum computer. *Physical Review A*, 94(2):022342, 2016.

6. Pranath Reddy and Aranya B Bhattacherjee. A hybrid quantum regression model for the prediction of molecular atomization energies. *Machine Learning: Science and Technology*, 2(2):025019, 2021.

7. Andrey Kardashin, Yerassyl Balkybek, Vladimir V.Palyulin, and Konstantin Antipin. Predicting properties of quantum systems by regression on a quantum computer. *Phys. Rev. Res.*, 7:013201, Feb 2025.

Calculations of energies, matrix elements, polarizabilities, and corresponding QED corrections for many-electron monovalent atoms and ions

A. Bobylev[1,2], T. Zalialiutdinov[1,2], D. Solovyev[1,2]

[1] Department of Physics, St. Petersburg State University, Petrodvorets, Oulianovskaya 1, 198504, St. Petersburg, Russia

[2] Petersburg Nuclear Physics Institute named by B.P. Konstantinov of National Research Centre 'Kurchatov Institut', St. Petersburg, Gatchina 188300, Russia

artem.bobyljow@gmail.com

This paper presents calculations of the scalar and dynamical polarisabilities as well as the corresponding thermal shifts of the atomic levels, in addition the Bethe logarithm [1] is worked out. The Bethe logarithm determines the dominant part of the QED self-energy correction. When calculating these quantities, it is necessary to summarize all intermediate states. Even worse, in the case of the Bethe logarithm, the largest contribution is made by states from the continuum. In precisely solvable problems (e.g., hydrogen-like atoms and ions), calculations can be performed by direct summation over intermediate states, tracking convergence. However, for atoms and ions with several electrons, and even more so for many-electron systems, the task is complicated by the possibility of reproducing the full spectrum of states. To solve this problem, there are various methods used to approximate the interaction potential. In particular, model potentials have become widespread, which are most natural for atoms and ions of the alkaline group of the periodic table (monovalent systems).

In this paper, calculations were performed using the combined Dirac-Fock plus Core-Polarization (DFCP) method [2], which is based on the local version of the Dirac-Hartree-Fock potential [3]. In this approach, the total spectrum, including discrete, continuous, and negative continuum, is replaced by a suitable discrete pseudo-spectrum [4], enabling summation over intermediate states in a manner similar to hydrogen-like systems. The pseudo-spectrum is constructed in such a way that several lower positive energy states correspond exactly to the de facto low-lying bound states of the valence electron (the calculated energies are compared with the corresponding experimental values). In doing so, the valence electron is considered in the self-consistent field of the frozen core. Correlation interactions between the core electrons and the valence electron are accounted for by means of the semi-empirical core polarisation potential.

The paper presents a comparative analysis of the calculated quantities: the values are compared both with theoretical results obtained in the framework of other approaches and with the corresponding experimental values. The value of the Bethe logarithm is to be used to calculate the leading-order QED correction (one-loop self-

energy of the bound electron) to different energy levels of atoms and ions of the alkali group and their two-atom molecular compounds [5].

References

1. Yan, Z.-C. *et al.*, Phys. Rev. Lett. **100**, 243002 (2008).

2. Tang Yong-Bo *et al.*, Chin. Phys. B **23** 063101 (2014).

3. V. M. Shabaev *et al.*, Phys. Rev. Lett. **94**, 213002 (2004).

4. V. M. Shabaev *et al.*, Phys. Rev. Lett. **93**, 130405 (2004).

5. M. Lesiuk *et al.*, Phys. Rev. A **108**, 042817 (2023).

On the generation of twisted photons in elliptical undulators

O. Bogdanov[1] and S. Bragin[1]

[1] Tomsk Polytechnic University

bov@tpu.ru, svb38@tpu.ru

Various methods are employed to generate photons with non-zero orbital angular momentum. Contemporary theoretical developments in twisted photon generation are based on the concept of inverse Compton scattering [1], along with more exotic proposals, such as twisted radiation during the channeling of relativistic particles in crystals [2]. Another potential method for producing twisted photons is undulator radiation. The suggestion to use undulator radiation as a pure source of twisted photons could significantly expand the range of applications for such devices.

Previously, fundamental formulas for the average number of twisted photons radiated by relativistic electrons in electromagnetic fields, considering the radiation reaction, were derived [3]. Numerical calculations of the probability of twisted photon radiation in undulators have also been presented.

Furthermore, the generation of twisted photons during the motion of relativistic electrons in elliptical undulators has been studied. The influence of the undulator's ellipticity on the intensity of twisted photon radiation, as well as asymmetry and selection rules in dipole and wiggler regime, has been investigated [4, 5].

In this work, new results on the radiation of twisted photons in elliptical undulators. The properties of such radiation are presented using of a promising undulator with parameters of the SKIF beams, as well as other operational elliptical undulators.

Список литературы

1. B.A. Knyazev, V.G. Serbo, Physics–Uspekhi 61 (2018).

2. O.V. Bogdanov et al., Phys. Lett. A 451, 128431 (2022)

3. O.V. Bogdanov et al., Phys. Rev. D 99, 116016 (2019).

4. P.O. Kazinski, V.A. Ryakin, Russ. Phys. J. 64, 717 (2021)

5. O.V. Bogdanov, S.V. Bragin, Nucl. Instrum. Methods Phys. Res. A 1075, 170337 (2025).

Analytical theory of the skewed wake effect

A. N. Chuprina[1] and S. S. Baturin[1]

[1] School of Physics and Engineering, ITMO University, St. Petersburg, Russia 197101

anna.chuprina@metalab.ifmo.ru, s.s.baturin@gmail.com

The Panofsky-Wentzel theorem [1] states that any asymmetry in the transverse distribution of the longitudinal electric field will inevitably lead to the appearance of the transverse component of the Lorentz force, which in turn results in emittance growth and may even cause beam break-up instability [2]. Such interactions between particles within a beam or between different beams (e.g., driver and witness) through radiation are typically described within a convenient framework known as wakefield interactions [3]. Recently, it has been shown that wakefield interactions depend significantly on the geometry of the problem. For example, a highly elliptical beam generates significantly weaker transverse wakefields [4].

Regarding geometry, one might intuitively conclude that not only the shape of the guiding channel (e.g., round or slab) matters, but also the shape of the driver and its relative position within the guide channel. This is especially true if one of the transverse dimensions of the beam is comparable to the minimum characteristic size of the vacuum channel. This intuition has recently been experimentally confirmed. In Ref. [5], the authors report the discovery of the "skew wake effect", which manifests as a rotation of the dipole and quadrupole wake toward the beam when the beam is tilted in the transverse plane relative to the boundary of the guiding slab channel. This discovery and the detailed study of this effect represent a critical step in understanding the prospects and limitations of the flat-beam concept.

In this work, we have investigated the skew wake effect in slab structures, focusing on its dependence on beam geometry and tilt angle. By employing both a three-particle model and a more realistic elliptic beam model, we derived analytical expressions for the skew angle ϕ and scaling factor λ of the transverse wake potential. Our analysis reveals that these quantities are strongly influenced by the beam's tilt angle α and ellipticity parameter $\varkappa = \sigma_x/a$. For highly elliptic beams ($\varkappa \gg 1$), the skew angle approaches $\phi \approx -\frac{3}{2}\alpha$, while the scaling factor λ is suppressed as $\lambda \approx 1 + \frac{4(\sin\alpha)^2}{\varkappa^2}$. In contrast, for beams with low ellipticity ($\varkappa \ll 1$), the skew angle scales as $\phi \approx -\frac{\pi^2}{8}\varkappa^2 \sin 2\alpha$, and the scaling factor grows as $\lambda \approx 1 + \frac{\pi^2}{2}\varkappa^2(\sin\alpha)^2$.

The sensitivity of the wake amplitude to the skew effect is most pronounced for beams with low ellipticity ($\varkappa \leq 1$), where the scaling factor λ reaches its maximum. However, for highly elliptic beams ($\varkappa \gg 1$), the scaling factor is naturally suppressed due to the constraint $\varkappa \leq \frac{1}{3\sin\alpha}$, which ensures the beam does not clip. Despite this suppression, the skew effect, characterized by the rotation of the quadrupole wake's

principal axis, persists even for highly elliptic beams. The skew angle ϕ is always proportional to the tilt angle α, with a limiting value of $\phi \approx -\frac{3}{2}\alpha$ for $\varkappa \gg 1$.

The basic theory we used is independent of the specific nature of the wake field (as demonstrated in Refs. [6, 7]), leading to the conclusion that the skew wake is a purely geometric phenomenon. It manifests itself in any interaction with asymmetric beams and results from imperfect beam alignment, which is inherently random. Consequently, the skew effect is likely to cause instabilities or emittance growth, especially in applications that require precise control of beam dynamics, such as colliders and wakefield accelerators.

The stochastic nature of the skew wake effect poses significant challenges for beam control and compensation. Unlike the case of a pure quadrupole wake, where alternating slab structures can mitigate the effect, the skew wake's dependence on random beam misalignment makes it difficult to suppress. This underscores the importance of advanced beam diagnostics and feedback systems to manage the impact of the skew wake effect in practical applications.

Looking ahead, further experimental studies are needed to investigate this effect, particularly for beams with extreme ellipticity and small tilt angles. These efforts will be essential for the design and operation of future accelerators and colliders, where understanding and controlling the skew wake effect will play a crucial role in achieving optimal beam performance.

In summary, our results show that the skew wake effect is an intrinsic feature of transversely asymmetric beams in slab structures. While the scaling factor λ is naturally suppressed for highly elliptical beams, the skew angle ϕ remains significant and can lead to beam instabilities. These results highlight the importance of considering the skew wake effect in the design and operation of future accelerators and colliders, and emphasize the need for continued research and innovation in this area.

References

1. Panofsky, W. K. H. and Wenzel, W. A., Review of Scientific Instruments **11**, (2004).

2. Alex Chao, Physics of Collective Beam Instabilities in High Energy Accelerators, (1993).

3. Bane, K. L. F. and Chen, Pisin and Wilson, P. B., IEEE Transactions on Nuclear Science **5**, (1985).

4. Tremaine, A. and Rosenzweig, J. and Schoessow, P.,Phys. Rev. E **56**, (1997).

5. Lynn, W. and Xu, T. and Andonian et al., Phys. Rev. Lett. **132**, (2024).

6. Baturin, Stanislav S. and Kanareykin, Alexey D., Phys. Rev. Lett. **113**, (2014).

7. Baturin, S. S. and Kanareykin, Phys. Rev. Accel. Beams **19**, (2016).

Angle-resolved three-dimensional distributions of electron-positron pairs in slow heavy-ion collisions

N. K. Dulaev[1,2,*], D. A. Telnov[1,†], R. V. Popov[2,1], V. M. Shabaev[1,2,‡], Y. S. Kozhedub[1], I. A. Maltsev[1], I. I. Tupitsyn[1]

[1]St. Petersburg State University

[2]Petersburg Nuclear Physics Institute named by B. P. Konstantinov of National Research Center "Kurchatov Institute"

[*]st069071@student.spbu.ru, [†]d.telnov@spbu.ru, [‡]v.shabaev@spbu.ru

Nonperturbative effects of quantum electrodynamics in the presence of strong electromagnetic fields have been the subject of extensive theoretical investigations since the first half of the XX century. One such effect is the spontaneous vacuum decay in heavy-ion collisions. When two nuclei with a total charge $Z > Z_{\rm cr}$, where $Z_{\rm cr} \approx 173$, approach each other closely enough, the lowest quasimolecular electronic state, $1s\sigma$, dives into the negative-energy continuum as a resonance. This process can result in the creation of electron-positron pairs, with the positrons escaping the collision area to infinity as free particles due to the Coulomb repulsion from the nuclei. Collisions in this regime are classified as supercritical.

Experimental observation of this phenomenon is challenging because of the competing dynamical mechanism of electron-positron pair production, which stems from the time-dependent electromagnetic field of the colliding nuclei. Therefore, precise theoretical modeling is required to isolate distinctive signatures of the transition to the supercritical pair-creation regime while accounting for the dynamical channel.

Over the past decade, the theoretical research group at Saint Petersburg State University has made substantial progress in understanding pair production in heavy-ion collisions. In Refs. [1, 2], key indicators of the transition to the supercritical regime were identified in the total probabilities and energy spectra of emitted positrons. These studies, based on nuclear trajectories with a fixed minimal internuclear distance, provided crucial insights into the onset of supercritical effects. More recently, two-center calculations [3] have facilitated a detailed analysis of the angular distributions of emitted positrons.

In previous studies, the effects of rotational coupling were neglected based on the argument that they have a negligible influence on the total pair-creation probabilities and the energy spectra of emitted positrons. However, rotational coupling may play a role in shaping the angular distributions of positrons. In the present work [4], we investigate the impact of the rotational term on the total probabilities of pair creation, as well as on both angle-integrated and angle-resolved positron energy distributions. We solve the time-dependent two-center Dirac equation using the generalized pseudospectral method in modified prolate spheroidal coordinates, incorporating the rotational term explicitly into the Hamiltonian.

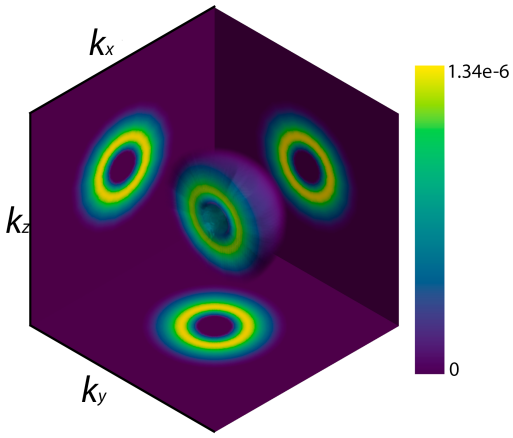

Figure 1: Pseudocolor plot of the angle-resolved differential probabilities of positron creation corresponding to the positron momentum components k_x, k_y, and k_z for head-on collision of the nuclei with $Z = 92$ at $R_{\min} = 17.5$ fm.

A subset of the obtained results is presented in Fig. 1, which depicts the three-dimensional angle-resolved energy distribution of outgoing positrons for a head-on collision of two identical nuclei with charge numbers $Z = 92$. The momentum components in Fig. 1 are shown against the axes of the fixed frame, with the z axis directed along the initial relative velocity of the nuclei. For improved clarity, only one half of the three-dimensional distribution is displayed. Additionally, two-dimensional cross-sections of the full distribution are provided in the $k_z - k_x$, $k_x - k_y$ and $k_z - k_y$ planes, each passing through the center of the distribution and aligned with the respective coordinate planes. As evident from Fig. 1, the three-dimensional distributions of emitted positrons exhibit a high degree of isotropy.

This work was supported by the Russian Science Foundation (Grant No 22-62-00004, https://rscf.ru/project/22-62-00004/).

References

1. I. A. Maltsev, V. M. Shabaev, R. V. Popov *et al.*, Phys. Rev. Lett. **123**, 113401 (2019).

2. R. V. Popov, V. M. Shabaev, D. A. Telnov *et al.*, Phys. Rev. D **102**, 076005 (2020).

3. N. K. Dulaev, D. A. Telnov, V. M. Shabaev *et al.*, Phys. Rev. D **109**, 036008 (2024).

4. N. K. Dulaev, D. A. Telnov, V. M. Shabaev *et al.*, Phys. Rev. D **111**, 016018 (2025).

Decay of the twisted relativistic electron in a strong inhomogeneous magnetic field

M.S. Epov and S.S. Baturin

ITMO University

mikhail.epov@metalab.ifmo.ru

Recent theoretical and experimental studies reveal that electrons in free space or in a constant magnetic field can carry a nonzero orbital angular momentum projection. Such quantum states are called twisted electrons. While many basic properties of twisted electrons have already been studied, several open questions remain. One of these is the stability of the vortex state. Unlike twisted photons, which are stable, twisted electrons can undergo spontaneous decay — a lowest-order QED process. It turns out that the decay rate depends heavily on the structure of the magnetic field interacting with the twisted electron. Specifically, in a z-dependent inhomogeneous magnetic field, the decay rate can be several times higher than in a homogeneous magnetic field (e.g., during transitions between Landau levels). One of the important practical consequences of this conclusion is that the decay rate increases when a free twisted electron is being focused. The sharper the focusing, the higher the decay rate becomes.

In the present study, we develop a theoretical framework based on the Foldy-Wouthuysen transformation and the Ermakov mapping operator to support the above statement. The proposed technique allows us to evaluate decay rates (and higher-order interactions of the twisted electron in an inhomogeneous magnetic field with the quantized electromagnetic field) for different configurations of the magnetic field. We analyze standard magnetic field models, such as the Glazer field and Faraday coils, as well as examine field configurations that may appear in astrophysical environments, particularly in stellar and relativistic jets.

We show that the propagation of a twisted electron in a transversely uniform but z-dependent magnetic field dramatically increases the decay rate. Additionally, we demonstrate that focusing a twisted electron results in a reduction of its lifetime.

Half-ring evolution in a spatially varying magnetic field

N. Filina[1] and S. Baturin[2]

[1,2] School of Physics and Engineering, ITMO University

[1]nvfilina@bk.ru, [2]s.s.baturin@gmail.com

We provide a complete description of the half-ring evolution of twisted electron in the axially symmetric spatially varying magnetic field. We use the formalism of Ermakov operators [1] to construct the evolution operator for our system. To apply it to the half-ring, we choose the trial system and search for the evolution of the initial state in it. We study the rotation and deformation of the half-ring in the magnetic field and make the conclusion about the physics under this effect.

Imagine that our initial state is the upper half-ring of the LG mode with quantum numbers n_a, l_a. We close the half-ring on the diameter as in the papers [2, 3] and assume that diffractive effects are negligibly small at far distances. We can therefore write the corresponding wave function in polar coordinates as

$$\Psi_{arc}(\rho,\phi,0) = N_{n_a,l_a}\left(\frac{\rho}{\rho_H}\right)^{|l_a|}\mathcal{L}_{n_a}^{|l_a|}\left[\frac{2\rho^2}{\rho_H^2}\right]\exp\left\{-\frac{\rho^2}{\rho_H^2}+il_a\phi\right\}(\theta(\phi)-\theta(\phi-\pi)), \tag{1}$$

where N_{n_a,l_a} - the normalization constant, $\mathcal{L}_{n_a}^{|l_a|}(x)$ - the generalized Laguerre polynomials, ρ_H - the Landau radius, $\theta(\phi)$ - the Heaviside step function. To find the evolution of the wave function (1) in any spatial-dependent symmetric magnetic field, we use the idea of unitary equivalence between this system and the trial one with the equation of motion in paraxial approximation

$$i\frac{k}{m_e}\frac{\partial\psi}{\partial z} = \left[\frac{p_x^2+p_y^2}{2m_e}+\frac{m_e\omega_0^2(x^2+y^2)}{2}\right]\psi. \tag{2}$$

The half-ring evolved in this system can be described by the wave function in the form

$$\Psi_{arc}(\rho,\phi,z) = \sum_{n,l}c_{n,l}\Psi_{n,l}(\rho,\phi,z) =$$

$$= \sum_{n,l}c_{n,l}N_{n,l}\left(\frac{\rho}{\rho_H}\right)^{|l|}\mathcal{L}_n^{|l|}\left[\frac{2\rho^2}{\rho_H^2}\right]\exp\left\{-\frac{\rho^2}{\rho_H^2}+il\phi-i(2n+|l|+1)\frac{m_e\omega_0}{k}z\right\}, \tag{3}$$

where the coefficients $c_{n,l}$ are the expansion coefficients of the initial state (1) over the Laguerre-Gaussian mode basis $\Psi_{n,l}(\rho,\phi,z)$. To find the answer for the real system,

we apply the unitary transformation in the form

$$\hat{\mathcal{E}}^{2D}_{1\mapsto 2} = \exp\left\{-i\frac{m_e}{k}\int\limits_0^z \omega_2(z'')\hat{L}_z dz''\right\}\hat{\mathcal{E}}_{1\mapsto 2}(x,y), \tag{4}$$

where the operator $\hat{\mathcal{E}}_{1\mapsto 2}(x,y)$ is a two-dimensional Ermakov operator

$$\hat{\mathcal{E}}_{1\mapsto 2}(x,y) : \begin{cases} \rho_2 = \rho b(z_2) \\ z = \int\limits_0^{z_2} \frac{dz''}{b^2(z'')} \\ \widetilde{\psi}_2(x_2,y_2,z_2) = \frac{1}{b}\,\widetilde{\psi}\,(x,y,z)\, e^{\frac{i}{2}k\frac{\dot{b}}{b}(x_2^2+y_2^2)}. \end{cases} \tag{5}$$

Above, z is the same spatial variable as in Eq. (3) and z_2 is the coordinate in the physical system. The function $b(z_2)$ is the parameter of the transformation that satisfies the Ermakov-Pinney equation of the form $\ddot{b} + \frac{m_e^2\omega_2^2}{k^2}b = \frac{m_e^2\omega_0^2}{k^2 b^3}$.

So the evolved wave function for half-ring in real system with spatially varying magnetic field is

$$\Psi_{arc}(z_2) = \sum_{n,l} c_{n,l}\frac{N_{n,l}}{b}\left(\frac{\rho}{b\rho_H}\right)^{|l|}\mathcal{L}_n^{|l|}\left[\frac{2\rho^2}{b^2\rho_H^2}\right]\exp\left\{-\frac{\rho^2}{b^2\rho_H^2} + il\left(\phi - \int\limits_0^{z_2}\omega(z')dz'\right)\right\} +$$
$$+\exp\left\{\frac{i}{2}k\frac{\dot{b}}{b}\rho^2 - i(2n+|l|+1)\frac{m_e\omega_0}{k}\int\limits_0^{z_2}\frac{dz'}{b^2(z')}\right\}. \tag{6}$$

We plot the spatial evolution of the half-ring in the homogeneous magnetic field in Fig. 1. We see the rotation with twice the speed compared to the speed in the trial system due to the $\hat{L}_z$ operator in the exponent in (4). It's important to note that our state rotates even when we don't have an external magnetic field. The reason of this is that the half-ring state isn't the solution to equation of motion for the trial system. The scaling of the state in the magnetic field follows the Ermakov-Pinney equation. In general, the situation is the same as in the case of non-stationary Landau states.

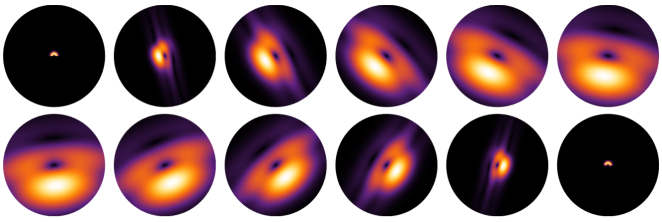

Figure 1: Evolution of the half-ring in a homogeneous magnetic field with quantum numbers $n = 0,\ l = 2$.

References

1. N. V. Filina and S. S. Baturin, "Unitary equivalence of twisted quantum states," Phys. Rev. A, **108**, p. 012219, Jul 2023.

2. T. Schachinger, S. Loeffler, M. Stoeger-Pollach, P. Schattschneider. (2015). Peculiar rotation of electron vortex beams. ULTRAMICROSCOPY. 10.1016/j.ultramic.2015.06.004.

3. Qi Meng, Xuan Liu, Wei Ma, Zhen Yang, Liang Lu et al. Generalized Gouy Rotation of Electron Vortex beams in uniform magnetic fields, e-Print: 2407.02788 [quant-ph]

Attosecond Compton backscattering using multicolour laser

D. V. Gavrilenko [1] and A. A. Tishchenko [1]

[1]National Research Nuclear University «MEPhI», Moscow, Russia

dvgavrilenko@mephi.ru,tischenko@mephi.ru

Compton backscattering of laser light on relativistic electrons is one of the most promising methods for generating bright quasi-monochromatic X-ray radiation. For many applications, such as studying electron dynamics at the atomic scale or performing ultrafast measurements [1], pulses of attosecond duration are required. However, generating such pulses remains technically challenging, as it typically necessitates coherent, ultrashort electron beams achieved through methods like microbunching or the Self-Amplified Spontaneous Emission (SASE) regime [2]. Obtaining attosecond pulses via laser beam chirping has also been proposed [3].

In this work, we examine the scattering process based on a set of lasers with varying frequencies. We demonstrate that parameters can be chosen such that the scattered radiation from this multicolour laser combines coherently to form a beam with a predefined shape. In particular, it is possible to generate an attosecond-duration beam whose duration is shorter than that of any of the initial laser pulses.

References

1. D.Hui, H. Alqattan, M. Sennary, N. V. Golubev, M. Th. Hassan, Attosecond electron microscopy and diffraction, Sci. Adv. **10**, 5805(2024).

2. E. A. Schneidmiller, Application of a modified chirp-taper scheme for generation of attosecond pulses in extreme ultraviolet and soft X-ray free electron lasers, Phys. Rev. Accel. Beams **25**, 010701 (2022).

3. B.H. Schaap, P.W. Smorenburg, O.J. Luiten, Isolated attosecond X-ray pulses from superradiant thomson scattering by a relativistic chirped electron mirror, Sci Rep 12, 19727 (2022). R. M. Arkhipov, I. Babushkin, M. K. Lebedev et al., Transient Cherenkov radiation from an inhomogeneous string excited by an ultrashort laser pulse at superluminal velocity, Phys. Rev. A **89**, 043811 (2014).

Preparation of Schrödinger cat quantum state using parametric down-conversion interaction

V. L. Gorshenin[1,2]

[1] Russian Quantum Center, Skolkovo 121205, Russia

[2] Moscow Institute of Physics and Technology, 141700 Dolgoprudny, Russia

valentine.gorshenin@yandex.ru

One of the most well-known types of non-Gaussian states is the Schrödinger cat (SC) state. The mainstream method for preparing these states is based on photon subtraction and conditional measurement (see Refs. [1]). Using this approach, SC state amplitudes up to $\alpha \sim 2$ were demonstrated using this method.

In the following work [2], we propose a novel procedure for preparing a squeezed even SC state with amplitude $\alpha > 10$. This method uses degenerate spontaneous parametric down-conversion (SPDC) taking into account pump depletion described by Hamiltonian:

$$\hat{H} = \gamma \left(\hat{a}^2 \hat{b}^\dagger + \hat{a}^{\dagger 2} \hat{b} \right), \tag{1}$$

where $\hat{a}$ and $\hat{b}$ are annihilation operator of the signal(first harmonic) and pump mode (second harmonic). We will introduce non-dimensional time $\tau = \gamma t$.

A well-known way to obtain bistability in the classical limit is to use degenerate SPDC, producing two possible output radiation variants with opposite phases. By analogy with the classical limit, the initial conditions are as follows: vacuum in the signal mode and a coherent state $|\beta\rangle$ in the pump mode.

The novel result of this paper is that after performing a projective measurement of zero photons in the pump mode at a specific interaction time τ_{opt} (depends on the pump Hamiltonian in Eq. (1)), the output state $|\psi\rangle$ in the signal mode closely approximates an SC state. The projective measurement should be performed when the probability of detecting zero photons in the pump mode is maximized. The schematic of the procedure is shown in Figure 1 (left). The Wigner function of the output state is presented in Figure 1 (right).

Output state was approximated by following wavefunction:

$$|\psi_{\text{out}}\rangle = \frac{1}{\sqrt{N}} e^{-i\pi\hat{n}/4} \hat{S}(r)(|\alpha\rangle + |-\alpha\rangle) \tag{2}$$

where N – wavefunction normalization factor, $\hat{S}(r)$ – squeeze operator with r – squeeze parameter, $\hat{n}$ – number operator. Amplitude of the prepared SC state $\alpha = 1.001 \cdot \beta \approx \beta$. The output state fidelity with the closest squeezed SC state is greater than 99.7%. Was performed approximations of the squeezing parameter r, the interaction time

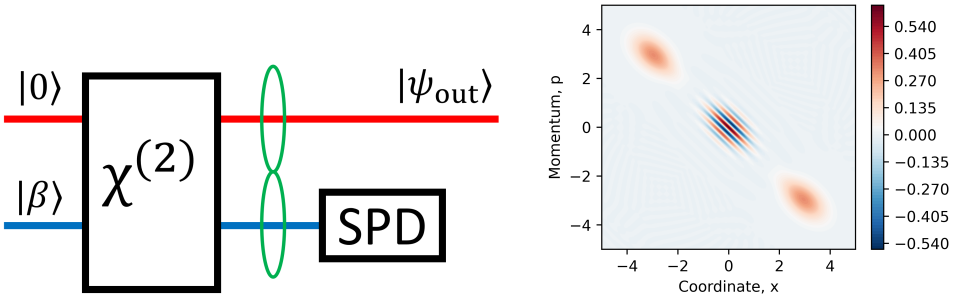

Figure 1: (Left) Scheme of proposed preparation procedure; (Right) Wigner function of the output state at the optimal time τ_{opt}. ($\beta = 3$)

τ_{opt}, and the probability of successfully SC state preparation by initial coherent input amplitude β in the pump mode (for more details see [2]).

Whispering gallery mode microresonators [3] combine low optical losses with a high concentration of the optical energy looks as a possible platform for pratical realization. The evident necessary condition for our protocol is that the preparation time t_{opt}, have to be shorter than optical mode relaxation time $t^* = Q/\omega_s$, where Q is the quality factor of the mode. Using the modern state of the art lithium niobate microresonators [4] with Q-factor $Q = 10^8$, estimation of factor $\gamma \sim 2 \cdot 10^6$ Hz and for the values of $\beta > 10$, Schröedinger cat state preparation time equal to:

$$t_{\text{opt}} \simeq \left(\frac{10}{\beta}\right)^{0.84} \times 10^{-7}\,\text{s}\,. \tag{3}$$

Taking into account the rapid progress in technologies of fabrication of the optical microresonators, the method proposed in this work can be a possible approach for preparation of bright (with $\beta \gg 1$) SC states.

This work was supported by Russian Science Foundation (Project 25-12-00263).

References

1. Dakna, M. *et al.* Phys. Rev. A **55**, 4 (1997).

2. V. L. Gorshenin, JOSA B **42**, 2 (2025).

3. D. V. Strekalov *et al.*, J. Opt. **18**, 12 (2016).

4. R. Gao *et al.*, New J. Phys. **23**, 12 (2021).

Analytical expressions for trace distance and measure of non-Markovianity for a single qubit interacting with damped single qubit environment

I. Gridnev[1,2], L.A. Mazhorina[1,2], E. A. Polyakov[1], K. Lakhmanskiy[1]

[1] Russian Quantum Center, RQC, Moscow, Russia

[2] Moscow Institute of Physics and Technology, MIPT, Dolgoprudny, Russia

gridnev.io@phystech.edu

Open quantum system is a system that interacts with the surrounding environment. Most of the existing real and experimentally accessible quantum systems have to be considered as open systems. Usually, the dynamics of open systems is described by the Gorini–Kossakowski–Sudarshan–Lindblad (GKSL) master equation [1]. This is the main equation that covers a large number of phenomena and describes many types of noise in quantum processors. However, the equation is derived under a number of simplifying approximations: The Born approximation (separability of the initial states of the open system and the environment, as well as the weakness of their interaction), the Markov approximation (the evolution of the open system at each moment in time depends only on its current state), and the rotating wave approximation (neglecting rapidly oscillating terms in the Hamiltonian). Systems whose dynamics are described by the GKSL equation are called Markovian, while violations from approximations generate the so-called non-Markovian dynamics. The development of a formalism and mathematical description of non-Markovian quantum dynamics, as well as experimental investigation and quantitative characterization of deviations from Markovianity, are the subject of active current research.

In this work, we consider how the violation of approximations in the derivation of the GKSL equation for the simple case of two interacting qubits generates non-Markovian dynamics. To quantitatively characterize the degree of non-Markovianity of the quantum dynamics we consider the Breuer-Laine-Piilo (BLP) trace distance based non-Markovianity measure [2]. This measure is experimentally accessible, has a clear intuitive interpretation and allows us to obtain results in an analytical form.

The trace distance $D(\rho_1, \rho_2)$ between two states of the system ρ_1 and ρ_2 is defined as:

$$D(\rho_1, \rho_2) = \frac{1}{2}||\rho_1 - \rho_2||, ||A|| = \sqrt{A^\dagger A} \tag{1}$$

And BLP measure has the following definition:

$$\chi = \max_{\rho_1, \rho_2} \int_0^\infty \sigma_{12}(t)\theta(\sigma_{12}(t))dt, \sigma_{12}(t) = \frac{d}{dt}D(\rho_1(t), \rho_2(t)) \tag{2}$$

where θ is the Heaviside function, and the integration is performed over time intervals where the trace distance between two evolving states of the open quantum system increases. For Markovian dynamics $\chi = 0$. Non-zero values of the measure characterise a backflow of information from the environment to the system, which is a distinct feature of non-Markovian processes.

Our model consists of system and environment qubits interacting by the following Hamiltonian:

$$H = \hbar\frac{\omega}{2}\sigma_z^S + \hbar\frac{\Omega}{2}\sigma_z^R + \hbar\frac{g}{2}(\sigma_+^S\sigma_-^R + \sigma_-^S\sigma_+^R), L = \sqrt{\gamma}\sigma_-^R \tag{3}$$

where Ω and ω – are system and environment frequencies respectively, g is the coupling constant. The reservoir qubit is subject to Markovian decay with Lindblad jump operator σ_-^R and decay γ. The decay constant of reservoir qubit controls the environment correlation time, while the coupling g sets the system-environment interaction strength. For the model, we analytically calculate the dependence of the trace distance on time for various initial states and values of coupling and environment decay, and analyze the value of the BLP measure of non-Markovianity. This work allows us to study the deviations from Markovian dynamics caused by different physical reasons and compare them quantitatively with each other.

This work was supported by Rosatom in the framework of the Roadmap for Quantum computing (Contract No. 868-1.3-15/15-2021 dated October 5).

References

1. Lindblad G. On the generators of quantum dynamical semigroups //Communications in mathematical physics. – 1976. – T. 48. – C. 119-130.

2. Breuer H. P., Laine E. M., Piilo J. Measure for the degree of non-Markovian behavior of quantum processes in open systems //Physical review letters. – 2009. – T. 103. – №. 21. – C. 210401.

Analysis of angular momentum loss experienced by a vortex electron accelerated to relativistic energies

D.V. Grosman

School of Physics and Engineering, ITMO University, St. Petersburg, Russia

dmitry.grosman@metalab.ifmo.ru

The physics of vortex particles is a rapidly developing field with a growing number of theoretical and experimental research. The common methods to generate vortex particles are diffraction on a fork grating and imprinting a helical phase with a phase plate. These methods are applicable for generating both vortex photons and charged vortex particles. However, they are limited on the energy scale and only allow to generate low-energy vortex particles. One of the possible ways to produce high-energy vortex electrons would be to employ one of the common methods to generate a vortex charged particle and then accelerate it in a linear accelerator. The only possible problem in such a scenario is that due to acceleration the charged particle will emit photons. The latter can carry away angular momentum. Thus, it is crucial to investigate the angular momentum loss due to acceleration and find a way to control the parameters of experimental set ups such that an electron does not effectively lose its vorticity upon acceleration to relativistic energies.

This study was carried out with the support of the Russian Science Foundation (project No. 23-62-10026) and the Foundation for the Advancement of Theoretical Physics and Mathematics “BASIS” (project No. 24-1-5-65-1).

Space charge region in quantum dot p-n junction

V.I. Gusev[1,2]

[1]Ioffe Institute

[2]Saint Petersburg Academic University

vlad_suns@mail.ru

Creation of photosensitive elements based on a p-n junction composed of quantum dots (QDs) (the contact between p- and n-doped QD layers) is the promising approach in the development of efficient and cost-effective photosensitive devices [1]. These quantum dots are fabricated from semiconductor materials (e.g., HgTe or CdSe) and have typical sizes ranging from 3 to 10 nm. Experimental studies have shown that in such structures the dark current under reverse bias differs just slightly from the one under forward bias [2]. It is assumed that this effect arises from the formation of a conductive channel within the QD array due to disorder — both geometric (variations in sizes and distances between quantum dots) and in the distribution of dopant impurities. However, there is currently no unified theory that could describe the behavior of such systems for different doping levels, sizes, permittivities, and other QD parameters.

This work presents a theoretical model describing a p-n junction in an array of doped quantum dots. Using computer simulations, we have obtained: the dependence of the space charge region thickness on dopant concentration, the energy band diagrams of the p-n junction under equilibrium and applied reverse bias conditions (Fig. 1). The results for weakly doped quantum dots agree with the classical bulk semiconductor p-n junction theory. At high dopant concentrations, the density of states reveals the presence of a Coulomb gap resulting from disorder in the distribution of dopants according to the Efros-Shklovskii criterion [3].

References

1. V. P. Ponomarenko, V. S. Popov, I. A. Shuklov, V. V. Ivanov, V. F. Razumov, Russian Chemical Reviews, **93**, RCR5113 (2024).

2. V. S. Popov, et al.,Technical Science, **68**, 233–236 (2023).

3. B. I. Shklovskii and A. L. Efros, Electronic Properties of Doped Semiconductors, pp. 395 (Springer, 1984).

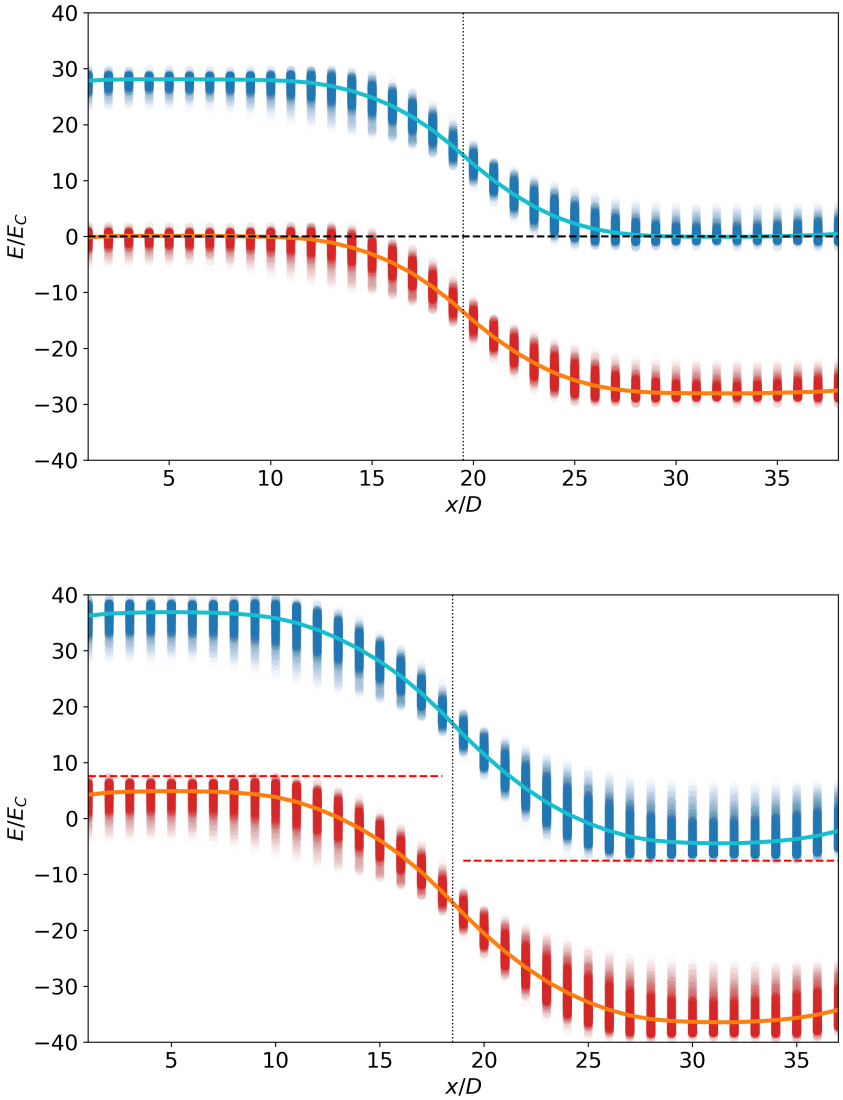

Figure 1: Example of energy diagrams of a QD p-n junction. The top figure shows the system in equilibrium; the bottom — under an applied external voltage $V = 15E_C/e$. Here, $E_C = e^2/\kappa D$ — charging energy of a quantum dot (κ - effective permittivity of a system), D — diameter of quantum dots. For each quantum dot the states in the conduction and valence bands are calculated and are shown by blue and red points, respectively. A dotted black horizontal line is Fermi level in the system. Red dotted lines are quasi Fermi level for p- and n-sides.

Quantum circuits for learning transport maps

D. Guskov

Skolkovo Institute of Science and Technology

d.guskov@skoltech.ru

We introduce a quantum circuit-based framework to learn transformations between data distributions by treating interpolation as a boundary-value problem. The key idea is to train a variational quantum circuit $Q_\theta(x, z)$ that distinguishes between points from a source distribution and a target distribution by evaluating pairs (x, z). For each sample pair (x, y), the circuit is trained to satisfy:

$$Q_\theta(x,z) = \begin{cases} 0 & \text{if } z = x \text{ (source anchor)}, \\ 1 & \text{if } z = y \text{ (target match)}, \\ \sin(\frac{\pi}{2}t) & z_t = (1-t)x - ty, \end{cases} \tag{1}$$

The last one to encourage meaningful paths between source and target, we enforce a smooth interpolation constraint, where z_t defines a linear path in data space between x and y. The sinusoidal target ensures smoothness and monotonicity along the path, aligning with a notion of flow from x to y. Once trained, the circuit implicitly defines a transformation from the source to the target distribution. To recover the transport map $T(x)$, we solve:

$$T(x) = \arg\min_{x^*} \underbrace{(Q_\theta(x, x^*) - 1)^2}_{\mathcal{L}(x^*)} \quad \text{(gradient-based inversion)} \tag{2}$$

The quantum circuit's ability to encode complex mappings is enabled by a reuploading architecture, where alternating input embeddings and trainable unitaries build expressive correlations between x and z.

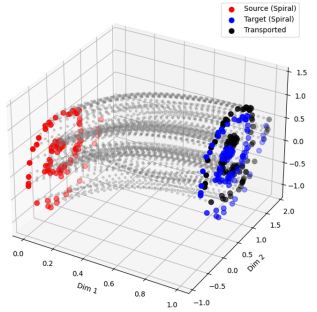

(a) Spiral-to-spiral Transform

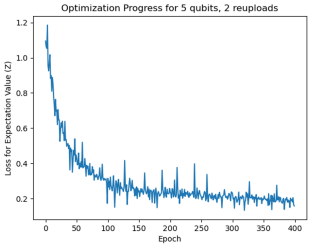

(b) Interpolation loss $||Q_\theta(x, z_t) - \sin(\frac{\pi}{2}t)||^2$

Sturmian basis and finite-size nucleus calculations

V.K. Ivanov[1] and D.A. Glazov[1]

[1]School of Physics and Engineering, ITMO University, 197101 St. Petersburg, Russia

[1]vladislav.ivanov@metalab.ifmo.ru

One of the powerful computational methods in atomic physics is the Raylaigh-Ritz method, in which one use a finite basis set of functions to find atomic spectra or to approximate a Green's function. Such method is applied for both relativistic and non-relativistic problems, to find quantum-electrodynamic corrections.

The problem of finding an appropriate basis set is a complicated task, since different basis sets, such as B-splines or Gaussians, have their own drawbacks and fit a certain range of problems. One such set is the so-called Sturmian basis [1]:

$$S_{nl}(x) = N s_{nl}(x), \tag{1}$$

$$s_{nl} = x^{l+1} e^{-x/2} L^{2l+1}_{n-l-1}(x) \tag{2}$$

and N is a normalization factor (Fig. 1). These functions have a tridiagonal Gram matrix and are orthogonal with $1/x$ weight. These features make Coulomb the Sturmians very convenient for being used in finite-basis-set [2]

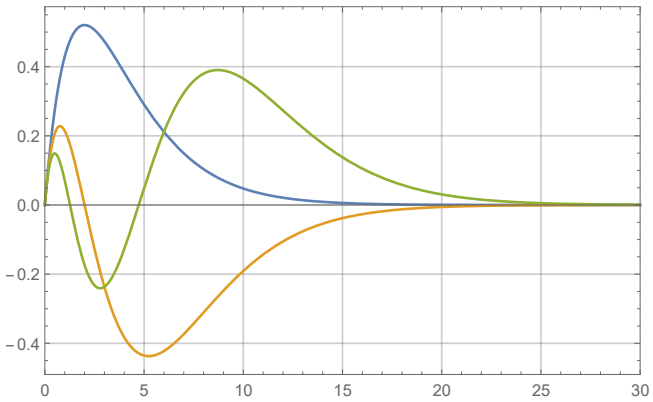

Figure 1: Normalized Coulomb Sturmian functions $S_{nl}(x)$, $l = 0$, $n = 1, 2, 3$.

We provide calculations of atomic spectra of hydrogen-like heavy ions, using the Coulomb Sturmian basis set. We consider both Coulomb and hollow shell potentials. While Coulomb Sturmians are defined by solving a non-relativistic equation with Coulomb potential, it provides good results for a relativistic problem with arbitrary

potential; for shell potential, such functions have correct asymptotics near zero. For example, in yields $E_{1S_{1/2}} = 0.931\ 063\ 254\ 367\ 882$ (a.u.) for $Z = 50$. These developments have the potential to facilitate atomic calculations, especially in cases where the application of other basis sets poses significant challenges.

References

1. M. Rotenberg, Annals of Physics **19**, 262-278 (1962).

2. I. P. Grant and H. M. Quiney, Phys. Rev. A **62**, 022508 (2000).

The single-qudit phases accumulated in entanglement gates in trapped ions

P. Kamenskikh[1,2], N. Semenin[1,2], I. Zalivako[1,2], I. Semerikov[1,2], A. Borisenko[1,2], K. Khabarova[1,2], N. Kolachevsky[1,2]

[1] P.N. Lebedev Physical Institute of the Russian Academy of Sciences, Moscow 119991, Russia

[2] Russian Quantum Center, Skolkovo, Moscow 121205, Russia

kamenskikh.pa@gmail.com

The use of qudits nowadays is an efficient tool to scale a quantum computer. However, with the use of qudits, quantum logic becomes more complex and requires careful monitoring of relative phases between different qudit levels. In particular, when considering entangling operations between qudits in trapped ions, it is essential to account for the phases that accumulate on certain levels. These additional phases are no longer global, as they are in qubit architecture. We present research that explores the theory behind additional two-qudit phases that arise from various entangling operations in trapped ion systems. We consider $\sigma_\phi \otimes \sigma_\phi$ and $\sigma_Z \otimes \sigma_Z$ gates including their variations with amplitude/phase-modulated laser pulses and take into account interaction with multiple motional modes.

The scheme, to implement the $\sigma_X \otimes \sigma_X$ gate or Mølmer and Sørensen(MS) gate [1] is shown in Fig. 1a. The evolution operator for MS gate has the form:

$$\hat{\mathrm{MS}} = \prod_{j=1,2} e^{i\chi_{jj}^{MS}(|0_j\rangle\langle 0_j| + |1_j\rangle\langle 1_j|)} \exp\Big(2i\chi_{12}^{MS}\sigma_X^{(1)}\sigma_X^{(2)}\Big), \tag{1}$$

the first term in the evolution operator represents the single-qudit phase χ_{jj}^{MS}, on which we are focusing in this work. The second term in (1) stands for the entanglement between the target ions.

The scheme, to implement the $\sigma_Z \otimes \sigma_Z$ gate or Light Shift(LS) gate is shown in Fig. 1b. The evolution operator for LS gate:

$$\hat{\mathrm{LS}} = \exp\left(2i\chi_{12}^{LS}\sum_{s,s'=0}^{d-1}\theta_s\theta_{s'}\left|ss'\right\rangle\!\left\langle ss'\right| + i\sum_{j=1}^{2}\hat{\Phi}_j\right), \tag{2}$$

where θ_s is the ratio between the light shift of the states $|s\rangle$ and $|0\rangle$. The $\hat{\Phi}_j$ is an operator that changes phases on the single qudits states.

We propose three methods to compensate for single-qudit phases. The first method involves optimizing gate parameters to ensure phase cancellation by the end of the operation(see Fig. 1c). The second method employs single-qudit rotations to compensate

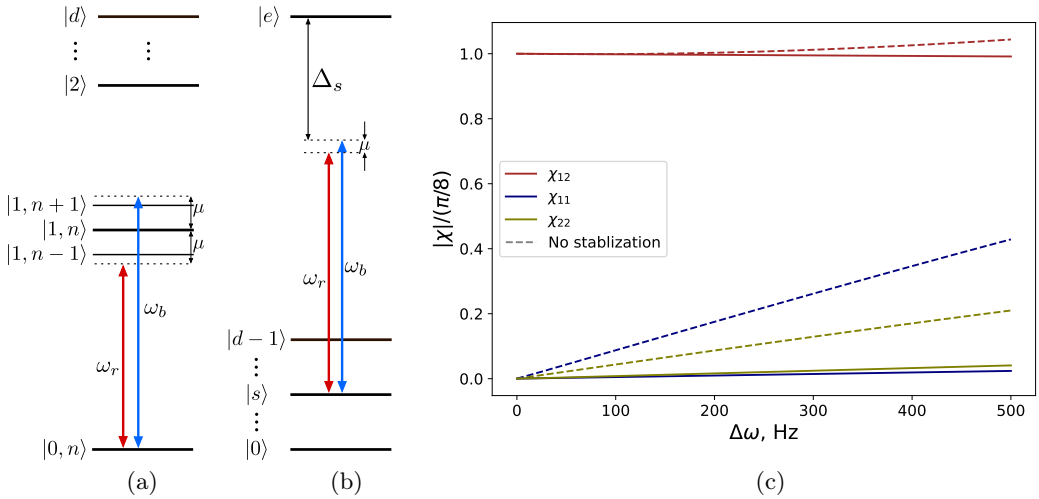

Figure 1

for unwanted phase shifts. The third method, applicable only to the $\sigma_Z \otimes \sigma_Z$ gate, is a spin-echo sequence. The spin-echo sequence has previously been applied to qudits in [2]. However, in this work, we examine the most general case of the $\sigma_Z \otimes \sigma_Z$-gate, where the light shifts of all qudit levels are significant. The spin-echo sequence not only allows us to mitigate single-qubit phases, but it also helps symmetrize the LS-gate.

We measured the single-qudit phases accumulated in $\sigma_\phi \otimes \sigma_\phi$-gate in our experimental setup. In the experiment, numerous factors can influence the phase of qudit levels, including interaction with the carrier, the AC-Stark shift, etc. Some of these phase shifts can be mitigated through careful calibration of experimental parameters. Aligning the experimental phases with theoretical predictions enables precise calibration of two-qudit operations.

References

1. Mølmer K and Sørensen A, Physical Review Letters. 82.9 (1999): 1835.

2. Hrmo, Pavel, et al. Nature Communications 14.1 (2023): 2242.

Attosecond-Scale Features of Cherenkov Radiation in Phase Space

D. Kargina[1] and D. Karlovets[1]

[1] School of Physics and Engineering, ITMO University, 197101
St. Petersburg, Russia

daria.kargina@metalab.ifmo.ru

The classical theory of Cherenkov radiation developed by I.Tamm and I.Frank [1] allowed the phenomenon to be commonly used in particle detection experiments, for instance, in neutrino telescopes [2] and gamma-ray astronomy [3]. Despite the simplicity of the classical interpretation of the mechanism, which consists in the polarization of atomic shells by the field of the charge, the complete quantum picture of the Cherenkov radiation has remained hidden.

The quantum description in phase space provides access to the spatiotemporal dynamics at femto- and attosecond time scales, as well as to microscopic features within the formation zone. Such predictions cannot be obtained using the momentum-space approach under the far-field approximation. Here, we present a quantum optics interpretation of Cherenkov radiation using a Wigner function to describe the emitted photon field. By analyzing the correlation radius, it is possible to determine the regions where the spatiotemporal dependence of the Wigner function becomes negligible. We focus on the formation zone, where the Cherenkov cone has not yet formed. In this regime, we observe a quantum shift in photon detection time on the attosecond scale, emphasizing the atomic-scale nature of Cherenkov radiation and suggesting a connection to the Stark effect.

The proposed quantum theory in phase space reveals several novel features, including a negative quantum shift, a negative diffraction time near the Cherenkov angle and a correlation between the duration of the Cherenkov flash and the length of the initial electron wavepacket.

References

1. I. Frank and I. Tamm, Doklady Akad. Nauk SSSR **14**, 107 (1937).

2. V. A. Allakhverdyan *et al.*, Phys. Rev. D **107**, 042005 (2023).

3. E. Aliu *et al.*, Astroparticle Physics **30**, 293 (2009).

Theoretical modeling of the electronic structure of ytterbium halide crystals

P.A. Khadeeva[1,2], V.M. Shakhova[1], Y.V. Lomachuk[1], N.S. Mosyagin[1], A.V. Titov[1,2]

[1] NRC "Kurchatov Institute" – PNPI, Gatchina, Russia

[2] Saint-Petersburg State University, Saint Petersburg, Russia

khadieieva_p@pnpi.nrcki.ru

A combined method for modeling the electronic structure of materials using compound-tunable embedding potentials (CTEP) has been developed in the Department of Quantum Physics and Chemistry of the NRC «Kurchatov institute» - PNPI [1, 2, 3]. The CTEP for a given crystal fragment is constructed in three stages. At the first stage, the CRYSTAL program calculates the electronic structure of a crystal with periodic boundary conditions. At the second stage, the main cluster is selected and the compound-tunable pseudopotentials with a large core (which will be used to describe the immediate environment of the crystal fragment of interest within the framework of the embedding potential) are optimized so that the electron density in the region around the central atom up to its immediate environment is reproduced with required accuracy as in the crystal. In the third stage, cluster calculations of the crystal fragment are performed, and the properties of the compound are studied.

The chemical shift (CS) of the X-ray emission spectra (XES) lines was chosen as an independent criterion to verify the accuracy of reproducing the electron density of the crystal fragment. For each compound, the CSs of the XES lines are characteristic and highly sensitive to the electronic state of the d- or f-element. Direct methods for calculating this property are practically inapplicable to the study of such compounds, so a new two-step calculation method was developed [4].

However, this approach still has limited capabilities due to its enormous computational complexity, so pilot calculations were carried out. For this, ytterbium fluorides and chlorides were chosen, as these systems predominantly contain ionic bonds that simplify the analysis of contributions to the CS of XES lines [5, 6].

Using this combined method, crystals with an ionic-covalent bond type and a lanthanide atom in a periodic structure were studied. In the work, an analysis of the structural parameters of the crystals was carried out, obtained within the framework of calculations with periodic boundary conditions, and the various versions of pseudopotentials (PPs) were used to describe the ytterbium atom. A fragment models for crystals was constructed using the CTEP method. For ytterbium fluorides and chlorides, preliminary calculations of chemical shifts of X-ray emission spectrum lines for CTEP crystal fragments were carried out using the relativistic coupled cluster method with single and double exitations.

This work was supported by Russian Science Foundation, grant No. 24-73-00076 (https://rscf.ru/project/24-73-00076/)

References

1. V. M. Shakhova *et al*, Phys. Chem. Chem. Phys. **24**, 19333–19345 (2022).
2. Y. V. Lomachuk *et al*, Phys. Chem. Chem. Phys. **22**, 17922–17931 (2020).
3. D. A. Maltsev *et al*, Phys. Rev. B. **103**, 205105 (2021).
4. Y. V. Lomachuk *et al*, PRA. **88**, 062511 (2013).
5. P. A. Khadeeva *et al*, Mosc. Univ. Chem. Bull. **79**, 288–293 (2024).
6. P. A. Khadeeva *et al*, Molecular Physics, (2025).

Ultrastable lasers and optical clocks for fundamental research

O. V. Khronusova[1,2], K. S. Kudeyarov[1], A. M. Russkih[1,2], N. O. Zhadnov[1], D. A. Mishin[1], K. Yu. Khabarova[1], N. N. Kolachevsky[1,3]

[1] P. N. Lebedev Physical Institute

[2] Moscow Institute of Physics and Technology

[3] Russian Quantum Center

olya.hronusova@gmail.com

Nowadays ultrastable lasers with highly narrow spectral linewidth are widely used in precision measurements. Modern technologies allow creating lasers with linewidth less than 0.1 Hz and fractional frequency instability below 10^{-16} [7]. Ultrastable lasers have a wide range of applications, from sensing to spectroscopy. Besides, their exceptional precision as measurement tools enables tests of fundamental theories, including searches for phenomena beyond the Standard Model.

The most established method to create an ultrastable laser is to lock its frequency to a high-finesse Fabry-Perot cavity using the Pound-Drever-Hall (PDH) method [1]. The ultimate frequency stability of such a laser is typically limited by thermal noise-induced mirror surface fluctuations, which constrain the reference cavity length stability.

Ultrastable lasers serve as the local oscillator in optical atomic clocks [4], which are among the most precise tools for testing Einstein's theory of general relativity. According to this theory, a clock at a higher altitude ticks faster than one at a lower altitude, so one can detect the gravitational potential difference by comparing them. The unprecedented low frequency uncertainty of optical clock enables resolving height differences at millimetre-scale [6].

Our laboratory is also building an experiment to measure the gravitational potential using two optical lattice clocks based on cold thulium atoms [8]. The straightforward way to enhance its resolution is to replace the current clock laser (that has fractional frequency instability of 2×10^{-15}) with a better one. In order to achieve that goal we are developing the laser based on a cryogenic silicon cavity with thermal noise limit 2×10^{-16} [2]. However, reaching this limit requires the studying and suppression of various technical noise sources.

Other fundamental features that can be probed by optical clock are parameters of dark matter particles and variation of fundamental constants [3, 5]. By comparing two optical clocks with different types of clock transitions (and therefore, different sensitivity to studied phenomenon), one can place constraints on these effects. Additionally, ultrastable optical cavities themselves can serve as detectors [3]: the comparison of

resonant frequencies of cavity with suspended mirrors and rigid one allows to study particularly the sector of ultralight dark matter.

References

1. R. W. P. Drever *et al.*, Appl. Phys. B **31**, 97–105 (1983).
2. N. O. Zhadnov *et al.*, Quantum Electronics. **47**, 421–425 (2017).
3. A. A. Geraci *et al.*, Phys. Rev. Lett. **123**, 031304 (2019).
4. M. Takamoto *et al.*, Nat. Photonics **14**, 411–415 (2020).
5. E. Savalle *et al.*, Phys. Rev. Lett. **126**, 051301 (2021).
6. T. Bothwell *et al.*, Nature, **602**, 420–424 (2022).
7. D. Kedar *et al.*, Optica. **10**, 464–473 (2023).
8. A. Golovizin *et al.*, Jetp Lett. **119**, 659–664 (2024).

Does Brownian motion become quantum at zero temperature?

D. O. Kondaurov[1] and E. A. Polyakov[1]

[1] Russian Quantum Center

kd8466@mail.ru, evgenii.poliakoff@mail.ru

Classical Brownian motion is a well-known and well-studied process that occurs in a large number of applied problems where one has to consider the motion of a particle in some environment with dissipation and random noise, for example, when describing chemical reactions, microscopic biological processes, etc. Such a problem also occurs at smaller scales, for example, to describe the decay of metastable states, surface effects in superconductors, diffusion in metals, where it is already necessary to take into account quantum effects [1]. Attempts to quantize Brownian motion began more than 50 years ago, but there is still no single theory.

In the classical case, we have the Langevin equation, which allows for the Markov limit. The actual problem is how can we describe this in the quantum case? In quantum optics, the Markov limit usually leads to the Lindblad equation. By analogy, the papers related to quantum Brownian also usually consider the Lindblad equation. However, for Brownian motion at low temperatures, it is not completely positive. To correct this, an additional term is added in the literature, which is non-physical and diverges in the limit of low temperatures, when quantum effects are important [2]. Therefore, the open problem remains how to correctly preform the Markov limit in the quantum Brownian motion.

The goal of our work is to consider the low-temperature limit of classical Brownian motion with white noise within the framework of a microscopically justified model and to answer two questions: does Brownian motion become quantum at low temperatures and does it remain Markovian?

We consider the Caldeira-Leggett model [3]

$$H = \frac{p^2}{2m} + V(x) + \sum \left(\frac{p_i^2}{2m_i} + \frac{m_i\omega_i^2 x_i^2}{2}\right) + \sum \left(-c_i x_i x + \frac{c_i}{2m_i\omega_i^2}x^2\right)$$

Environment can be described by spectral density $J(\omega) = \frac{\pi}{2}\sum \frac{c_i^2}{m_i\omega_i}\delta(\omega - \omega_i)$, which leads to the Langevin equation in the Ohmic case $J(\omega) = \gamma m\omega e^{-\varepsilon\omega}$.

Classic closed equation of motion for particle

$$\dot{p} = -\frac{\partial V}{\partial x} - x(0)M(t) - \int_0^t p(\tau)M(t-\tau)\,\mathrm{d}\tau + \xi(t)$$

Memory function $M(t) = \frac{2\gamma}{\pi}\frac{\varepsilon}{\varepsilon^2+t^2}$ leads to delta-function at small ε, so in the limit

$\gamma\varepsilon \to 0$ we obtain classic Markovian Langevin equation with white noise.

$$\dot{p} = -\frac{\partial V}{\partial x} - \gamma p + \xi(t), \quad \langle \xi(t_1)\xi(t_2)\rangle = 2m\gamma T\delta(t_1 - t_2)$$

We considered this limit in quantum case, using influence functional method [3],[4]. Exact solution for quantum Caldeira-Legget model with taking into account initial correlations between particle and environment leads to prefactor $exp(-\frac{mE_{vac}}{\hbar^2}q^2)$ in density matrix, where $E_{vac} = \frac{\gamma\hbar}{2\pi}ln(\frac{1}{\gamma\varepsilon})$, so in the limit $\gamma\varepsilon \to 0$ it becomes quasi-diagonal and corresponds to classical probability distribution.

Using path integral approach for classical stochastic processes [5], we have shown that the path integral for quantum Brownian motion reduces to the path integral for the classical stochastic process in this limit.

In the classical case, we have the Langevin equation, which becomes Markovian in the limit $\gamma\varepsilon \to 0$. We conclude that, in contrast to quantum optics, the Brownian motion does not become quantum-Markovian (i.e. does not satisfy any Lindblad-type equation while retaining quantum coherences in the particle's density matrix) in this limit. Instead, the spatial coherences die away in this limit, and the particle dynamics becomes effectively classical stochastic, but with different noise statistics, caused not by the thermal nature, but by vacuum fluctuations, which leads to non-Markovian behavior and logarithmic diffusion.

$$m\ddot{x} = -m\gamma\dot{x} + \tilde{\xi}(t), \quad \langle \tilde{\xi}(t)\tilde{\xi}(t+\tau)\rangle = \frac{2\gamma m\hbar}{\pi}\frac{\varepsilon^2 - \tau^2}{(\varepsilon^2 + \tau^2)^2}$$

This work was supported by Rosatom in the framework of the Roadmap for Quantum computing (Contract No. 868-1.3-15/15-2021 dated October 5).

References

1. P. Hänggi, P. Talkner, M. Borkovec, *Reaction-rate theory: fifty years after Kramers*, Rev. Mod. Phys. **62**, 251 (1990).

2. H.-P. Breuer and F. Petruccione, *The Theory of Open Quantum Systems*, Oxford University Press (2002).

3. A. O. Caldeira and A. J. Leggett, *Path integral approach to quantum Brownian motion*, Physica A **121**, 587 (1983).

4. H. Grabert, P. Schramm, and G.-L. Ingold, *Quantum Brownian motion: The functional integral approach*, Phys. Rep. **168**, 115 (1988).

5. P. Hänggi, *Path Integral Solution for Nonlinear Generalized Langevin Equations*, in: *Path Integrals from meV to MeV: Tutzing '92*, eds. H. Grabert, A. Inomata, L. Schulman, U. Weiss, World Scientific (Singapore, 1993), pp. 289–301.

A new type of artificial Josephson atom for quantum simulation of topological models

E. Konopleva[1,2], G. Fedorov[2], O. Astafiev[1,2]

[1] Skolkovo Institute of Science and Technology

[2] Moscow Institute of Physics and Technology

Ekaterina.Konopleva@skoltech.ru

1. Introduction

Topologically non-trivial phenomena are not limited to fermionic structures and have been predicted in a number of other systems, including photonic platforms. Photonic extensions of topological models, such as the "Zig-Zag" model [1], possess an additional degree of freedom—polarization and have been studied in systems of plasmonic and dielectric nanoparticles, as well as in polariton microcavities. Considering the aforementioned limitations of photonic systems related to medium linearity and high losses, Josephson artificial atoms offer several advantages, such as easy scalability and relative freedom in choosing the topology [2].

2. Results

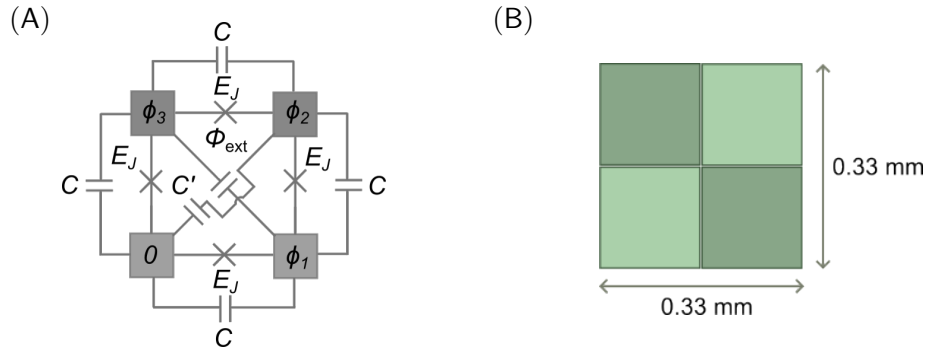

Figure 1: (A) Electrical scheme and (B) a physical element

In this work, we present and numerically study the design of a polarization transmon as a component base for simulators of photonic topological models. The electrical

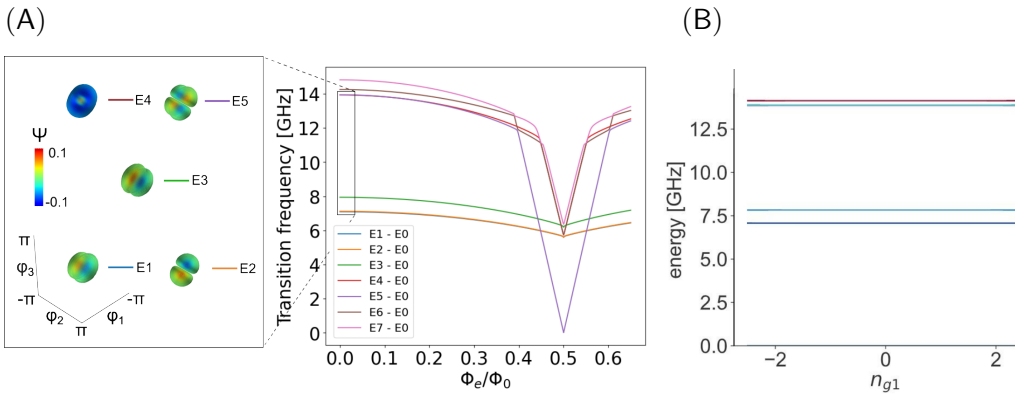

Figure 2: *(A)* External flux spectrum Φ_{ext}/Φ_0 and *(B)* charge dispersion

circuit of the studied nonlinear system and its physical element are shown in Figure 1.

The capacitances and Josephson energy of the given topology have the following values: $C = 33.9\,\text{fF}$, $C' = 7.7\,\text{fF}$, and $E_J = 14.9\,\text{GHz}$. The transition eigenenergies were numerically calculated as $\omega_{1-3} = 7.07, 7.07, 7.83$ GHz at $\Phi_{\text{ext}} = 0$. The two lowest levels are degenerate and characterized by orthogonal dipole fields.

The spectrum as a function of external flux was plotted and is presented in Figure 2 (A). At $\Phi_{\text{ext}}/\Phi_0 \approx 0.5$, the potential becomes double-welled, leading to hybridization between localized states. The spectrum as a function of charge noise is shown in Figure 2 (B), demonstrating charge noise suppression due to the high $E_J/E_C \approx 100$ ratio.

3. Conclusion

Thus, we have presented and characterized the design of an artificial atom capable of supporting arbitrary polarization states. Our analysis revealed the presence of degenerate ground-state transitions with orthogonal dipolar modes and demonstrated charge noise suppression in the operational regime.

This work was supported by Russian Science Foundation, project №25-22-00280

References

1. A. Poddubny, ACS Photonics. 1. 101–105. (2014).

2. T. P. Orlando, Physical Review B. 60(22), 15398. (1999)

Evaluation of spectroscopic parameters of a thorium tetrafluoride crystal fragment

A.E. Krasnikova [1,2], P.A. Khadeeva [1,2], V.M. Shakhova [2], N.S. Mosyagin [2], A.V. Titov [1,2]

[1] Saint-Petersburg State University, Saint Petersburg, Russia

[2] NRC "Kurchatov Institute" – PNPI, Gatchina, Russia

st085026@student.spbu.ru

High-precision theoretical modeling of the electronic structure and properties of materials based on d- and f-elements is important for understanding the atomic-level processes occurring within them and for planning experiments aimed at minimizing systematic errors in measuring physical-chemical characteristics. Additionally, it is crucial for interpreting the results of experiments searching for new physics.

However, studying the electronic structure of compounds containing heavy d- and f-elements faces several challenges. To describe crystalline compounds, the "compound-tunable" embedding potential method (CTEP) was developed in the Department of Quantum Physics and Chemistry at PNPI (Petersburg Nuclear Physics Institute) [2, 3, 4].

Constructing the embedded clusters with CTEP is carried out in three stages. The first stage involves modeling the electronic structure of the crystalline compound using periodic boundary conditions. The second stage consists of constructing the embedded cluster, with the primary goal of reproducing the electron density in the region around the central atom up to its nearest neighbors. The third stage involves investigating the electronic structure of the crystal fragment using CTEP.

This work presents a theoretical study of the electronic structure of thorium tetrafluoride (ThF4) crystals, which could be used in experimental searches for hypothetical variations in fundamental constants, such as the fine-structure constant and the proton-to-electron mass ratio. The study [1] demonstrates that thin films based on ThF4 crystals could be utilized to create integrated and universal solid-state nuclear clocks. The high density of nuclear emitters (Th-229) in ThF4 also suggests greater sensitivity in experiments searching for new physics.

Using the combined theoretical approach, a crystal ThF4 was investigated. An embedded cluster with CTEP was constructed for this compound, and its spectroscopic parameters were analyzed.

This work was supported by Russian Science Foundation, grant No. 24-73-00076 (`https://rscf.ru/project/24-73-00076/`)

References

1. Zhang et al., arXiv:2410.01753 (2024).

2. Y. V. Lomachuk, D. A. Maltsev, N. S. Mosyagin, L. V. Skripnikov, R. V. Bogdanov and A. V. Titov, Phys. Chem. Chem. Phys., 2020, 22, 17922–17931.

3. D. A. Maltsev, Y. V. Lomachuk, V. M. Shakhova, N. S. Mosyagin, L. V. Skripnikov and A. V. Titov, Phys. Rev. B, 2021, 103, 205105.

4. V. M. Shakhova, D. A. Maltsev, Y. V. Lomachuk, N. S. Mosyagin, L. V. Skripnikov and A. V. Titov, Physical Chemistry Chemical Physics, 2022, 24, 19333–19345.

P,T-odd polarization of levels in triatomic molecules

I. Kurchavov[1], L. Skripnikov[1,2], A. Petrov[1,2]

[1] Petersburg Nuclear Physics Institute

[2] Saint Petersburg State University

kurchavov_ip@pnpi.nrcki.ru, petrov_an@pnpi.nrcki.ru

The search for the electric dipole moment (EDM) of the electron and the magnetic quadrupole moments (MQM) of the nuclei, especially in triatomic molecules such as $LuOH^+$ [1], opens new perspectives in searches beyond the standard model. These laser-cooled molecules are sensitive to T, P-violating interactions. In this work, an improved method for calculating the degree of polarization of molecules was used to study the contributions of the EDM and MQM.

Calculations performed for the $^{175}LuOH^+$ molecule [2] with the spin of the lutetium nucleus $I = 7/2$ showed that the contribution of the MQM can vary significantly depending on the external electric field. The results obtained so far are presented in Table 1 and Figure 1. The degree of polarization of the levels turned out to be less than $P_e < 0.58$ for the EDM and $P_M < 0.12$ for the MQM for most states of the molecule, which is almost identical to the results previously obtained for the YbOH molecule [3]. This limitation is associated with the peculiarities of the l-doubling structure of linear triatomic molecules, for which the polarization saturation at high external fields does not reach 100%. Also, the stretching mode was taken into account for the first time, and it leads to a decrease in the values of polarization for the electron EDM and the nuclear MQM by about 4-5% at an electric field of E = 50-100 V/cm.

The results of the studies show that the use of these calculations can improve the accuracy of experiments aimed at measuring the MQM and EDM. These experiments will help to better understand T, P-violating interactions and expand understanding of the properties of elementary particles such as quarks and nucleons [4].

The work was supported by the grant of the Russian Science Foundation No. 24-12-00092.

References

1. Daniel E. Maison *et al.*, Phys. Rev. A **106**, 062827 (2022).

2. I. Kurchavov *et al.*, Phys. Rev. A **108**, 052815 (2023).

3. I. Kurchavov, A. Petrov, Phys. Rev. A **106**, 062806 (2022).

4. L.V. Skripnikov *et al.*, Phys. Rev. Lett. **113**, 263006 (2014).

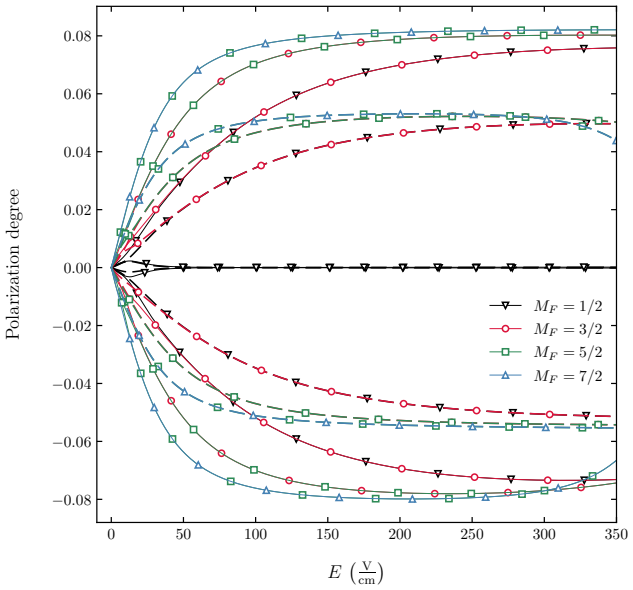

Figure 1: Calculated polarizations $P_e/7$ (solid) and P_M (dashed) for the selected levels for the different values of M_F of the lowest $N = 1$ rotational level of the first excited the $\nu_2 = 1$ bending vibrational mode of ^{175}LuOH$^+$ as functions of the external electric field.

Table 1: Calculated vibrational energy levels (cm^{-1}) rotational constants B (cm^{-1}), and $l-$doubling (MHz) for the excitation modes of stretching $\nu_1 = 0 - 1$ and bending $\nu_2 = 0 - 2$ quanta of ^{175}LuOH$^+$.

Parameter	CCSD(T) (R-frozen)	CCSD	CCSD(T)
$\nu_1 = 0, \nu_2 = 0$	0	0	0
$\nu_1 = 0, \nu_2 = 1$	442	438	434
$\nu_1 = 1, \nu_2 = 0$		750	745
$\nu_1 = 0, \nu_2 = 2^0$	871	864	856
$\nu_1 = 0, \nu_2 = 2^2$	898	887	879
$B(\nu_1 = 0, \nu_2 = 0)$	0.2879	0.2874	0.2868
$B(\nu_1 = 0, \nu_2 = 1)$	0.2881	0.2869	0.2863
$B(\nu_1 = 1, \nu_2 = 0)$		0.2862	0.2855
$B(\nu_1 = 0, \nu_2 = 2^0)$	0.2883	0.2870	0.2864
$B(\nu_1 = 0, \nu_2 = 2^2)$	0.2882	0.2919	0.2912
l-doubling $(\nu_1 = 0, \nu_2 = 1)$	23.5	24.4	24.5
l-doubling $(\nu_1 = 0, \nu_2 = 2^2)$	0.005	0.005	0.005

Two-loop self-energy corrections to one-photon recombination process in hydrogen atom

P. Kvasov[1], D. Solovyev[1,2], T. Zalialiutdinov[1,2]

[1]Department of Physics, St. Petersburg State University, Petrodvorets, Oulianovskaya 1, 198504, St. Petersburg, Russia

[2]Petersburg Nuclear Physics Institute named by B.P. Konstantinov of National Research Centre "Kurchatov Institut", St. Petersburg, Gatchina 188300, Russia

st103333@sudent.spbu.ru

Abstract

In this work, two-loop self-energy corrections to the single-photon recombination process are examined. Within the framework of rigorous relativistic quantum electrodynamics and the S-matrix formalism, we derive analytical expressions and perform numerical computations for radiative corrections to the one-photon recombination cross-section. We demonstrate that the imaginary component of the one-loop bound-electron self-energy operator, when averaged over continuum wave functions, naturally leads to the well-established expression for the one-photon recombination cross-section. Furthermore, we extend this approach to show that the dominant correction to the free-bound one-photon process can be extracted in a similar fashion by examining the imaginary part of the two-loop self-energy. The findings of this work may provide deeper theoretical insight into hydrogen recombination kinetics and could prove valuable for astrophysical studies of the primordial hydrogen plasma in the early universe.

Key words: Theoretical Physics, Atomic Physics, Astrophysics

Recently, in the previous work of our scientific group, it was shown that in the presence of cascade processes, there is a fundamental difference between the two-photon level width of the excited atomic state and the corresponding two-photon transition rate [1, 2]. In particular, in [1], using the example of bound $ns/nd - 1s(n \geq 3)$ transitions in hydrogen, it was shown that the two-photon widths of the excited levels, evaluated as the imaginary part of the two-loop bound electron self-energy correction to the energy level, differ from the corresponding two-photon decay rates when one-photon cascade processes are taken into account. The obtained results can be interpreted as radiative corrections to the one-photon width.

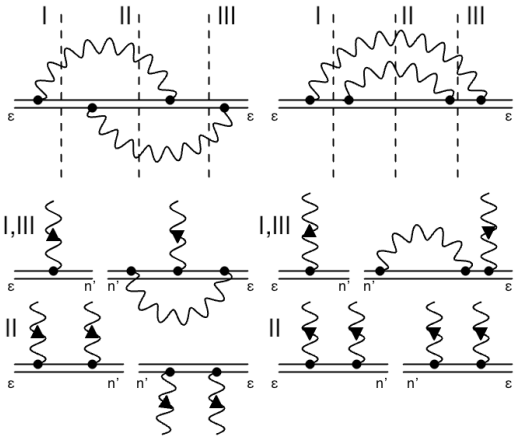

Figure 1: The Feynman diagram of irreducible contributions to the two-loop self-energy of the bound electron: "loop within a loop" and "crossed loops". The irreducible contribution is obtained only by cutting in the region II.

In the present work, we continue our investigation by focusing on free-bound processes, and consider the dynamics of two-photon recombination in the hydrogen atom. Within the framework of quantum electrodynamics and the S-matrix formalism, we provide an analytical derivation and numerical results for the radiative corrections to the one-photon recombination cross-section, as well as to the recombination coefficients. Following the approach developed in [4], we consider the imaginary part of the two-loop self-energy operator averaged over the wave functions of the continuum spectrum, see Fig. 1. It is shown that, within this approach, the resulting expression contains no resonance terms and represents a radiative correction to the one-photon recombination cross-section.

References

1. T. Zalialiutdinov, D. Solovyev, L. Labzowsky, and G. Plunien, Phys. Rev. A 89, 052502 (2014)

2. T. Zalialiutdinov, A. Anikin, and D. Solovyev, Phys. Rev. A 102, 032204 (2020)

3. U. D. Jentschura, Phys. Rev. A 69, 052118 (2004)

4. D. Solovyev, T. Zalialiutdinov, A. Anikin, J. Triaskin, and L. Labzowsky Phys. Rev. A 100, 012506 , (2019)

Gauge invariance of self-energy diagram: Lamb shift and g factor

E. Lazarev[1] and M. Reiter[2]

[1] School of Physics and Engineering, ITMO University, St. Petersburg, Russia

[2] Department of Physics, St. Petersburg State University, St. Petersburg, Russia

egor.lazarev@metalab.ifmo.ru

Quantum electrodynamics (QED) predictions are well known as the best in agreement with experimental results. Such a phenomenon could be seen in Lamb shift QED predictions [1, 2]. Modern spectroscopy methods improved the accuracy of g-factor measurements up to 10^{-11} [3]. Moreover, recent study [4] has shown detection of g-factor difference in coupled ions on the level of accuracy of 10^{-13}. In order to compare these experimental results with bound state QED calculations, it's necessary to evaluate at least first and second order QED corrections with significant precision, which is a challenging problem.

Common methods of determining self-energy corrections use potential decomposition, which helps to cancel ultraviolet and infrared divergences [5, 6]. The main error of the self-energy correction consists in the partial wave expansion of the many-potential term. Accelerated convergence of these series could be obtained by subtracting the quasi-two-potential contribution from the many-potential term. This approach is proposed by Sapirstein and Cheng [7, 8]. The self-energy correction to the bound-electron g factor has been evaluated, e.g., in [9, 10, 11]. In general, both experimental and theoretical accuracy for the g factor of few-electron ions is quite high, up to 10^{-12}, so the precision calculations of the QED corrections are in demand.

The global idea of the current work is to change the gauge of the photon propagator in the self-energy loop. Invariance of the first-order diagrams towards this change is trivial. However, for higher-order diagrams with two or more photons, changing the gauge only in the self-energy loop while keeping the other photons' gauge the same is not invariant in general. It turns out that some diagrams or sets of diagrams are invariant to that change of gauge, so this approach allows us to improve the accuracy of calculations by using the most appropriate gauge in the self-energy loop. Accordingly, we evaluated SE corrections to the Lamb shift and g factor and compared the convergence of many-potential terms in Feynman and Coulomb gauges. From Fig. 1 one can see that contributions of zero-, one- and quasi-two-potential terms in the Coulomb gauge are less in magnitude than in the Feynman gauge (a). But at the same time, the many-potential term converges more slowly in the Coulomb gauge than in the Feynman one (b).

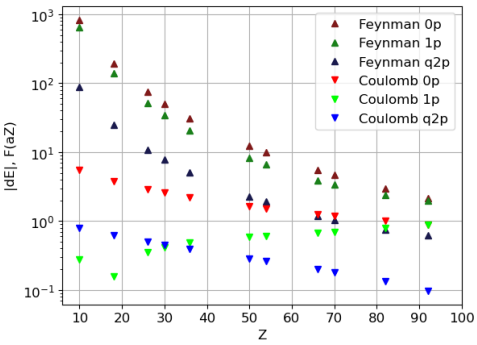

(a) The absolute value of zero-, one- and quasi-two-potential contributions to the self-energy correction to Lamb shift in Feynman and Coulomb gauges.

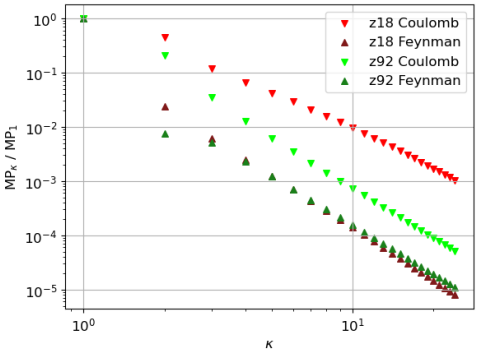

(b) Many-potential contributions as a function of angular quantum number κ with normalization on the first contribution of expansion.

Figure 1: Comparison of Feynman and Coulomb gauges.

References

1. A. Gumberidze et al., Phys. Rev. Lett. **94**, 223001 (2005).

2. P. Beiersdorfer et al., Phys. Rev. Lett. **95**, 233003 (2005).

3. S. Sturm et al., Phys. Rev. Lett. **525**, 620–635 (2013).

4. T. Sailer et al., Nature **606**, 479–483 (2022).

5. V.A. Yerokhin and V.M. Shabaev, Phys. Rev. A **60**, 800 (1999).

6. D. Hedendahl and J. Holmberg, Phys. Rev. A **85**, 012514 (2012).

7. J. Sapirstein and K.T. Cheng, Phys. Rev. A **108**, 042804 (2023).

8. A.V. Malyshev, E.A. Prokhorchuk and V.M. Shabaev, Phys. Rev. A **109**, 062802 (2024).

9. V.A. Yerokhin and U.D. Jentschura, Phys. Rev. A **81**, 012502 (2010).

10. D.A. Glazov et al., Phys. Lett. A **357**, 330–333 (2006).

11. D.A. Glazov et al., Phys. Rev. A **81**, 062112 (2010).

Compound-tunable embedding potential method for precise electronic-structure study of $LuPO_4$: comparative analysis of calculations with and without fragment-PP on phosphorus

A.A. Lutchenko[1,2], V.M. Shakhova[1], A.V. Titov[1,2]

[1] Petersburg Nuclear Physics Institute named by B.P.Konstantinov of NRC «Kurchatov Institute»

[2]St Petersburg University

lutchenko.aleksandra@yandex.ru

The current capabilities of modern quantum chemical methods for periodic systems (DFT methods, different versions of "soft" pseudopotentials and atomic basis sets of moderate size) are limiting the accuracy of theoretical lanthanide crystal studies. Overcoming these challenges would unlock precise modeling for fundamental and practical tasks.

The distinctive features of $LuPO_4$ crystal structure, particularly, the strongly bonded PO_4^{3-} group, served as the key motivation for this study. The electronic structure calculations of $LuPO_4$ using the compound-tunable embedding potential (CTEP) method were performed. Within the framework of this research, two approaches were compared: one employing fragment-PP to model the PO_4^{3-} group, and a standard way to treat the group.

In this research, the electronic structure of the crystal is studied by using the "compound-tunable" embedding potentials (CTEP) method [1-4]. The investigation of a crystal by the CTEP method is carried out in three stages. First, a perfect crystal with periodic boundary conditions is calculated by the CRYSTAL code. Second, short-range large-core "compound-tunable" pseudopotential (CTPP) is built for the chosen crystal by using the CRYSTAL code as well. Third, cluster calculations of the crystal fragment are performed, and the long-range Coulomb potential of the environment is constructed as a part of CTEP. A crystal fragment of a "minimal size" (a minimal cluster includes a heavy atom and its immediate environment) is cut out, within which the electron density must be reproduced with high accuracy. The atoms of the near environment of the crystal fragment are described by point charges and CTPPs ("pseudoatoms") to take into account the influence on a chosen fragment of the "whole crystal" excluding the atoms of the fragment.

Analysis of the crystal fragment's structural parameters demonstrates a notable improvement in accuracy when using fragment-PP for the PO_4^{3-} group. Bond length calculations revealed 2-4 times increase in agreement with experimental equilibrium distances. These results confirm the efficiency of this approach for describing the PO_4^{3-} groups in the studied crystal structure.

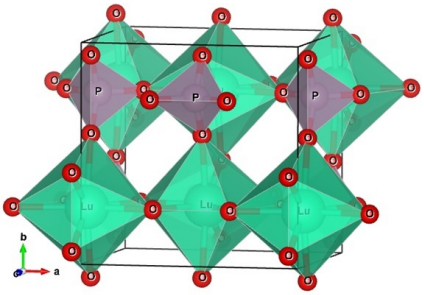

Figure 1: Crystal structure of $LuPO_4$ (141, I41/amd).

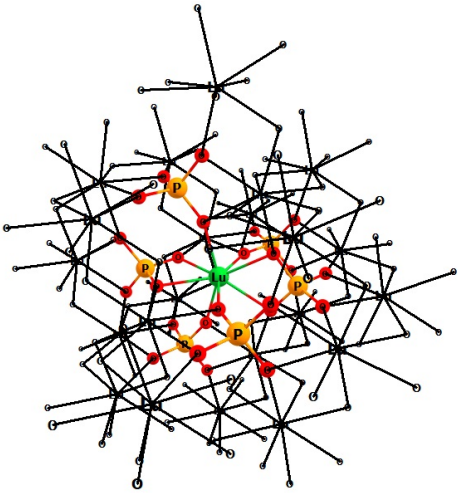

Figure 2: Cluster with CTEP for $LuPO_4$, where "balls" atoms are represent crystal fragment of a "minimal size" and "sticks" are "pseudoatoms" of CTEP.

References

1. Lomachuk Y. V., Maltsev D. A., Mosyagin N. S., Skripnikov L. V., Bogdanov R. V. and Titov A. V., Phys. Chem. Chem. Phys., 22:17922-17931, (2020).

2. Maltsev D. A., Lomachuk Y. V., Shakhova V. M., Mosyagin N. S., Skripnikov L. V. and Titov A. V., Phys. Rev. B., 103:205105, (2021).

3. Shakhova V. M., Maltsev D. A., Lomachuk Y. V., Mosyagin N. S., Skripnikov L. V. and Titov A. V, Phys. Chem. Chem. Phys., 24:19333-19345, (2022).

4. Maltsev D. A., Lomachuk Y. V., Shakhova V. M., Mosyagin N. S., Kozina, D. and Titov A. V, Sci. Rep., 15:10645, (2025).

Shape and size effects in discrete metamaterials with huge amount of coupled resonators

A.O. Makarenko,[1], M. Lapine[1,2,3], A.A. Shcherbakov[1]

[1] ITMO University, Russia

[2] University of Technology Sydney, Australia

[3] Qingdao Innovation and Development Centre of Harbin Engineering University, China

aleksandr.makarenko@metalab.ifmo.ru

Metamaterials are well-known concept for creation of materials with unusual electromagnetic properties [1]. Moreover, it is quite attractive to describe metamaterials in a similar way to conventional materials, i.e. using macroscopic parameters such as permittivity and permeability [2]. However, such theoretical descriptions often differ significantly from practical structures [3], that forces us to remind some necessary conditions for such description:

1. all structural features should be significantly smaller than the wavelength;
2. there should be a huge amount of structural units to ensure that averaging is meaningful.

In practice, the latter condition is often not satisfied, but it is still an open question how many metaatoms are needed to ensure that continuous media theory is applicable [4]. Moreover, the role of mutual interaction between structural elements is extremely important, but the plausible number of structural elements is limited. The role of shape and size then becomes quite essential, because mutual interaction between metamaterial elements is much stronger than for conventional materials [5] (fig.1).

In this work we describe electromagnetic properties of finite metamaterial structures using a novel way to solve matrix equations from [3] based on discrete spatial symmetry of the problem. This allows us to efficiently compute the response of millions of coupled resonators, so large effects of borders and shape were studied:

1. Despite previously described better convergence to continuous media theory for small structures in ragged borders case [5]; for large structures convergence to continuous media theory is incredibly slower;
2. Introduced centred metaatoms shows remarkable size-stable spectra and also better convergence for sharp geometry metastuctures, where centred structures with 5000 resonators has same behaviour as smooth with 3 million resonators;
3. 1D-structures is the only case when convergence is not possible at all, independently of number of resonators;
4. 2D squared and circles shows very similar behaviour, despite huge difference in spatial distribution of magnetic moments.

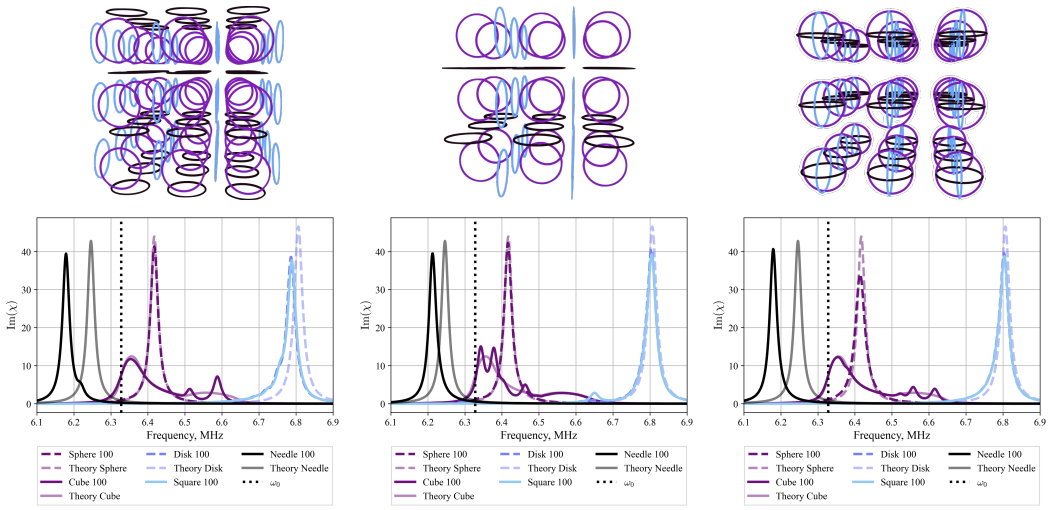

Figure 1: Imaginary part of polarizability spectra for different shapes and types of metaatoms: smooth and ragged borders (left and center), then centered metaatoms (right). Different colors correspond to different shapes while different line styles correspond to continuous media theory (dashed transparent lines) and discrete solution for 100 metacells per dimension (solid lines). Black vertical dotted line shows resonance frequency for single resonator.

References

1. M. Gorkunov, M. Lapine, S.A. Tretyakov, Methods of crystal optics for studying electromagnetic phenomena in metamaterials: Review, Crystallography Reports, 51(6), 1048–1062 (2006).

2. M. Gorkunov, M. Lapine, E. Shamonina, K.H. Ringhofer, Effective magnetic properties of a composite material with circular conductive elements, Eur. Phys. J. B, 28, 263–269 (2002).

3. M. Lapine, L. Jelinek, R. Marques, M. J. Freire, Exact modelling method for discrete finite metamaterial lens, Microwaves, Antennas & Propagation, IET, 4(8), 1132–1139 (2010), doi:10.1049/iet-map.2009.0598.

4. M. Lapine, R.C. McPhedran, C.G. Poulton, Slow convergence to effective medium in finite discrete metamaterials, Phys. Rev. B, 93, 235156 (2016).

5. M. Lapine, L. Jelinek, R. Marquйs, Surface mesoscopic effects in finite metamaterials, Opt. Express, 20, 18297–18302 (2012).

Radiation of relativistic electrons created in ionization of atomic gases by laser beams of extreme intensity

N. V. Makarenko [1] and S.V. Popruzhenko[1,2]

[1] National Research Nuclear University MEPhI

[2] Prokhorov General Physics Institute RAS

nikrussia1111@gmail.com, sergey.popruzhenko@gmail.com

Recent development of the new generation of femtosecond laser sources with peak power in the interval 1-10 petawatts (PW) has opened a way to systematic laboratory studies of laser-matter interactions at intensities $10^{22}\mathrm{W/cm}^2$ and higher. The field strength and its distribution inside the laser focus are key characteristics that determine the probabilities of nonlinear effects of classical and quantum electrodynamics, so that reliable diagnostics of such extremely strong electromagnetic fields is extremely important for upcoming experiments.

One of the proposed methods for measuring the peak laser intensity is based on the observation of tunneling ionization of heavy atoms [1]. In this contribution, we consider the process directly connected with ionization: electrons liberated from ions through tunnel ionization will be accelerated by the same electromagnetic field, which caused the ionization process, and will emit radiation predominantly in the direction of the laser pulse propagation. The spectral-angular distribution of such radiation depends both on the peak intensity of the laser and on its distribution inside the focus, which provides an additional tool for analyzing the structure of the electromagnetic field. However, as is known, the radiation of relativistic particles in the field of an external electromagnetic wave is strongly suppressed during co-propagating motion [2], as a result, even in a laser focus with a peak intensity of $\simeq 10^{22}$ W/cm^2, the electrons resulting from tunneling ionization emit, before leaving the strong field region, only several high-frequency photons. A relatively weak counter-propagating probe pulse is needed to enhance the signal and make it useful for analysis of the focal volume field distribution.

The initial conditions for the classical trajectories of photoelectrons are determined by the instants of ionization, which are randomly set for an ensemble of 10^3 argon atoms distributed in a laser focus. The rate of tunneling ionization is calculated using the Perelomov-Popov-Terentyev formula [3]. The ionized electrons are accelerated by the main laser pulse to Lorentz-factors $\gamma \sim 10^2 - 10^3$ and collide with a co-propagating weakly focused probe pulse of intensity $\simeq 10^{18}$ W/cm^2. The wavelength of both pulses is 1 μm. The main pulse is a Gaussian beam with waist radius $w_0 = 3$ microns. To calculate the spectral-angular distribution of radiation in a weakly focused probe pulse, we used the plane wave approximation and adapted the results of [4] by transforming them to a reference frame in which the electron is at rest on average.

The calculation results show that the angular distribution of radiation has the form of a cone with the angle depending on the intensity of the main laser beam. The propagation directions of emitted photons are concentrated in a small range of angles near the cone surface, which is a consequence of the characteristic shapes of the photoelectron trajectories, which all start with zero velocity inside the laser focus and leave the strong field region mainly through its lateral surface. The dependencies of the total radiated energy and its spectral distribution on the maximum intensity of the main beam and the lateral size of the laser focus are investigated.

This work was supported by the Russian Science Foundation through Grant No.25-22-00308.

References

1. M. Ciappina, S. Popruzhenko, S. Bulanov, T. Ditmire, G. Korn, and S. Weber, Physical Review A 99, 043405 (2019).

2. L.D. Landau, E.M. Lifshits, Theoretical Physics. Field Theory, M. Nauka Publ., 1988.

3. V.S. Popov, UFN 174, 921 (2004)

4. E. Sarachik and G. Schappert, Physical Review D 1, 2738 (1970).

Diffraction of twisted waves on different apertures

M. Maksimov[1], D. Kargina[1], D. Karlovets[1]

[1] School of Physics and Engineering, ITMO University, 197101 St. Petersburg, Russia

maksim.maksimov@metalab.ifmo.ru

The diffraction of electron wavepackets is a promising technique for diagnosing quantum states of electrons, particularly for analyzing their orbital angular momentum (OAM). Unlike photons, electrons possess mass and charge, enabling unique interactions with electromagnetic fields and matter.

A fundamental example of such interactions is the diffraction of twisted electron beams carrying OAM on apertures with tailored geometries. While experiments with twisted light have demonstrated the profound influence of aperture shape on diffraction patterns [1, 2, 3], analogous studies for electrons remain sparse. This gap impedes advances in precise electron-beam diagnostics and limits our understanding of how OAM manifests in charged-particle systems compared to photonic analogs.

In this work, we systematically model the diffraction of OAM-carrying electron beams through apertures of varying complexity. Our approach combines three frameworks: (1) scalar diffraction based on the stationary Schrödinger equation, (2) paraxial diffraction of Laguerre-Gaussian (LG) and Bessel beams, and (3) relativistic Klein–Gordon wave dynamics.

By comparing results across these models, we elucidate how aperture geometry (e.g., circular or triangular) and topological charge alter the intensity profiles of diffracted beams. For instance, triangular apertures introduce symmetry-breaking effects that redistribute intensity, as illustrated in Figure 1. These findings highlight the critical role of geometry in controlling OAM-dependent interference, offering insights for designing electron-optical systems with tailored angular momentum transfer.

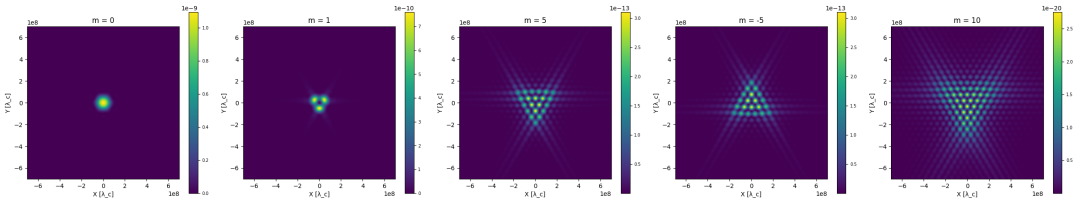

Figure 1: Simulated diffraction of a Bessel beam with different OAM on a triangular aperture.

References

1. J. Hickmann *et al.*, Phys. Rev. Lett. **105**, 053904 (2010).

2. S. Wada *et al.*, Sci. Rep. **13**, 22962 (2023).

3. L. de Araujo and M. Anderson, Opt. Lett. **36**, 787-789 (2011).

Constraining Lorentz Invariance Violation using the Muon Excess in Extensive Air Showers

N. S. Martynenko[1,2], G. I. Rubtsov[2,1], P. S. Satunin[2,1],
A. K. Sharofeev[1,2], S. V. Troitsky[2,1]

[1] Lomonosov Moscow State University

[2] Institute for Nuclear Research of the Russian Academy of Sciences

martynenko@ms2.inr.ac.ru

Extensive air showers (EASs) produced by cosmic rays in Earth's atmosphere allow us to study particle physics at energies beyond those accessible to current particle accelerator experiments. A combined analysis of relevant EAS measurements from multiple observatories has revealed [1, 2] a significant but yet unexplained excess of muons compared to theoretical predictions based on Monte-Carlo (MC) simulations. Conventionally, this discrepancy is quantitatively described by the so-called z-measure, which is expected to

$$z \equiv \frac{\ln N_\mu[\text{observed}] - \ln N_\mu[p\text{-induced EAS MC}]}{\ln N_\mu[^{56}\text{Fe-induced EAS MC}] - \ln N_\mu[p\text{-induced EAS MC}]}.$$

Here we consider a violation of Lorentz invariance (LIV) which leads to a modified photon dispersion relation,

$$E_\gamma^2 = k_\gamma^2 - \frac{k_\gamma^4}{M_{\text{LIV}}^2}.$$

Under this LIV scenario, the electron-positron pair production cross-section is significantly suppressed at high energies [3], which inhibits the development of electromagnetic cascades in the EASs.

We demonstrate that this may lead to a biased reconstruction of the primary particle's energy. It is shown that, assuming a reasonable and experimentally allowed LIV scale $M_{\text{LIV}} = \mathcal{O}(10^{16})$ GeV, this effect could produce $z \simeq (1...2)$, which corresponds to the muon excess observed at the Pierre Auger Observatory, see Figure 1, Panel (a).

On the other hand, the absence of a much larger discrepancy between EAS data and simulations induces a stringent constraint on the LIV scale, $M_{\text{LIV}} \gtrsim \mathcal{O}(10^{14})$ GeV, see Figure 1, Panel (b). The reader is referred to [4] for a detailed discussion.

This work was supported by the Russian Science Foun-dation, grant 22-12-00253. N.M. and A.S. thank the Theoretical Physics and Mathematics Advancement Foundation «BASIS» for the student fellowships under the contracts 24-2-10-39-1 and 24-2-10-33-1, respectively.

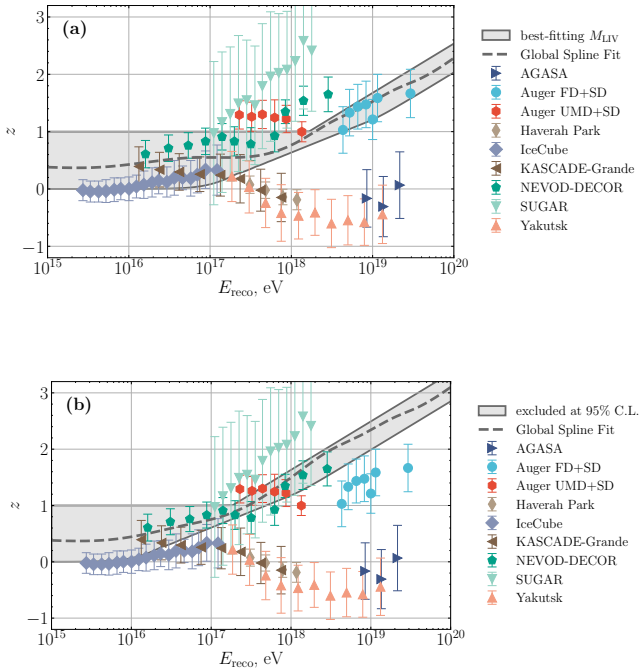

Figure 1: z-scale measured in experiments [2] in comparison with that predicted by the LIV scenario. Top: M_{LIV} favored by the Pierre Auger observations. Bottom: M_{LIV} excluded at 95% C.L. by the Pierre Auger observations.

References

1. J. Albrecht *et al.*, Astrophys. Space Sci. **367**, 27 (2022).

2. J. C. Arteaga Velazquez, PoS **ICRC2023**, 466 (2023).

3. G. Rubtsov, P. Satunin, and S. Sibiryakov, JCAP **05**, 049 (2017).

4. N. S. Martynenko *et al.*, Phys. Rev. D. **111**, 063010 (2025).

Boson sampling validation approach by examining the sample space filling

A A Mazanik[1,2]

[1]Russian Quantum Center

[2] Moscow Institute of Physics and Technology

mazanik.aa@phystech.su

Reaching the regime of quantum computational advantage — and thereby challenging the extended Church-Turing thesis — remains one of the central goals in modern science. Boson sampling is considered a promising route toward this objective. However, to confidently claim entry into the advantage regime, it is essential to demonstrate that the device samples from the true boson sampling distribution, rather than from a classically simulable alternative. This issue, known as the validation problem, is a significant obstacle to establishing clear evidence of quantum advantage.

In this work, we employ the recently introduced wave function network framework to study how the sample space becomes populated as the number of collected samples increases. We demonstrate that, owing to the inherent structure of the boson sampling wave function, its filling behavior can be computationally efficiently distinguished from several classically simulable alternatives, such as distinguishable particle sampling or mean-field sampling. Based on this, we propose a new validation technique grounded in sample space filling analysis, and we test it for systems involving up to 20 photons in a 400-mode interferometer. Thanks to its simplicity and efficiency, this method can complement existing approaches in validating future experiments and strengthening the case for quantum computational advantage.

This talk is based on the work [1].

This work was supported by Rosatom in the framework of the Roadmap for Quantum computing (Contract No. 868-1.3-15/15-2021 dated October 5).

References

1. Mazanik A. A., Rubtsov A. N. Sample space filling analysis for boson sampling validation //arXiv preprint arXiv:2411.14076. – 2024.

Relativistic expansions for the correlation correction of highly charged ions

A. D. Moshkin[1,2*]

[1] Department of Physics, Saint-Petersburg State University

[2] School of Physics and Engineering, ITMO University

[*]a.d.moshkin@gmail.com

Highly charged ions provide a unique opportunity to test bound-state quantum electrodynamics (QED) [1], such as the study of the Lamb shift in lithium-like uranium [2]. Furthermore, the experimental precision of g factor measurements for hydrogen-like, lithium-like and boron-like ions has reached the level of 10^{-9}—10^{-11} [3–6]. These studies have led to the most precise determination of the electron mass [7, 8] and provided a rigorous test of relativistic nuclear recoil effects in the presence of a magnetic field [5]. Further advances in both theoretical and experimental approaches to g factor measurements could allow the independent determination of the fine structure constant, the refinement of nuclear parameters, and the search for physics beyond the Standard Model [9–11]. This has opened up new possibilities for exploring QED effects in the strong coupling regime beyond the Furry picture [12–14].

In this work, correlation effects are studied for the Coulomb and various screening potentials. In particular, this work uses four different screening potentials, the core-Hartree potential and x_α – potentials derived from density functional theory. The core-Hartree potential is of the form:

$$V_{scr} = \alpha \int_0^\infty dr' \frac{\rho_c(r')}{r_>}, \tag{1}$$

where $r_> = \max(r, r')$, $\rho_c(r)$ is the electron density of the closed shell.

The remaining screening potentials are determined by the expression:

$$V_{scr} = \alpha \int_0^\infty dr' \frac{\rho_t(r')}{r_>} - x_\alpha \frac{\alpha}{r} \left(\frac{81}{32\pi^2} r \rho_t(r) \right)^{1/3}, \tag{2}$$

where the coefficient x_α for different potentials takes the value: $x_\alpha = 0$ for the Dirac-Hartree potential, $x_\alpha = 2/3$ for the Kohn-Scham potential, and $x_\alpha = 1/3$ for the Dirac-Slater potential. First, the convergence of the perturbation series for energies depending on the zero approximation potential is analyzed. Then, within the rigorous QED approach, a second-order relativistic expansion for the energies of lithium-like ions is derived. The energy corrections provide an excellent training ground for developing and validating methods before applying them to the g factor. Later, the convergence of perturbative theory is analyzed and a relativistic expansion for the g factor is

derived. The first-order contribution is treated rigorously, while higher-order terms are considered within the Breit approximation. A power expansion in the αZ parameter is then performed for lithium-like ions in the ground $(1s)^2 2s_{1/2}$ and excited $(1s)^2 2p_{1/2}$ and $(1s)^2 2p_{3/2}$ states. The analysis of these expansions, combined with high-precision non-relativistic calculations [15], is expected to improve the theoretical accuracy of g factor predictions.

References

1. V.M. Shabaev et al., J. Phys. Chem. Ref. Data **44**, 031205 (2015).
2. V.M. Shabaev, Phys. -Usp. **51**, 1175 (2008).
3. I. Arapoglou et al., Phys. Rev. Lett. **122**, 253001 (2019).
4. D.A. Glazov et al., Phys. Rev. Lett. **123**, 173001 (2019).
5. J. Morgner et al., Nature **622**, 53 (2023).
6. F. Heiße et al., Phys. Rev. Lett. **131**, 253002 (2023).
7. S. Sturm et al., Nature **506**, 467 (2014).
8. E. Tiesinga, Rev. Mod. Phys. **93**, 025010 (2021).
9. V.M. Shabaev et al., Phys. Rev. Lett. **96**, 253002 (2006).
10. V.A. Yerokhin et al., Phys. Rev. Lett. **116**, 100801 (2016).
11. V. Debierre et al., Phys. Rev. A **106**, 062801 (2022).
12. A.V. Malyshev et al., JETP Lett. **106**, 765 (2017).
13. V.M. Shabaev et al., Phys. Rev. Lett. **119**, 263001 (2017).
14. V.P. Kosheleva et al., Phys. Rev. Lett. **128**, 103001 (2022).
15. V.A. Yerokhin et al., Phys. Rev. A **95**, 062511 (2017).

Stabilizer Tensor Networks are Canonical in the Heisenberg Picture

A. Nasrallah

Skolkovo Institute of Science and Technology

aly.nasrallah@skoltech.ru

A graphical rewrite system that is both confluent and also terminates uniquely is called canonical. Applying alternate sequences of rewrites to the same initial diagram, a rewrite system is confluent whenever all resulting diagrams can be manipulated to establish graphical equivalence. We show that a reduced ZX-rewrite system is already confluent in the Heisenberg picture for stabilizer quantum mechanics. Moreover, any application of a subset of ZX-rewrites terminates uniquely and irrespective of the order of term rewrites in the Heisenberg picture for stabilizer quantum mechanics. The ZX-system is hence Heisenberg-canonical for stabiliser quantum mechanics. For a stabilizer circuit on n-qubits with l singlequbit gates and g two-qubit gates, the circuit output can be derived graphically in the Heisenberg picture using no more than $(\frac{1}{2} \cdot g + l) \cdot n$ graphical rewrites, thereby resulting in the Gottesman-Knill theorem as a corollary. Finally, we consider the application of this tool as a graphical means to derive parent Hamiltonians which can be used as penalty functions in variational quantum computation. Hence, we establish that each stabilizer state described by a Clifford circuit gives rise to a non-negative parent Hamiltonian with $n + 1$ terms and a one-dimensional kernel spanned by the corresponding stabilizer state. Such parent Hamiltonians can be derived with $\mathcal{O}(t \cdot n)$ graphical rewrites for a low energy state prepared by a t-gate Clifford circuit.

Accounting for quantum fluctuations of order parameter in systems of correlated fermions

S. S. Onuchin[2], Ya. S. Lyakhova[1,2], A. N. Rubtsov[1,3]

[1] Russian Quantum Center

[2] National Research Nuclear University MEPhI

[3] Moscow State University

semyon_onuchin@vk.com

The description of fluctuation phenomena in correlated systems remains a challenging problem for condensed matter physics. Despite the wide range of known computational methods in this field, the question of creating a scheme that is both simple and maintains good results over a wide range of parameters remains open. One of the latest perspective methods is the Fluctuating Local Field (FLF) approach [1].

The central idea of the FLF method is approximation of the exact partition function with a parental method (e.g. mean-field) functions averaged over ensemble of external fields ν artificially introduced in the leading fluctuation channel. Considering the example of antiferromagnetic fluctuations in a one-dimensional Hubbard chain of N sites with half-filling, the FLF transformation can be written as [2]:

$$Z_{FLF} = \iint \exp\Big\{-\mathcal{S}_h - \frac{\beta N}{2\lambda}(\boldsymbol{\nu} - \mathbf{h} - \lambda \mathbf{s})^2\Big\}\mathcal{D}[c^\dagger, c]d^3\nu \tag{1}$$

up to constant, where $\boldsymbol{\nu}$ is introduced fluctuating field, β is inverse temperature, $\mathcal{S}_h$ - action for the system in the external field $\boldsymbol{h}$, $\boldsymbol{s}$ - AF spin. The parameter λ remains arbitrary and should be chosen in accordance with parental method to account for fluctuations around it. This way, an effective long-range spin-spin interaction appears, which reduces the fluctuations in the corresponding channel. It allows to treat them as Gaussian.

The present work is devoted to the development of a method for accounting for quantum fluctuations of the order parameter. For this purpose, the field ν is expanded at Matsubara frequency representation. Assuming that the contribution of the non-zero modes in the expansion is relatively small in comparison to the zeroth one:

$$\sum_{n=-\infty}^{+\infty} \nu_n^\alpha e^{iw_n\tau} \approx \nu_0^\alpha + \nu_{\pm 1}^\alpha e^{iw_{\pm 1}\tau}, \quad \text{where} \quad w_n = 2n\frac{\pi}{\beta} \tag{2}$$

In this approximation, a formula for partition function was obtained, which allows us to calculate any averaged over FLF ensemble $< ... >_{FLF}$ value, and as an approbation of

Vortex dynamics in the vicinity of the Bogomolny point

V. Pashkovskaia[1], A. Vasenko[1], T. T. Saraiva[1]

[1] HSE University

vpashkovskaia@hse.ru

The Bogomolny point of the Ginzburg-Landau (GL) theory marks a point of infinite degeneracy of the stationary states. The solutions to the Bogomolny equations in superconductors have very particular properties and go beyond Meissner and vortex solutions, e.g. vortex lines and giant vortices. As we decrease the temperature and keep the GL parameter next to $\kappa_0 = \frac{1}{\sqrt{2}}$ the degeneracy is broken, the condensate and magnetic characteristic lengths become well defined and several elements of the system may influence in the electromagnetic response of the superconductor. In this work, we investigated non-simply connected 2D systems submitted to a perpendicular magnetic field using a generalization of the Time-Dependent Ginzburg-Landau theory, admitting local variations of temperature due to heat dissipation. We simulated a continuous increase of the external magnetic field for different thermal parameters of the system, i.e. thermal diffusivity, conductivity, etc and different sizes of the sample. We found that in the vicinity of the critical penetration field, Hc1, where the first magnetic fluxes moved through the sample, the local increase in temperature produced a trail of dissipation causing more elongation of vortices, resembling "vortex lines" found in the analytic solutions to the Bogomolny equations

References

1. Valeriia D. Pashkovskaia, Elwis C. S. Duarte, Rafael Zadorosny, Edson Sardella, Dmitrii A. Abrameshin, Andrey S. Vasenko, and Tiago T. Saraiva. Dynamics of vortex matter in 2d gapless su perconducting materials with impurities. The Journal of Physical Chemistry Letters, 0(0):10742– 10748, 2024. PMID: 39422296.

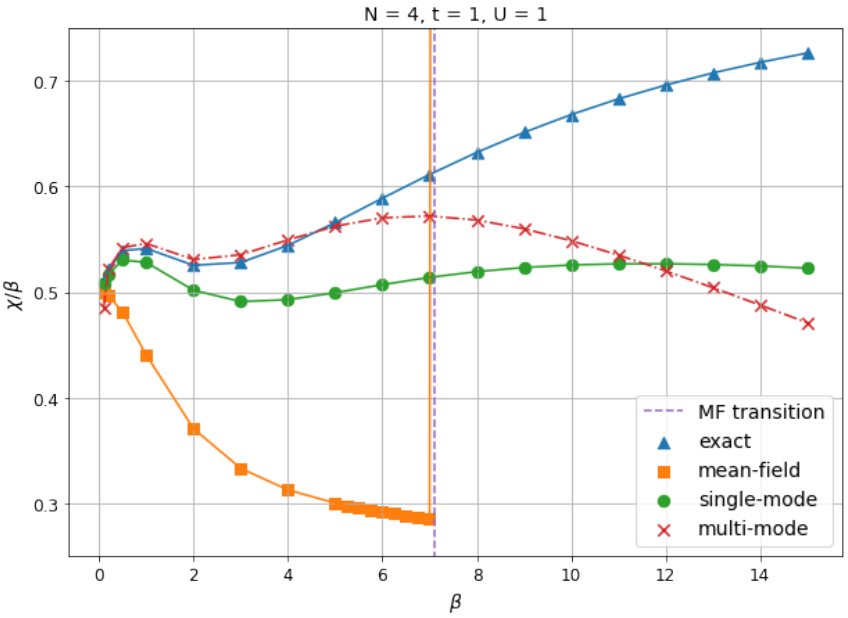

Figure 1: Temperature dependence of magnetic susceptibility in various approximations for a Hubbard chain (4 sites).

the method, susceptibility χ was obtained and temperature dependencies were plotted (Fig.1).

One can see an improvement of results for comparatively small β, which is expected behavior of the solution because of our assumption of smallness for non-zero modes in ν expansion. Presumably, taking further modes into account may allow us to improve the results in wider range of parameters.

The obtained results demonstrate a significant improvement in accuracy compared to the parental mean-field method. Also, the proposed approach eliminates the nonphysical phase transition that arises in the mean-field treatment of this system. These advantages establish the FLF method as a promising approach for describing correlated systems.

References

1. A. N. Rubtsov, Phys. Rev. E **97**(5), (2018).

2. Ya. S. Lyakhova *et al.*, Phys. Rev. B **110**(24), (2024).

Angular momentum effects in neutron decay

I.I. Pavlov[1], A. D. Chaikovskaia[1], D.V. Karlovets[1]

[1]School of Physics and Engineering, ITMO University, 197101 St. Petersburg, Russia

[1]ilya.pavlov@metalab.ifmo.ru

Recent advancements in neutron optics have enabled the generation and detection of free neutrons in structured quantum states, which go beyond simple plane waves. Among these are so-called vortex states with a phase singularity and a corresponding orbital angular momentum (OAM) projection onto a propagation direction [1, **?**] and spin correlated OAM (spin-orbit) states [2, 3], which have emerged as promising tools for material characterization and fundamental physics exploration.

We investigate the phenomenon of beta decay of a free neutron in a non-plane-wave (structured) state. Our analysis covers three types of states: unpolarized vortex (Bessel) neutrons that possess nonzero orbital angular momentum (OAM), Laguerre-Gaussian wave packets, and spin-orbit states characterized by unique polarization patterns. The spectral-angular distributions (SAD) of the emitted electrons and protons are examined. We show that the high sensitivity of the protons SAD to the structure of the neutron wave packet can be used as a tool to extract the distinctive features of the non-plane-wave neutron states. Furthermore, we demonstrate that the angular distribution of the emitted particles serves as a reflection of the spatial symmetries inherent to the neutron wave packet.

This work was supported by the Foundation for the Advancement of Theoretical Physics and Mathematics "BASIS" and by the Russian Science Foundation (Project No. 23-62-10026).

References

1. D. Sarenac *et al.*, Science Advances **8**, 46 (2022).

2. N. Geerits *et al.*, Communications Physics **6**, 1 (2023).

3. D. Sarenac *et al.*, New journal of physics **20**, 10 (2018).

4. D. Sarenac *et al.*, PNAS **116**, 41 (2016).

Quantum-electrodynamics corrections to the quadratic Zeeman effect via Green's function method

E. A. Prokhorchuk[1,*]

[1]St. Petersburg State University

[*]st068889@student.spbu.ru

High-precision experiments designed to measure various properties of highly charged ions provide a stringent test of theoretical methods in bound-state quantum electrodynamics (QED). Notably, measurements of the g-factor in hydrogenlike ions have reached an extraordinary accuracy of 10^{-11} [1]. Achieving theoretical predictions at a high level of precision requires a careful treatment of QED effects in the evaluation of atomic properties.

Among the most significant QED corrections is the self-energy (SE) contribution, which influences energy levels, the g-factor, the quadratic Zeeman effect, and other fundamental quantities. *Ab initio* calculations for highly charged ions have to be conducted in all orders in the electron-nucleus coupling parameter. The primary source of theoretical uncertainty arises from the slow convergence of partial-wave expansions [2, 3]. For high-precision calculations, the Green's function of an electron in a central potential—obtained via solutions to the corresponding system of differential equations—has proven to be an extremly useful tool [4, 5].

In this work, we investigate the electron Green's function in the presence of one and two interactions with an external field. We consider general forms of perturbing potentials that do not conserve angular quantum numbers and derive explicit expressions for the radial Green's functions. These results enable precise calculations of various one- and two-electron SE corrections. To demonstrate the efficacy of the method, we apply it to compute the SE contribution to the quadratic Zeeman effect in hydrogenlike ions.

This work was supported by the Theoretical Physics and Mathematics Advancement Foundation "BASIS" (Grant No 24-1-2-74-3).

References

1. H. Häffner *et al.*, Phys. Rev. Lett. **85**, 5308 (2000).

2. V. A. Yerokhin *et al.*, Phys. Rev. A **60**, 3522 (1999).

3. V. A. Yerokhin *et al.*, Phys. Rev. A **69**, 052503 (2004).

4. P. Mohr *et al.*, Phys. Rep. **293**, 227 (1998).

5. V. A. Yerokhin, A. V. Maiorova, Symmetry **12**, 800 (2020).

Calculation of isotope shift parameters in neutral atoms

S.D. Prosnyak[1] and L.V. Skripnikov[1,2]

[1] NRC «Kurchatov Institute» - PNPI

[2] Saint Petersburg State University

prosnyak.sergey@yandex.ru, leonidos239@gmail.com

The root mean square charge radius is one of the most interesting properties of the atomic nucleus. By studying changes in this parameter in a chain of isotopes of an element, one can draw conclusions about how the structure of the nucleus changes with changing number of neutrons, as well as about how well nuclear theory describes the dependencies obtained in experiment. In the case of short-lived isotopes, the main experimental method of charge determination is the measurement of isotopic shifts of transition energies in atoms.

In order to interpret such experiments, it turns out to be necessary to perform electronic structure calculations with the calculation of field and mass shift constants. The field shift constant is related to the different charge distribution over the nucleus for the isotopes under consideration, and the mass shift constant is related to the recoil effect of the nucleus. We have developed a technique for the theoretical calculation of these constants with a detailed analysis of the resulting uncertainties. It has been shown that the approach used allows us to obtain a much higher accuracy of the electronic factors of isotope shifts [1, 2, 3]. The developed approach was applied in calculations for gold [4] and mercury atoms for the interpretation of future experiments.

The calculation of matrix elements of considered properties was supported by the Foundation for the Advancement of Theoretical Physics and Mathematics “BASIS” Grant according to Projects No. 24-1-1-36-1. The electronic structure calculations was supported by the Russian Science Foundation grant no. 24-12-00092.

References

1. L. Filippin, R. Beerwerth, J. Ekman, S. Fritzsche, M. Godefroid, P. Jönsson, Phys. Rev. A, **94(6)**, 062508 (2016).

2. H. Heylen, et al., High-resolution laser spectroscopy of Al 27–32. Phys. Rev. C, **103(1)**, 014318 (2021).

3. A. Rosen, B. Fricke, G. Torbohm, Zeitschrift fur Physik A Atoms and Nuclei, **316(2)**, 157-16 (1984).

4. J. G. Cubiss, et al., Phys. Rev. Lett., **131(20)**, 202501 (2023)

Self-energy diagram for axially symmetric systems

M. Reiter[1], D. Glazov[2,3], A. Malyshev[1,3]

[1] Department of Physics, St. Petersburg State University

[2] School of Physics and Engineering, ITMO University

[3] Petersburg Nuclear Physics Institute named by B.P. Konstantinov of NRC "Kurchatov Institute"

mikh.reiter@gmail.com

Theoretical description of atomic spectra is a computationally complex area of physics. When considering the heavy atoms' spectra, an important task is to take into account quantum electrodynamic (QED) corrections. The leading QED corrections for a bound electron correspond to the self-energy (SE) and vacuum polarization (VP) diagrams. Methods for calculating QED corrections for systems with spherical symmetry – atoms and ions – are well developed to date [1]-[5]. On the other hand, when considering systems with a more complex structure, e.g. molecules, there are only approximate methods that rely on the results obtained for individual atoms [6].

In addition to molecules, there are various systems with axial symmetry, where the accuracy of theory and experiment allows observing QED contributions. In particular, these are atoms and ions in electromagnetic fields. Notwithstanding the fact that the external field is considered small, its inclusion in the zero-order Hamiltonian allows one to go beyond the perturbation theory, which provides a number of advantages. Another important example of such systems is quasimolecules consisting of two heavy nuclei and one or more electrons. Such systems are formed in collisions of heavy ions, and the possibility of spontaneous production of electron-positron pairs arises due to the fact that the bound states for such a system can plunge into the negative continuum (see e.g. [7]). In the future, studies of such collisions will be possible in projects such as NICA, HIAF and GSI/FAIR.

In this work, a rigorous calculation of the SE diagram contribution to the ground state energy of the one-electron uranium quasimolecule U_2^{183+} is performed. The Dirac equation with a two-center potential is solved numerically. In order to construct the electron Green's function on the basis of a finite basis set, a generalization of the dual kinetic balance (DKB) method to auxiliary symmetric systems, termed as A-DKB, is used [8]. The formal expression corresponding to the self-energy diagram contains ultraviolet divergences. They are canceled with the mass counterterm within the potential expansion approach. As a result, the SE diagram is divided into three contributions: zero-, one-, and many-potential terms [1]. The zero- and one-potential contributions are calculated in the momentum representation. For the many-potential contribution, the calculation of the two-electron matrix elements of the photon propagator is performed with subsequent summation over the spectrum and numerical

integration over the energy parameter in the complex plane, resulting in a rigorous and complete calculation of the SE diagram. The results we obtained are in reasonable agreement with the results of Refs. [9, 10], where the contributions of the SE and VP diagrams to the ground state energy of a one-electron uranium quasimolecule and two heteronuclear molecules were calculated using the partial expansion of the two-center potential.

This work was supported by the Russian Science Foundation grant №22-12-00258.

References

1. V. A. Yerokhin and V. M. Shabaev, Phys. Rev. A **60**, 800 (1999).
2. V. A. Yerokhin *et al.*, Phys. Rev. A **111**, 012802 (2025).
3. D. A. Glazov *et al.*, Phys. Rev. A **81**, 062112 (2010).
4. A. V. Malyshev *et al.*, Phys. Rev. A **109**, 062802 (2024).
5. O. V. Andreev *et al.*, Phys. Rev. A **85**, 022510 (2012).
6. V. M. Shabaev, *et al.*, Phys. Rev. A **88**, 012513 (2013).
7. I. A. Maltsev *et al.*, Phys. Rev. Lett. **123**, 113401 (2019).
8. E. B. Rozenbaum *et al.*, Phys. Rev. A **89**, 012514 (2014).
9. A. N. Artemyev and A. Surzhykov, Phys. Rev. Lett. **114**, 243004 (2015).
10. A. N. Artemyev *et al.*, Phys. Rev. A **106**, 012813 (2022).

Using tensor decompositions to solve the equations of the coupled cluster method

A.S. Rumiantsev[1,2], A.V. Oleynichenko[1,3], A.V. Zaitsevskii[1,4]

[1] NRC «Kurchatov Institute» - PNPI, Gatchina

[2] SPbU, Saint-Petersburg

[3] MIPT, Dolgoprudny

[4] MSU named after M.V. Lomonosov, Moscow

attoatom@gmail.com

In theoretical modeling of the electronic structure of materials containing f-elements, such as lanthanides and actinides, it is necessary to take into account both relativistic and correlation effects with high accuracy. Some of the most effective methods for this purpose are approaches based on wave function theory, such as the relativistic coupled cluster (CC) method, but the study of such structures significantly increases the resource intensity of the task. Computational complexity can be reduced by using tensor decompositions to store data and optimizing the algorithms used in modeling.

In this work, the equations of the relativistic coupled cluster method with single and double excitations (CCSD) were formulated in terms of Goldstone diagrams. The parameterization of double cluster amplitudes, following [1, 2], will take the following form:

$$t_{ai}^{bj} = \sum_{XY} U_{ai}^{X} U_{bj}^{Y} T^{XY}, \tag{1}$$

where U is the projector onto the subspace of compressed amplitudes, T is the tensor of compressed amplitudes. It is worth noting that the rank (size in each dimension) of the tensor should behave almost linearly with increasing size of the system. Also, to reduce the computational complexity, it is necessary to use the representation of molecular two-electron integrals in the form of an expansion:

$$(pr|qs) = \sum_{Q} B_{pr}^{Q} B_{qs}^{Q}. \tag{2}$$

Using projectors obtained by simpler methods of the theory of many-particle systems, the equations of the coupled cluster method were reformulated in terms of the compressed amplitude tensor and the expansion of two-electron integrals. Thus, thanks to these approaches, it is possible to reduce the computational complexity of the CCSD method from $O(N^6)$ to $O(N^5)$. A software implementation of the compressed equations of the LCCD method was completed, with the help of which pilot calculations of various compounds were carried out.

This work was supported by Russian Science Foundation (project No. 24-73-00076, https://rscf.ru/project/24-73-00076/).

References

1. M. Lesiuk , J. Chem. Phys. **156**, 064103 (2022).

2. R. M. Parrish *et al.*, J. Chem. Phys., **137**, 224106 (2012).

Design of a photonic interconnect for ion qubits based on a concentric Fabry-Perot cavity

A.M. Russkikh[1,2], N.O. Zhadnov[1,3], N.N. Kolachevsky[1,3]

[1] P.N. Lebedev Physical Institute of the Russian Academy of Sciences, Moscow, Russia

[2] Moscow Institute of Physics and Technology,Dolgoprudny, Russia

[3] Russian Quantum Center, Moscow, Russia

russkikh.am@phystech.edu

Qubit systems based on chains of ultracold ions trapped in radiofrequency traps demonstrate promising characteristics for building an efficient quantum processor [1, 2]. One promising approach for scaling ion-based quantum computers involves combining a set of individual ion traps, where communication and quantum entanglement are achieved through the exchange of photons. To implement this multi-core solution, it is necessary to collect photons emitted by an atomic ion very efficiently. This can be accomplished by placing the atom inside the mode of an optical cavity, the frequency of which matches one of the atomic transitions.

Designing such a system requires solving several key problems. First, it is essential to calculate the cavity parameters, particularly the cooperativity parameter C, defined as: $C = \frac{g^2}{\kappa\gamma}$, where γ is the atomic level decay rate, κ is the cavity decay rate, and g is the ion-cavity coupling strength (single photon Rabi frequency). The best parameters for quantum state transfer efficiency between remote qubits, operation speed, and error rates are achieved in the "strong coupling" regime between the atom and the cavity mode [3]. The strength of this coupling is characterized by the cooperativity parameter, which in modern experimental studies rarely exceeds values of 1, making it difficult to achieve the desired operational regime.

This report is devoted to the development of a resonator for achieving the strong coupling regime with a single ion qubit, as well as the calculation and optimization of parameters for a photonic interconnect based on it. As such a device, we plan to use a Fabry-Perot cavity in a configuration that is as close as possible to concentric. Due to strong mode focusing and high quality factor, it becomes possible to achieve a cooperativity parameter exceeding 10. The report will discuss the use of various types of ions and optical transitions to implement such an interconnect, and provide estimates of the scale of cavity quantum electrodynamics effects in such system (e.g. Purcell effect, vacuum Rabi splitting, etc.). The work will also present the latest experimental results on the development of a microchip-based ion trap and approaches to the precision alignment of the ion's position with the mode of an external resonator.

References

1. Moses, Steven A. et al. "A race-track trapped-ion quantum processor." Physical Review X 13.4 (2023): 041052.

2. Zalivako, Ilia et al. "Quantum computing with trapped ions: principles, achievements and prospects" Phys. Usp. (2025), accepted.

3. Takahashi, Hiroki et al. "Strong coupling of a single ion to an optical cavity." Physical Review Letters 124.1 (2020): 013602.

Radiation from Dirac fermions caused by a projective measurement

P.O. Kazinski[1], V.A. Ryakin[1,2], P.S. Shevchenko[1]

[1] Physics Faculty, Tomsk State University, Tomsk 634050, Russia

[2] Mathematics and Mathematical Physics Division, Tomsk Polytechnic University, Tomsk 634050, Russia

kpo@phys.tsu.ru, vlad.r.a.phys@yandex.ru, psh-work@yandex.ru

We shall show that the properties of radiation appearing solely due to measurement are similar to edge or transition radiation [1, 2]. This is a consequence of the fact that the measurement of the intermediate state of the radiating particles undresses this particle, the virtual photons bound to it decouple and become real [1]. Therefore, in order to trace the dynamics of the wave function one can employ a proper modification of the developed experimental technics for beam diagnostics based on transition and diffraction radiations [3].

In the report we further generalize the theory developed in [4] to the case where the intermediate state of a radiating particle is measured. We obtain the general formulas for the probability of a chain of events and for the conditional probability. Then we apply the elaborated formalism to several particular examples describing the radiation from free Dirac particles undergoing a measurement. We study spontaneous and stimulated radiations due to measurement in the leading nontrivial order of perturbation theory and describe their main properties. In the case of stimulated radiation from a single particle, its wave function creates photons coherently, i.e., the amplitudes of radiation from the points of the particle wave packet are summed. In the case of spontaneous radiation, the radiation of photons is incoherent, i.e., the probabilities of radiation from the points of the particle wave packet are added up. It is shown that stimulated radiation due to measurement can be used to trace the dynamics and collapse of the wave function of the Dirac particle. A systematic procedure taking into account a finiteness of the measurement time is presented. Several examples of radiation due to measurement of the state of free Dirac particles are investigated in detail. In particular, we consider radiation due to measurement of the particle spin projection, of the particle momentum, and of the particle coordinate. The initial state of the Dirac particles is assumed to be of a general form and is described by the many-particle density matrix. The particular case of radiation due to measurement of the spin projection of one of the pair of entangled particles is also investigated.

Acknowledgments. The report was supported by the Russian Science Foundation, grant No. 25-21-00283.

References

1. V. A. Bazylev, N. K. Zhevago, *Radiation from Fast Particles in a Medium and External Fields* (Nauka, Moscow, 1987) [in Russian].

2. V. G. Bagrov, G. S. Bisnovatyi-Kogan, V. A. Bordovitsyn, A. V. Borisov, O. F. Dorofeev, V. Ya. Epp, V. S. Gushchina, V. C. Zhukovskii, *Synchrotron Radiation Theory and its Development* (World Scientific, Singapore, 1999).

3. L. G. Sukhikh, G. Kube, A. P. Potylitsyn, Simulation of transition radiation based beam imaging from tilted targets, Phys. Rev. Accel. Beams **20**, 032802 (2017).

4. P. O. Kazinski, T. V. Solovyev, Coherent radiation of photons by particle wave packets, Eur. Phys. J. C **82**, 790 (2022).

Zero noise extrapolation via cyclically permuted circuit layouts

Z. Sayapin[1,2] and D. Rabinovich[1,2]

[1] Skolkovo Institute of Science and Technology

[2] Moscow Institute of Physics and Technology

saiapin.zi@phystech.edu

Quantum computing excels at solving certain problems vs. classical methods [1, 2], but noise limits its practical use [3]. While quantum error correction works theoretically [4], it demands many qubits and precision. For current noisy devices, methods like Zero Noise Extrapolation (ZNE) [5] are promising—running algorithms at different noise levels and extrapolating to zero noise, especially for variational quantum algorithms [6].

We improve an error mitigation method from [7] for estimating observable expectation values. The approach exploits the uneven error distribution across qubits and qubit pairs, allowing noise variation by choosing different physical embeddings of the quantum circuit. After computing results for selected embeddings, values are linearly extrapolated to zero noise. While [7] proved exact convergence for n! noisy values on n-qubit circuits, the method still performed well with far fewer samples, despite lacking theoretical guarantees.

We consider a simplistic noise model where the application of any two-qubit gate is followed by a transformation:

$$\rho \to (1-q)\rho + q\mathcal{E}(\rho) \tag{1}$$

where q is the operation's error rate and $\mathcal{E}$ is a fixed quantum channel applied to the qubit pair. Error inhomogeneity arises from varying q across operations and qubit pairs.

We enhanced the method's theoretical convergence guarantees and analyzed single-qubit errors and non-unital noise effects. For n-qubit circuits with linear/circular topology under noise model (1), we prove the noiseless observable expectation can be reconstructed with $O(q^2)$ accuracy using just $2n$ noisy values from cyclic circuit permutations.

We tested the method numerically using a noise model based on IBM Sherbrooke processor calibration data, incorporating both single- and two-qubit errors. The model matched experimental randomized benchmarking data and included depolarizing and thermal relaxation. Results agreed well with theory.

Figure 1 illustrates the method for 12 qubits, showing numerical calculations for a randomly parameterized transverse-field Ising Hamiltonian. The circuit was evaluated over two cycles of cyclic permutations

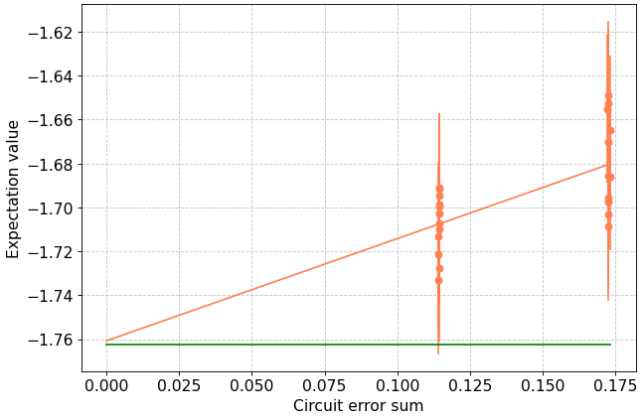

Figure 1: Linear extrapolation of noisy observable values obtained from cyclic permutations of a 12-qubit quantum circuit. Orange dots show noisy expected values; vertical lines indicate standard error. The green line marks the noiseless expected value.

References

1. P. Shor, SIAM Rev. **41**, 2 (1999)

2. S. Lloyd, Science **273**, 5278 (1996)

3. J. Preskill, Quantum **2**, 79 (2018)

4. D. Gottesman, Phys. Rev. A. **54**, 3 (1996)

5. K. Temme *et al.*, Phys. Rev. Lett. **119**, 18 (2017)

6. D. Wecker *et al.*, Phys. Rev. A. **92**, 4: (2015)

7. A. Uvarov *et al.*, Phys. Rev. A. **11**, 1 (2024)

Uncertainty of Bloch waves traveling in periodic structure

K. V. Semushev[1], Z. E. Munkueva[2], A. V. Dostovalov[2], S. A. Babin[2], E. E. Maslova[1], M. V. Rybin[1]

[1] School of Physics and Engineering, ITMO University, Russia

[2] Institute of Automation and Electrometry SB RAS, Russia

kliment.semushev@metalab.ifmo.ru

Optics unveils a multitude of phenomena that highlight the quantum character of light. Among them are topological photonic states [1], surface plasmon polaritons [2], and Anderson localization [3]. Moreover, any wave state can be characterized by a certain excitation length or localization length, which is especially significant for excitation in small structures. However, spatial confinement leads to momentum uncertainty due to the uncertainty principle, which ultimately destabilizes the wave state. The interplay between spatial confinement and momentum uncertainty imposes limits on the performance of devices of restricted size. Understanding and controlling this balance is crucial to optimize the systems used in quantum information processing [4], optical sensing [5], and other applications [6].

To illustrate the influence of the uncertainty principle on the formation of wave states, we explore the formation of Bloch waves. Here, we propose two approaches to defining a superperiodic dielectric medium inspired by structures commonly found in photonic devices, namely, photonic crystals and fiber Bragg gratings. Our investigation links the finite size of the constituent periodic regions to Bloch wave formation by examining the emergence of band gaps and performing a Fourier analysis, which is supported by both numerical simulations and experimental data.

Our theoretical framework allows us to analyze the band diagram in detail. We derive expressions for bandgap widths and estimate the spread of momentum values, leading to a condition for bandgap crossing. In addition, reflectance spectra are calculated using the transmission matrix method in our numerical simulations, which not only pinpoint the spectral positions of bandgaps but also yield results that are fully consistent with our theoretical predictions.

The role of dielectric permittivity contrast in bandgap crossing is particularly noteworthy. In fiber Bragg gratings, for instance, periodic perturbations typically exhibit low contrast, resulting in narrow band gaps. Under these conditions, the band gap crossing is predominantly driven by pronounced momentum uncertainty. Our numerical simulations agree with the theory, and experimental observations further emphasize the phenomena under study.

This work was supported by the Russian Science Foundation (No25-12-00213).

References

1. C. He *et al.*, Int. J. Mod. Phys. B **28**, 02 (2014).
2. F. Alpeggiani *et al.*, Plasm. **9** (2014).
3. M. Segev *et al.*, Nat. Phot. **7**, 3 (2013).
4. N. Gisin *et al.*, Nat. Phot. **1**, 165–171 (2007).
5. J. Anker *et al.*, Nat. Mat. **7**, 442–453 (2008).
6. V. Giovannetti *et al.*, Science **306**, 5700 (2004).

Autonomous discrete time crystal based on optical cavity-atom system

T. T. Sergeev[1,2,3,4], A. A. Zyablovsky[1,2,3], E. S. Andrianov[1,2,3]

[1] Dukhov Research Institute of Automatics

[2] Moscow Institute of Physics and Technology

[3] Institute for Theoretical and Applied Electromagnetics

[4] Institute of Spectroscopy Russian Academy of Sciences

sergeev.tt@phystech.edu

The concept of time crystals proposed by F. Wilczek [1] is closely related to the phenomenon of spontaneous breaking of time translation symmetry. Subsequently, this concept was extended to periodically driven Hamiltonian systems [2]. The periodical external driving leads to the appearance of a discrete time translation symmetry with respect to the time period of external driving. Spontaneous breaking of time translation symmetry causes some quantities in the system begin to change with a period multiple of the period of external driving [2].

In this work, we propose an optical cavity-atom system without periodic external driving where it is possible to observe spontaneous breaking of time translation symmetry [3]. We consider a system consisting of a two-level atom placed into a single-mode cavity coupled with a ring resonator. Here, the time scale arises not due to external driving, but due to the interaction of the system with the finite-sized environment. And, therefore, the discrete time translation symmetry is also created by the finite size of the environment. Usually, when an atom emits a photon, the photon needs to bypass the resonator length once to return the atom to an excited state. The bypass time is determined by the size of the resonator. We demonstrate that in considered system, there exists a parameter range, at which the photon emitted by the atom returns back, transitioning the atom to the excited state, after two bypasses of the resonator length, but not one bypass [3]. This is an indication of spontaneous breaking of discrete time translation symmetry. Moreover, this is a manifestation of time crystalline order in an autonomous system, where is no external periodical driving. We believe that this phenomenon opens a way to a new direction in the time crystal field.

This work was financially supported by a Grant from Russian Science Foundation (Project No. 23-42-10010).

References

1. F. Wilczek, Phys. Rev. Lett. **109**, 160401 (2012).

2. M. P. Zaletel, Rev. Mod. Phys. **95**, 031001 (2023).

3. T. T. Sergeev *et al.*, Opt. Lett. **49**(17), 4783-4786 (2024).

Non-Saturated Performance Scaling of Graphene Bilayer Sub-Terahertz Detectors at Large Induced Bandgap

Elena I.Titova[1], Mikhail A.Kashchenko[1], Andrey V.Miakonkikh[1], Alexander D.Morozov[1], Alexander V.Shabanov[1], Ivan K.Domaratskiy[1], Sergey S.Zhukov[1], Dmitry A.Mylnikov[1], Vladimir V.Rumyantsev[1], Sergey V.Morozov[1], Kostya S.Novoselov[1], Denis A.Bandurin[1], Dmitry A.Svintsov[1]

[1] Moscow Institute of Physics and Technology

Shabanov.AV@phystech.edu

Electrically induced p-n junctions in graphene bilayer have shown superior performance for detection of sub-terahertz radiation at cryogenic temperatures, especially upon electrical induction of the bandgap E_g. Still, the upper limits of responsivity and noise equivalent power (NEP) at very large E_g remained unknown. Here, the cryogenic performance of graphene bilayer detectors at $f = 0.13THz$ is studied by inducing gaps up to $E_g \approx 90meV$,a value close to the limits observed in recent transport experiments. High value of the gap is achieved by using high-κ bottom hafnium dioxide gate dielectric. The voltage responsivity, current responsivity, and NEP optimized with respect to doping do not demonstrate saturation with gap induction up to its maximum values. The NEP demonstrates an order-of-magnitude drop from $\approx 400fWHz^{-1/2}$ in the gapless state to $\approx 20fWHz^{-1/2}$ at the largest gap. At largest induced bandgaps, plasmonic oscillations of responsivity become visible and important for optimization of sub-THz response.

The devices were fabricated using the equipment of the Center of Shared Research Facilities (MIPT). E.I.T., M.I.K., A.V.S., I.K.D., S.I.Z., D.A.M., and D.A.S. acknowledged the support from grant FSMG-2025-0005. V.V.R. and S.V.M acknowledged the support from grant FFUF-2024-0045. E.I.T., M.A.K., A.D.M., and D.A.B. were supported by internal funding programme from the Center for Neurophysics and Neuromorphic Technologies.

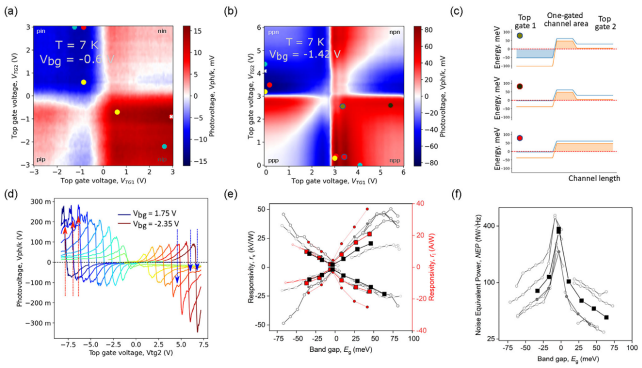

Figure 1: Terahertz photoresponce of BLG detector with induced p - n junctions. a,b) Color map of BLG sub-THz photovoltage as a function top gate voltages V_{tg1} and V_{tg2} controlling the density at two sides of the channel. k is the attenuation coefficient of the THz power. Panel (a) corresponds to the nominally gapless state, panel (b)– to the state with large induced band gap. Red dots on the color maps represent the optima of photovoltage V_{ph}^{max} , cyan dots– the optima of photocurrent I_{ph}^{max} , yellow– the optima of photovoltage per THz power dissipated in the channel $(V_{ph} \times R_{ch})^{max}$, white– the minima of NEP. c) Band diagrams along the BLG channel corresponding to high voltage responsivity. The respective doping voltages are indicated by color dots in panel (b). Red and black dots correspond to largest responsivity. d) Voltage responsivity obtained by scanning of the second gate voltage V_{tg2} while keeping the first gate voltage fixed, at different values of the back gate voltage marked by color. Red and blue arrows indicate the photovoltage oscillations arising from the excitation of graphene plasmons. e) Extracted maximum voltage responsivity (gray) and current responsivity (red) as a function of induced bandgap. Filled and hollow symbols correspond to slightly different focusing conditions at different days of the measurement f) Extracted noise equivalent power of the detector versus the induced bandgap.

The influence of correlations in medium microscopic structure on polarization radiation

P. G. Shapovalov and A. A. Tishchenko

National Research Nuclear University "MEPhI", Moscow, Russia

pgshapovalov@mephi.ru, tishchenko@mephi.ru

Polarization radiation occurs when a charged particle passes through a medium. The particle's electric field induces currents in the atoms of the medium, resulting in radiation, like Cherenkov, transition, X-ray parametric radiation. Polarization radiation is typically considered in homogeneous media using macroscopic electrodynamics. The only exception to this rule is the parametric X-ray radiation, in which taking into account (periodic) microscopic structure is a key effect; for other radiation types the yield of microstructure is usually not considered. Yet, we suppose that this problem has not been sufficiently investigated. Astapenko examined the influence of the structure within the framework of a microscopic consideration of the formation of polarization radiation [1, 2], however, as far as we know, consistent accounting of correlations has not yet been carried out.

This study aims to investigate the impact of the correlations in microscopic structure of matter on polarization radiation. We show that correlations in positions of separate particles (atoms) under certain conditions can result in a strong suppression of X-ray polarization radiation.

The study was partially supported by the Ministry of Science and Higher Education of the Russian Federation, Project No. FSWU-2023-0075.

References

1. V. A. Astapenko, L. A. Bureeva and V. S. Lisitsa, Physics-Uspekhi, **45**, 149 (2002)

2. V. A. Astapenko, L. A. Bureeva, and V. S. Lisitsa, JETP, **90**, 434 (2000).

Topological Phase Transitions in One-Dimensional Systems with Long-Range Interactions

V. Simonyan[1] and M. Gorlach[1]

[1] School of Physics and Engineering, ITMO University, Saint Petersburg 197101, Russia

vlad.simonyan@metalab.ifmo.ru

Topological phases of matter, initially discovered in condensed matter physics, have since been applied to diverse fields including metamaterial electrodynamics, photonics, electronics, and acoustics. A classic example is the Su–Schrieffer–Heeger (SSH) model, originally proposed to describe polyacetylene molecules [1]. The SSH model is particularly valuable due to its experimental simplicity and analytic solvability. However, this model typically includes interactions only between nearest neighbors, whereas realistic systems often possess significant long-range couplings [2].

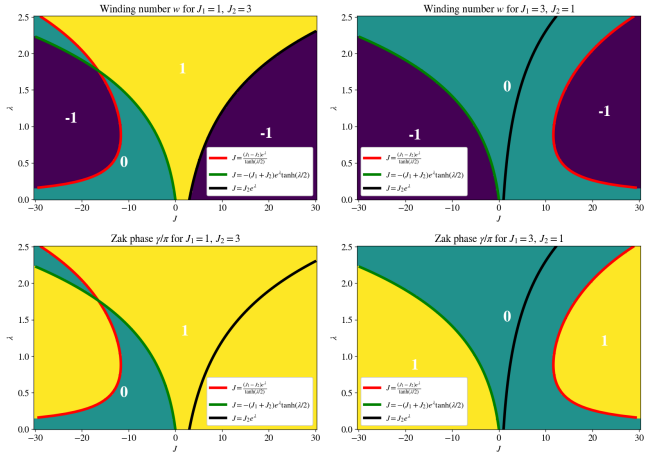

Figure 1: Phase diagram showing the influence of the long-range coupling amplitude and decay rate on the topological phases when couplings are decaying exponentially $J_s = Je^{-\lambda s}$.

Experimental systems such as waveguide arrays, characterized by exponentially decaying overlap integrals [3], or trapped-ion chains, featuring power-law decaying spin-spin interactions [4], exemplify scenarios where each lattice site is coupled to all others. To capture the essential physics of such systems while retaining simplicity, we introduce a single long-range hopping term at a separation of n unit cells into the SSH model. This modification preserves chiral symmetry, ensuring the existence of zero-energy modes.

We first consider coupling sequences whose sum $\sum_j t_j$ converges, allowing the use of standard Bloch theory to construct the Hamiltonian and define topological invariants. Our results, summarized in the phase diagram (Fig. 1), show that varying the strength of the coupling and its decay rate can induce clear topological transitions.

On the other hand, power-law decay interactions violate the conditions required by Bloch's theorem, complicating the analytical determination of phase boundaries and stability of edge modes. Nevertheless, we demonstrate that generalized summation methods allow us to identify these transition points effectively.

Significantly, adding a single long-range hopping interaction across n unit cells results in an increased winding number $\nu = 2n + 1$, supporting up to $2n + 1$ protected pairs of edge states. The winding diagrams become more intricate, and additional in-gap states with nonzero energies emerge.

These observations illustrate that even minimal incorporation of long-range couplings can significantly enrich the topological properties, revealing novel phase transitions and complex edge-state structures. These insights could facilitate the development of advanced topological systems with engineered boundary characteristics.

References

1. W. P. Su, J. R. Schrieffer, and A. J. Heeger, "Solitons in Polyacetylene," Phys. Rev. Lett. **42**, 1698 (1979).

2. B. Pérez-González, M. Bello, Á. Gómez-León, and G. Platero, "Interplay between long-range hopping and disorder in topological systems," Phys. Rev. B **99**, 035146 (2019).

3. B. A. Bell, K. Wang, A. S. Solntsev, D. N. Neshev, A. A. Sukhorukov, and B. J. Eggleton, "Spectral photonic lattices with complex long-range coupling," Optica **4**, 1433–1436 (2017).

4. D. Porras and J. I. Cirac, "Effective Quantum Spin Systems with Trapped Ions," Phys. Rev. Lett. **92**, 207901 (2004).

Theoretical study of the $^{29}Si^{16}O^{+}$ cation

P. D. Turchenko[1,2] and L. V. Skripnikov[1,2]

[1] Petersburg Nuclear Physics Institute named by B. P. Konstantinov of National Research Centre "Kurchatov Institute", Gatchina, Russia

[2] Saint-Petersburg State University, St Petersburg, Russia

p.d.turchenko@vk.com, leonidos239@gmail.com

An experiment aimed at detecting nuclear spin-dependent parity-violating effects in the $^{29}Si^{16}O^{+}$ cation [1] is currently being prepared by an international collaboration of scientists based at the Massachusetts Institute of Technology. A clear understanding of the electronic structure of this molecule is required for both setting up the experiment and interpreting its results. This topic has been addressed in several publications [2–8], but none of them employ the coupled-cluster method, which is currently considered the standard of accuracy. The accuracy of results is not analyzed in these works.

In the present study, the $^{29}Si^{16}O^{+}$ cation is investigated within multielectron approaches at the level of relativistic coupled-cluster theory. Scalar-relativistic potential energy curves are calculated near the equilibrium bond length for both the ground and excited electronic states, as well as the spin-orbit coupling curve between them. The excitation energy from the ground to the excited state is reported along with an estimate of its accuracy, enabled by systematic variation of basis sets and the level of electron correlation. The influence of spin-orbit interaction on the lowest vibrational levels of both the ground and excited electronic states is also evaluated.

This work was supported by the Russian Science Foundation grant no. 24-12-00092 and the "BASIS" grant no. 24-1-1-36-3.

References

1. J. Karthein *et al.*, Phys. Rev. Lett. **133**, 033003 (2024).
2. Z.-L. Cai, J. P. François, Chem. Phys. **234**, 59–68 (1998).
3. Z.-L. Cai, J. P. François, Chem. Phys. Lett. **282**, 29–38 (1998).
4. Z.-L. Cai, J. P. François, J. Mol. Spectrosc. **197**, 12–18 (1999).
5. S. Chattopadhyaya *et al.*, THEOCHEM. **639**, 177–185 (2003).
6. D. Shi *et al.*, Comput. Theor. Chem. **980**, 73–84 (2012).
7. R. Li *et al.*, Chem. Phys. **525**, 110412 (2019).
8. R. Li *et al.*, Chin. Phys. B. **28(4)**, 043102 (2019).

High-precision evaluation of magnetic hyperfine structure constants in $X^2\Pi$ and $A^2\Sigma^+$ states of OH molecule

D. P. Usov[1]*, Y. S. Kozhedub[1], A. V. Stolyarov[2], V. M. Shabaev[1,3]

[1] Department of Physics, Saint-Petersburg State University

[2] Department of Chemistry, Lomonosov Moscow State University

[3] Petersburg Nuclear Physics Institute named by B.P. Konstantinov of National Research Center "Kurchatov Institute"

*st054876@student.spbu.ru

Theoretical modeling of spectroscopic properties provides the foundation for understanding molecular structure enabling the interpretation of experimental observations and the prediction of new phenomena. For open-shell systems such as the hydroxyl radical OH, accurate *ab initio* calculations are essential to describe its complex electronic structure, including spin-orbit coupling, Λ-doubling, and hyperfine structure (HFS). These theoretical frameworks allow for the precise determination of transition frequencies, aiding in astrophysical observations [1], atmospheric chemistry [2], and tests of fundamental physics [3].

This study presents high-precision calculations of the parallel component of the hyperfine coupling constant in the OH molecule, induced by both the hydrogen ^{1}H and oxygen ^{17}O nuclei. Since the ground state of the OH molecule is a $X^2\Pi$ doublet, the calculations were carried out for projection of the total electron momentum on the molecular axis with values $\Omega = 3/2$ and $1/2$. Hydrogen-induced HFS constant was also obtained for excited state $A^2\Sigma^+$. The four-component relativistic single-reference coupled-cluster method was employed, incorporating single, double, and perturbative triple excitations (CCSD(T)). We also investigated the contribution of full triple excitations. Standard core-valence aug-cc-pCVNZ (N=3,4,5) basis sets were used, while an optimised basis set was constructed for calculations of hydrogen-induced HFS.

For the ground state, the calculated values of the HFS constants, induced by both nuclei, agree with the experimental values at the level of 1% for available $v = 0, 1, 2$ vibrational levels. The dependence on the internuclear distance was investigated, revealing significant variation for hydrogen-induced HFS, whereas oxygen-induced HFS exhibited a more monotonic behavior. This dependence of the hydrogen-induced HFS constant coincides with high accuracy with the available accurate semiempirical curve [4] in the range of distances corresponding to the experimental data.

This work was supported by the Russian Science Foundation (interdisciplinary grant No. 22-62-00004) and by the Foundation for the Advancement of Theoretical Physics and Mathematics "BASIS".

References

1. H. Weaver *et al.*, Nature **208**, 29–31 (1965).

2. M. Rex *et al.*, Atmos. Chem. Phys. **14**, 4827–4841 (2014).

3. N. Kanekar *et al.*, Phys. Rev. Lett. **95**, 261301 (2005).

4. L. D. Augustovičová, V. Špirko. J. Quant. Spectrosc. Radiat. Transf. **254**, 107211 (2020).

Theoretical investigation on possible indices of electromagnetic multipoles' singularities

N.A. Vlasov[1], V.P. Panurchenko[1], R. Nazarov[1], S.S. Baturin[1], E.E. Maslova[1], Z.F. Kondratenko[1]

[1] School of Physics and Engineering, ITMO University, 197101, St. Petersburg, Russia

nikolai.vlasov@metalab.ifmo.ru

Electromagnetic multipoles characterized by vector spherical harmonics are a widely used and convenient basis for the analysis of electromagnetic fields. Today, they are an active subject of both an applied and a fundamental research. One such example is nanophotonics, especially bound states in the continuum (BIC). The mechanism of BIC formation was shown to have multipolar origin [1]. The direction in which the mode does not emit corresponds to the singularity of the sum of multipoles coinciding with the open diffraction channel of the system. Meanwhile, a polarization vortex forms around the BIC point in reciprocal space [2, 3, 4]. Such vortices are characterized by their topological charge, which is the number of revolutions of the field around the BIC point. However, despite many numerical and experimental works in which the values of topological charges are calculated, little attention has been paid to giving an analytical description of the formation of polarization vortices around BIC points. Such a theory can be a very useful contribution to nanophotonics and can help us to take a step toward the formation of large topological charges, which today is one of the urgent and unresolved problems of BIC's research.

In the work [5] devoted to the singularities of electromagnetic multipoles, the authors analyze the number and indices of singularities of single multipoles. The authors conclude that if one multipole prevails in the mode, then at the Γ-point the topological charge is associated with its azimuthal index m, and out of Γ-point it is impossible to obtain a topological charge greater than 1 modulo. In our work, we extend the analysis of topological charges by considering an arbitrary sum of multipoles. Our goal is to construct a theory that describes the formation of field swirls around the BIC point for an arbitrary sum of multipoles and to identify the conditions for the formation of a large topological charge.

We show that the topological structure of the vortices around the BIC point is described by phase portraits of singular points of a two-dimensional dynamical system on a sphere. In this case, each multipole creates its own phase portrait, which, when combined with each other, forms a general field distribution around the singularity point. When the Jacobi matrix for the field is non-degenerate, one cannot expect a topological charge greater than 1 modulo out of the Γ point. However, in contrast to the work [5], our research indicates that the degeneracy of the Jacobi matrix leads to the possible appearance of a larger topological charge out of the Γ-point. In this case, the possible topological charge has an estimate of its modulus above $|q| < \Pi_2(3)$,

where $\Pi_2(3)$ is the Petrovskii number. It is also worth noting that for orders of multipoles actually excited in photonic structures, we show that there is no point in the reciprocal space where the Jacobi matrix of at least one of the multipoles degenerates. This means that the degeneracy of the Jacobi matrix is achieved only by selecting coefficients that satisfy a system of linear algebraic equations for each of the components of the Jacobi matrix of a general field. Different points in the reciprocal space and different combinations of multipoles give different numbers of equations necessary for the degeneracy of the field's Jacobi matrix at the singularity point. The number of such equations gives the lower limit of the required number of multipoles for the possibility of forming a large topological charge. Thus, we show that the formation of a possible high topological charge out of the Γ-point is associated with certain conditions on the coefficients before the multipoles and the quantity of these multipoles. In the case of the Γ-point, our analysis shows that the topological charge is associated with a minimum nonzero degree of the multipole asymptotics at this point. Thereby, we show a complex interplay between phase portraits of multipoles and generated topological charges. Our analytical analysis takes a serious step towards a deep understanding of the formation of topological charges of BIC.

References

1. Z. Sadrieva et al.: Phys. Rev. B 100, 115303 (2019)
2. B. Zhen et al.: Phys. Rev. Lett. 113, 257401 (2014)
3. T. Yoda et al.: Phys. Rev. Lett. 125, 053902 (2020)
4. E. N. Bulgakov et al.: Phys. Rev. Lett. 118, 267401 (2017)
5. W. Chen et al.: Phys. Rev. Lett. **122**, 153907 (2019)

Recapturing of cold rubidium atoms in an optical dipole trap

T. A. Voronova[1] and G. A. Vishnyakova[1]

[1] Moscow Institute of Physics and Technology

tvoronova847@gmail.com

Ensembles of cold atoms represent one of the most powerful tools for research across multiple domains of modern physics. For instance, they enable the development of novel frequency standards, serve as qubit implementations and quantum sensors. Many experiments require long-term spatial confinement of atoms to ensure extended interaction times with electromagnetic fields. This confinement can be achieved through combinations of electric, magnetic, gravitational, or optical forces.

Among classical trapping configurations, the magneto-optical trap (MOT) stands as a fundamental solution. It employs counter-propagating laser beams along three orthogonal directions combined with a pair of anti-Helmholtz coils generating a radially symmetric quadrupole magnetic field with zero point at the trap center.

In contrast, optical dipole traps operate via electric dipole interaction with a focused off-resonant high-power laser beam, providing weaker confinement compared to the aforementioned mechanism. Typical trap depths are on the order of 1 mK [1] or below. Optical excitation can be extremely weak in such traps, unlike in MOTs, thereby eliminating limitations inherent to radiation pressure-based capture mechanisms. Furthermore, the trapping mechanism is independent of magnetic sublevels in the ground state with an accuracy that excludes tensor polarizability. This enables diverse trapping geometries, including optical lattice implementations.

Within this work, we have established a stable MOT configuration achieving atomic cloud confinement with temperatures of approximately 175 μK. For dipole trapping, we employ a far-red-detuned laser system operating at 1012 nm. This wavelength selection is motivated by its dual utility: serving both as a dipole trap beam and as one component in two-photon Rydberg excitation schemes [2]. An additional advantage of this dipole trap configuration lies in its potential for Rydberg atom confinement while simultaneously satisfying the magic wavelength condition for ground-to-Rydberg transitions [3].

We have calculated the characteristics of the intended dipole trap for subsequent transfer operations, determining a maximum achievable trap depth of 3 mK under our experimental conditions. This value exceeds the Doppler cooling limit, creating favorable conditions for efficient atom transfer.

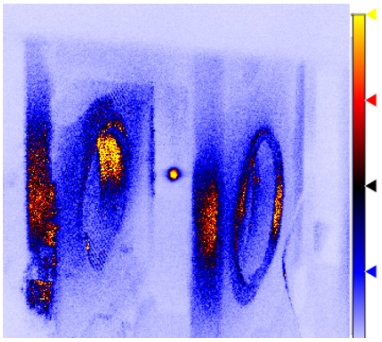

Figure 1: Image of atoms trapped in the MOT. The atomic cloud appears at the center of the image, with lens flare artifacts visible on both sides. The cloud dimensions are approximately 1 mm.

This study was supported by the Russian Science Foundation, project no. 25-22-00430.

References

1. 1. R. Grimm *et al.*, Adv. Atom. Mol. and Opt. Phys, **42**, 95–170 (1999).

2. 2. H. Bernien *et al.* Nature **551**, 579-584 (2017).

3. 3. Y. Li *et al.* Phys. Rev. A. **106**, L051701 (2022).

Modeling nuclear multipole transitions excited by Laguerre-Gaussian Beams

Y. Wang[1] and O.V. Bogdanov[1]

[1] Tomsk Polytechnic University

yanchzhao1@tpu.ru, bov@tpu.ru

In recent years, the interaction between matter and twisted light has been extensively studied, with particular interest in the forbidden multipole transitions induced by twisted light. Theoretical approaches for generating high energy twisted photons have been proposed in [1, 2], making the excitation of nuclear multipole transitions by twisted light experimentally feasible.

For the 7.8 eV nuclear transition in ^{229}Th induced by twisted photon absorption, theoretical calculations have been performed using Bessel mode wave functions, with the results expressed as impact parameter dependent transition probabilities [3].

A prediction was given in [3], that for this transition, when the impact parameter is small, the excitation by idealized Bessel modes and the Laguerre-Gaussian(LG) modes should give similar results in twisted light.

The nuclear multipole transition probabilities and selection rules for excitation by Bessel modes were presented in [4]. Applying a method similar to those in [4] and [5], we calculated the nuclear multipole transition probabilities for excitation by LG modes and compare the LG_{01} mode with the Bessel mode under the condition of small transverse momentum.

We obtained the general form of probability of nuclear multipole transitions excited by twisted light, that is described by $\mathrm{LG}_{\mathrm{nm}}$ mode. Confirmed that the nuclear multipole transition probabilities induced by the LG_{00} mode and those induced by plane waves are formally similar. Demonstrated that under condition of small impact parameter, the LG_{01} mode predicts the same behavior as the Bessel mode twisted light in nuclear excitation of multipole transitions.

References

1. U. D. Jentschura, V. G. Serbo, Phys. Rev. Lett. **106**, 013001 (2011).

2. O. V. Bogdanov *et al.*, Phys. Rev. D **99**, 116016 (2019).

3. T. Kirschbaum *et al.*, Phys. Rev. C **110**, 064326 (2024).

4. P. O. Kazinski, A. A. Cokolov, Phys. of Atom. Nuclei **87**, 561-569 (2024).

5. A. A. Peshkov *et al.*, Phys. Rev. A **96**, 023407 (2017).

Study of the surface [100] of Xenotime (YPO_4)

Oleg Yu. Andreev[1,2] and Igor A. Zhosan[2]

[1] Department of Physics, St. Petersburg State University, 7/9 Universitetskaya nab., St. Petersburg, 199034, Russia

[2] Petersburg Nuclear Physics Institute named by B.P. Konstantinov of National Research Centre Kurchatov Institute, Gatchina, Leningrad District 188300, Russia

iigorezhosan@gmail.com

The objective of this study is to develop and implement a novel cluster-based methodology for the analysis of solid surfaces. A similar approach has previously been applied to the study of three-dimensional solids, where it has demonstrated its effectiveness, particularly in the study of impurities of heavy elements in crystals.

The surface [100] of a Xenotime crystal YPO_4 has been selected as a modeling object. Previous calculations have been carried out in the framework of the cluster approach for the three-dimensional structure of this system, which allows the comparison of the results obtained in this work with previous ones and the evaluation of changes occurring when considering the surface of a solid.

The construction of the cluster surface model was executed in a series of stages. Initially, a periodic calculation was conducted in which the investigated structure was modeled as a finite number of infinite two-dimensional layers. The periodic calculation was performed using the CRYSTAL17 program code, whose fundamental approximation is the decomposition of the crystal orbital into a linear combination of Bloch functions (BF) defined in terms of atomic orbitals (LCAO CO approximation). All calculations at this stage were performed within the framework of density functional theory (DFT), employing the PBE exchange-correlation functional. The pseudopotential (ECP) method was used to describe the heavy yttrium atom (Y).

The corresponding ECP were specially developed by the group of the laboratory of quantum physics and chemistry of NRC «Kurchatov Institute» - PNPI for further application in the framework of the cluster approach. At this stage, primary data on surface relaxation and reconstruction, depth of the corresponding changes, electron density distribution, and other characteristics were obtained.

The data obtained function as a foundational basis for the construction of clusters and the subsequent emulation of their environment, utilizing the CTEP (Custom-Tailored Embedding Potential) approach and the point charge distribution (embedding) technique. The developed model incorporates relaxation effects on the solid surface and reproduces the crystal geometry around the central part of the cluster. Subsequent enhancement of the embedding and geometry of the cluster surface model was facilitated by using the software packages NWChem and ORCA 6.0. These packages, in addition to various density functional theory methods, support post-Hartree-Fock methods,

which allows for a significantly improve in the accuracy of the final results and obtain new information about the physical and chemical properties of the system.

The utilization of the obtained model facilitates the study of both the properties of the crystal surface itself, including local magnetic characteristics, and the processes occurring on it, particularly the adsorption of various elements and molecules. The study of adsorption is especially relevant for experiments on the study of superheavy elements.

References

1. Lomachuk Yu. V., Maltsev D. A., Mosyagin N. S., Skripnikov L. V., Bogdanov R. V., and Titov A. V. Compound-tunable embedding potential: which oxidation state of uranium and thorium as point defects in xenotime is favorable? // Physical Chemistry Chemical Physics. 2020. Vol. 22. P. 17922–17931.

2. Demidov Yu.A., Zaitsevskii A.V. Adsorption of the astatine species on a gold surface: A relativistic density functional theory study // Chemical Physics Letters. 2018. Vol. 691. P. 126-130.

One-electron quasimolecules: binding energies and critical distances in extreme magnetic field

D. V. Zinenko[1]

[1] Department of Physics, St. Petersburg State University,
Universitetskaya nab. 7/9, 199034 St. Petersburg, Russia

dmitrii.zinenko@gmail.com

The study of quantum electrodynamics (QED) effects in supercritical fields remains one of the most intriguing directions in modern theoretical physics. When the nuclear charge exceeds a critical value of $Z_{\rm cr} \geqslant 173$, the ground state of a hydrogen-like ion is predicted to dive into the negative-energy continuum, leading to spontaneous electron-positron pair production [1, 2]. Although nuclei with such a high charge have not yet been discovered, theoretical studies suggest that such a process is possible in slow collisions of heavy ions, whose total charge exceeds the critical value [3, 4, 5]. However, the effect of an ultra-strong external magnetic field on these processes remains insufficiently explored. It has been demonstrated [6, 7, 8] that in strong magnetic fields, magnetic forces dominate over Coulomb attraction, fundamentally altering atomic structure and increasing binding energies.

In particular, fields of the order of $B_0 = m^2c^2/(\hbar|e|) = 4.41 \cdot 10^9$ T and higher are typical for neutron stars and are also encountered in energetic heavy-ion collisions. Such strong fields significantly alter the conditions for vacuum decay in supercritical quasi-molecular systems, so that the corresponding theoretical investigations are in demand.

In this work, we study one-electron diatomic quasimolecules in a super-strong homogeneous magnetic field by solving the two-center Dirac equation using the dual-kinetic balance finite-basis-set method generalized for axially symmetric systems [9]. This approach has been successfully applied to quasimolecules with one and two electrons [10, 11, 12]. We focus on heavy-ion systems, such as $\mathrm{Pb}^{82+} - \mathrm{Pb}^{82+} - \mathrm{e}^-$ and $\mathrm{U}^{92+} - \mathrm{U}^{92+} - \mathrm{e}^-$, to determine how the binding energies and critical internuclear distances change under increasing field strength. Our calculations reveal that the presence of an external magnetic field significantly enhances the electron binding energy and reduces the critical internuclear distance at which the energy level dives to the negative continuum. In particular, the results for critical distances are shown in Figure 1.

This work was supported by the Russian Science Foundation No. 21-42-04411 and the BASIS foundation.

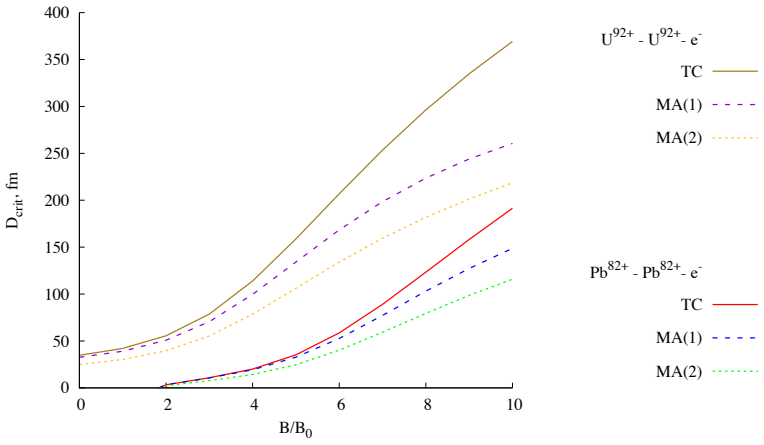

Figure 1: Dependence of the critical distance (in fm) for the ground electronic state of $Pb^{82+} - Pb^{82+} - e^-$ and $U^{92+} - U^{92+} - e^-$ on the magnitude of the magnetic field ($B_0 = 4.41 \cdot 10^9$ T). Calculations are performed for the two-center potential (TC) and the monopole potential with the origin at the center of mass of nuclei (MA(1)) and at one of the nuclear centers (MA(2)).

References

1. S. S. Gershtein and Y. B. Zel'dovich, Sov. Phys. JETP **30**, 358 (1970).

2. W. Pieper and W. Greiner, Z. Physik **218**, 327 (1969).

3. S. S. Gershtein and V. S. Popov, Lett. Nuovo Cimento **6**, 593 (1973).

4. I. A. Maltsev *et al.*, Phys. Rev. Lett. **123**, 113401 (2019).

5. R. V. Popov *et al.*, Phys. Rev. D **102**, 076005 (2020).

6. V. Oraevskii, A. Rex, and V. Semikoz, Sov. Phys. JETP **45**, 428 (1977).

7. P. Schlüter et al., J. Phys. B: At. Mol. Phys. **18**, 1685 (1985).

8. D. A. Tumakov et al., Opt. Spectrosc. **130**, 466 (2022).

9. E. B. Rozenbaum et al., Phys. Rev. A **89**, 012514 (2014).

10. A. A. Kotov et al., XRS **49**, 110 (2020).

11. A. A. Kotov et al., Atoms **9**, 44 (2021).

12. A. A. Kotov et al., Atoms **10**, 145 (2022).

School lectures

Schwinger effect in high energy physics, astrophysics and physics of nanostructures

S. P. Gavrilov

Herzen State Pedagogical University of Russia
gavrilovsergeyp@yahoo.com

Quantum field theories (QFTs) with external fields are to a certain extent the most appropriate models for calculating quantum effects in strong fields of electromagnetic, gravitational, or other nature. These calculations must be nonperturbative with respect to the interaction with strong backgrounds. One of the most interesting effect of such kind that attracts attention already for a long time is the particle creation from the vacuum by strong external backgrounds (the Schwinger effect). In the framework of the QFT, the particle creation is closely related to a violation of the vacuum stability with time. Backgrounds that violate the vacuum stability have to be electriclike fields that are able to produce nonzero work when interacting with charged particles. In such backgrounds any process is accompanied by new created particles and, thus, turns out to a many-particle process.

The Schwinger effect is currently considered in many field models of phenomena in high-energy physics, astrophysics, and physics of nanostructures. This is reflected in the new PhySH-Physics subject heading system used by journals in the Physical Review group, where a separate heading "Schwinger effect" has been introduced. It is believed that this is one of the main mechanisms, the appearance of matter in cosmological models, the production of a quark-gluon plasma by a chromoelectric field in the collision of heavy ions, is discussed in laser physics of extreme fields, the physics of black holes, neutron and quark stars, string theories and their dual theories of gauge fields. The effect arises in any model of quantum field theory (QFT), in which there is an interaction with the U(1) gauge field (for which the term "electriclike field" is used). This makes it possible to transfer the methods developed for studying the effects of QED in a strong electric field to other models and determines the scientific significance of this direction for QFT.

Lecture content:

1. The setting of a problem in the framework of strong-field QED.

2. Analogues of the Schwinger effect in the physics of nanostructures (Dirac fermions in graphene monolayer, antiferromagnetics magnons etc.; see, e.g., review [1]).

References

1. A. Fedotov, A. Ilderton, F. Karbstein, B. King, D. Seipt, H. Taya, G. Torgrimsson, *Advances in QED with intense background fields*, Phys. Rep. **1010**, 1-138 (2023) [arXiv:2203.00019].

Aharonov-Bohm interferometers

R.A. Niyazov[1,2], I.V. Krainov[2], D.N. Aristov[1,2], V.Yu. Kachorovskii[2]

[1] Petersburg Nuclear Physics Institute named by B.P. Konstantinov of NRC "Kurchatov Institute"

[2] Ioffe Institute

niyazov_ra@pnpi.nrcki.ru

Quantum wave interference plays a key role in fundamental physics and finds numerous applications. In condensed matter physics, interferometers based on systems with a small number of electron quantum channels have attracted significant attention in recent decades due to the growing interest in controllable nanoscale quantum devices. One of the simplest implementations of such an interferometer is a ring-shaped structure with metallic contacts (see Fig. 1(a)). Its operation can be controlled via the Aharonov-Bohm (AB) effect by applying a magnetic field. AB interferometers are highly promising for studying quantum-coherent phenomena and for applications such as miniature, highly sensitive magnetic field sensors.

We compare two types of interferometers: one based on a conventional conductor and another on a 2D topological insulator (TI). The conventional interferometer is modeled using one-dimensional electron states, where electrons can undergo backscattering at the contacts. In contrast, the TI has helical edge states (with opposite spins propagating in opposite directions), where backscattering at non-magnetic contacts is prohibited. To observe interference effects in the TI case, a magnetic defect must be placed at the edge.

The AB effect manifests itself as a dependence of measurable quantities on the magnetic flux through the interferometer's ring. We analyze two key observables: the conductance (relating current and voltage) [1], and the shot noise (current fluctuations due to electron discreteness) [2] (see Fig. 1(b)). Notably, interference persists even at relatively high temperatures (when temperature exceeds the level spacing in the ring).

Our results provide insights into experimentally observed time-reversal symmetry breaking in helical states [3], motivate further experimental studies of electron transport in high-temperature regimes, and suggest new potential applications for quantum interferometers. These findings may be relevant for spintronics, ultrasensitive magnetometry, and quantum computing.

This work was supported by the Russian Science Foundation (grant No. 25-12-00212).

References

1. R.A. Niyazov, D.N. Aristov, V.Yu. Kachorovskii, Npj Comput. Mater. **6**, (2020).

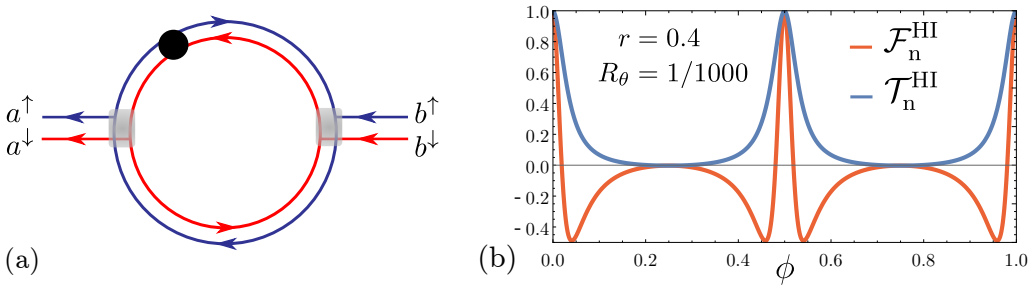

Figure 1: (a) Aharonov-Bohm interferometer based on the helical edge states of the 2D topological insulator. The magnetic defect is marked by black dot. (b) Dependence of the conductance (blue curve) and the shot noise (red curve) on the magnetic flux.

2. R.A. Niyazov, I.V. Krainov, D.N. Aristov, V.Yu. Kachorovskii, JETP Lett. **119**, 372 (2024).

3. I.V. Krainov, R.A. Niyazov, D.N. Aristov, V.Yu. Kachorovskii, arXiv:2410.04610 (2024).

What can we learn from 2+1-dimensional gravity?

A. Sheykin

Saint Petersburg State University

a.sheykin@spbu.ru

Since Ehrenfest's seminal paper [1] about the dimension of space, physicists started to treat the number of space dimensions as a free parameter of a theory rather than as a fixed number. Allowing it to vary often provides unexpected insights into the nature of physical theories, and gravity is not an exception.

At first glance 2+1D Newtonian gravity is not so different from its 3+1D analog; the only thing that changes is a radial dependence of gravitational force. However, in general relativity the situation drastically changes: it turns out that 2+1D GR has no Newtonian limit at all!

It can be shown in many different ways:

- observing that there is no Schwarzschild radius corresponding to a point mass in 2+1D, so the metric of spacetime with a point mass cannot depend on radius and therefore needs to be flat [2],
- through direct solution of vacuum field equations, as did Staruszkiewicz in his pioneering paper [3],
- using the fact that "gauge hits twice": there are six independent components of the metric, three of them are fixed by coordinate choice and another three are subject to constraints $G^{0\mu} = \varkappa T^{0\mu}$, so none of them are dynamic ones [4],
- via component counting of the Riemann and Ricci tensors: the fully antisymmetric part of the Riemann tensor, the Weyl tensor $C_{\mu\nu\alpha\beta}$, is necessarily zero in 2+1D as there are not enough spacetime dimensions for all its indices to be different, so the curvature of spacetime is completely defined by the Ricci tensor and (via Einstein equations) by the presence of matter, and where there is no matter, there is no curvature [4]. It also means that gravitational waves in 2+1D are absent as well.

Curiously enough, the absence of local degrees of freedom permits the spacetime to be topologically nontrivial. While the matter in 2+1D cannot curve spacetime around itself, it nevertheless can bend it. The space around a point mass can be constructed by cutting off a sector from a plane and gluing the edges together, so it represents a cone. In the presence of constant positive curvature one needs to cut a sector from a sphere instead, obtaining a spindle-like surface [5]. In particular, this means that in a spacetime with constant positive curvature one cannot assign a mass to a particle if it is single, since a spindle always has two endpoints.

The absence of locally nontrivial vacuum makes 2+1D GR somewhat boring at a classical level, so attempts have been made to study its non-vacuum solutions, which are relatively plentiful [6]. Another line of inquiry is a search for 2+1D gravity that has a Newtonian limit [7].

On the other hand, local vacuum triviality provides an immense advantage at a quantum level. As shown by Witten [8], 2+1D GR can be recast as a Chern-Simons theory, which makes it exactly solvable. Since then, quantum 2+1D GR has been extensively studied. An especially suitable toy model for quantum gravity is the 2+1D black hole (BTZ spacetime). The usual strategy here is to search for a QG phenomenon that can be studied and does not depend on the number of dimensions, so we can learn something about the 3+1D case from 2+1D.

However, the reverse thinking can also be fruitful. Facts from 3+1D that we treat as universal could disappear in 2+1D, as happens with the Einsteinian interpretation of GR as a theory of relativity between gravity and inertia[9].

To conclude, the weirdness of 2+1D gravity should encourage us not to try to make it more familiar to us, but rather to test our common knowledge on its grounds to see whether it still holds.

References

1. P. Ehrenfest, KNAW Proc. **20**, 200 (1918).

2. A. A. Sheykin, S. N. Manida, Universe **6**(10), 166 (2020), arXiv:2005.08196.

3. A. Staruszkiewicz, Acta Phys. Polon. **24**, 735 (1963).

4. S. Carlip, *Quantum gravity in 2+1 dimensions* (2023), arXiv:2312.12596.

5. A. A. Sheykin, M. V. Markov, S. A. Paston, J. Math. Phys. **62**, 102502 (2021), arXiv:2107.00752.

6. A. A. Garcia-Dias, *Exact Solutions in Three-Dimensional Gravity*, Cambridge, 2017.

7. J. H. C. Scargill, Phys. Rev. Research **2**, 013217 (2020), arXiv:1906.05336.

8. E. Witten, Nucl. Phys. **B 311**(1), 46 (1988).

9. A. A. Sheykin, Found. Phys. **52**, 34 (2022), arXiv:2103.13854.

Quantum computing and quantum simulation with neutral atoms

K.S. Tikhonov[1,2]

[1] St. Petersburg state University, 7/9 Universitetskaya Nab., 199034 St. Petersburg, Russia

[2] Russian Quantum Center, Skolkovo, 143025, Moscow, Russia

tikhonov.kyril@gmail.com

Arrays of neutral atoms are a very promising platform for building quantum computers and simulators. Their scalability, high-fidelity operations, and the ability to create reconfigurable connections between qubits (the quantum bits) make them a leading contender in the field [1].

In this talk, I will try to explain why neutral atoms are considered good qubits and how single-qubit and two-qubit operations are implemented in optical-tweezer arrays of neutral atoms. In particular, we will consider several protocols for implementing an entangling CZ gate based on the Rydberg blockade mechanism [2, 3]. In addition, we will discuss the challenges preventing the creation of a universal quantum computer today and explore some applications for the so-called NISQ (Noisy Intermediate-Scale Quantum) devices based on non-ideal qubits.

References

1. X. -F. Shi *et al.*., Quantum Sci. Technol. **7**, 023002 (2022).

2. T. M. Graham *et al.*., Phys. Rev. Lett. **123**, 230501 (2019).

3. H. Levine *et al.*, Phys. Rev. Lett. **123**, 170503 (2019).

4. N. Moroz *et al.*, Phys. Rev. A **-Accepted** 27 May (2025).

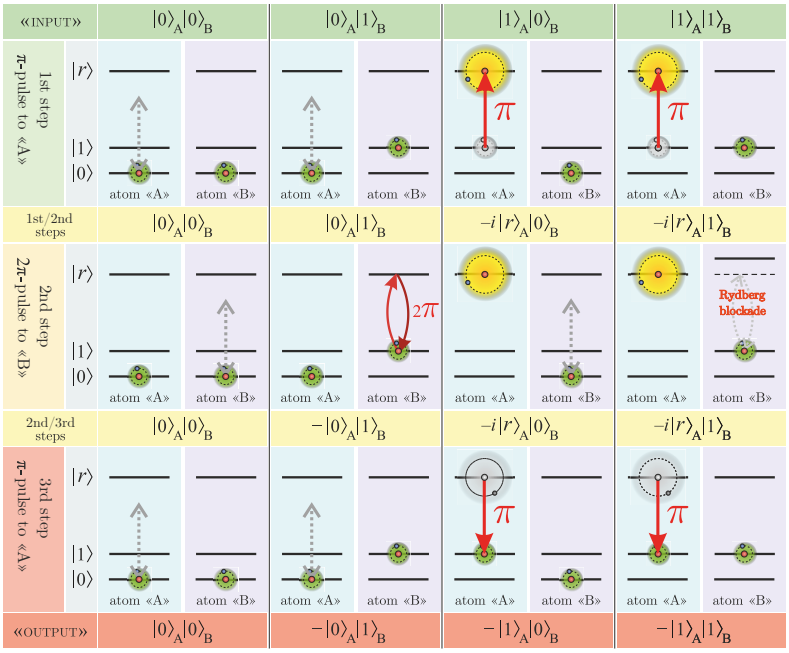

Figure 1: Implementation of the Controlled-Z gate using the π-2π-π protocol [2].

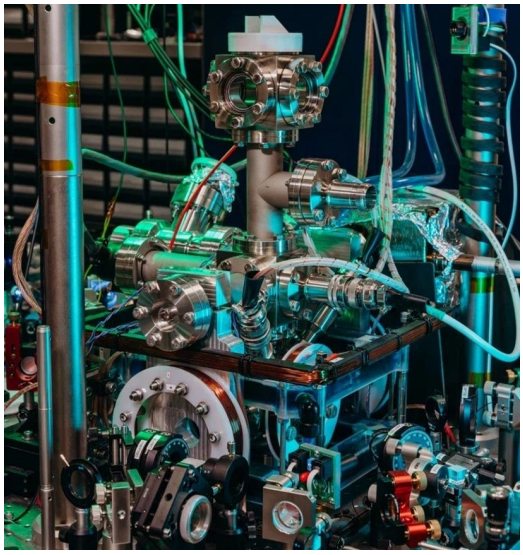

Figure 2: Atomic quantum computer under development in RQC. Source: https://rqc.ru